



FRAS 1.1.3; Weld Residual Stresses

Welding Residual Stress Relaxation in NPP Components Under Operation – A Literature Study

Author(s): Otso Cronvall




Confidentiality: Public

Report's title Welding Residual Stress Relaxation in NPP Components Under Operation – A Literature Study	
Customer, contact person, address State Nuclear Waste Management Fund (VYR), BeräkningsGrupp (BG, members of which are TVO Oyj, Oskarshamn Ab, Ringhals Ab, Forsmark Ab) and VTT	Order reference(s) 5280-08; TVO, 4090234; Oskarshamn, 594100-003; Ringhals, 4500175143; Forsmark
Project name FRAS 1.1.3; Weld Residual Stresses	Project number/Short name 32418/FRAS 09
Author(s) Otso Cronvall	Pages 80 / 2
Keywords WRS, RS, NPP, piping component, weld, FEM	Report identification code VTT-R-02200-10
<p>Summary</p> <p>This study concerns the welding process induced residual stresses in nuclear power plant (NPP) reactor circuit component welds, and their modelling for structural integrity analyses. The present study continues the work of the previous parts of the project. Here the emphasis is on a literature study concerning various weld residual stress (WRS) relaxation assessment procedures for NPP component welds. Also numerical simulations of WRS distributions were carried out with the same finite element method (FEM) model as was used in 2008, i.e. that consisting of a safe-end connecting to a nozzle and pipe. The scope of the analyses was extended so that here it was examined how the WRS distributions in the safe-end/pipe joint weld region behave under constant cyclic loading. Several load cycle sequences with different load amplitudes covering loading condition ranges from moderate to relatively severe were covered. Based on the obtained FEM simulation results analytical expressions for the assessment of WRS relaxation were formed. Also uncertainties and probabilistic aspects of WRS distributions are considered in this study.</p> <p>Selection of suitable WRS distribution estimates for structural integrity analyses is an issue requiring careful consideration. Several WRS definition procedures are currently available. Seven of those are compared in this study in the light of application examples for a representative set of NPP pipe components. One purpose for this is to have a starting point for WRS relaxation simulations, which are covered further in the study.</p> <p>The main results of this study are the altogether 25 discovered residual stress (RS) relaxation assessment procedures. These were found as a result of an extensive literature survey covering a great number of sources of information, including the major technical scientific journals, with tracing of cited references in each new article as it was obtained, as well as conference papers, academic theses, dissertations, handbooks and technical reports, both from libraries in paper format and from Internet databases. Brief descriptions of the main characteristics of the found WRS relaxation assessment procedures are given. In addition to the procedure equations/formulas, also mentioned are the original reference/authors, target of application, required input data, parameters to be fitted, range of applicability and the covered phenomena.</p> <p>Typically the available RS data contains measurement uncertainties, which vary from technique to technique. Generally the main uncertainties in RS measurement can be categorised to those that are technique specific, material specific, and component/geometry specific.</p>	

The published experimental as-welded state WRS data have a substantial scatter. Consequently the WRS distributions defined in the commonly used fitness-for-service procedures have been developed as tensile upper bound solutions based on the data. However, according to several authors, this approach not only lacks consistency for the same type of joints and welding parameters, but can either significantly overestimate the WRS level in some cases, or underestimate it in others.

Concerning probabilistic methods to define WRS distributions, the following procedures are described in this study: least-squares technique, Bayesian statistical approach, spatial Bayesian approach, spatial deconvolution approach, heuristic method, fuzzy-set approach, and goodness of fit technique. Also described in this study is the treatment of WRSs in some current notable probabilistic crack growth analysis codes. These PFM based codes are WinPRAISE, PRO-LOCA, ProSACC and PASCAL-SP.

Based on the numerical WRS simulation results and within their scope, two analytical WRS relaxation assessment equations were also developed for the considered safe-end/pipe weld region. The obtained results provide also an example of an approach to derive analytical WRS relaxation equations for practical applications. Moreover, as the involved computational effort is reasonable, it is considered that the approach used here is technically feasible, and can thus be applied to components with other geometries, materials and experienced loads.

Confidentiality		Public	
Espoo 6.5.2010			
Signatures	Signatures	Signatures	
			
Written by Otso Cronvall Research Scientist	Reviewed by Kim Calenius Research Scientist	Accepted by Arja Saarenheimo Deputy Technology Manager	
VTT's contact address P.O. Box 1000, 02044 VTT			
Distribution (customer and VTT) SAFIR2010 Reference Group 6 (Structural Safety of Reactor Circuit); SAFIR2010 FRAS Ad-Hoc Group; BeräkningsGrupp (2+2+2+2); VTT Archive (2)			
<i>The use of the name of the VTT Technical Research Centre of Finland (VTT) in advertising or publication in part of this report is only permissible with written authorisation from the VTT Technical Research Centre of Finland.</i>			

Foreword

This report has been prepared under the research project FRAS 1.1.3; Weld Residual Stresses, which concerns welding process induced residual stress distributions in Nuclear Power Plant (NPP) reactor circuit component welds. The project is a part of SAFIR2010, which is a national nuclear energy research program. FRAS 1.1.3 project work in 2009 was funded by the State Nuclear Waste Management Fund (VYR), the BeräkningsGrupp (BG), and the Technical Research Centre of Finland (VTT). The work was carried out at VTT. The author of the report expresses his gratitude to Mr Paul Smeekes from Teollisuuden Voima Oy (TVO) for valuable co-operation. The support from BG is also gratefully acknowledged.

Espoo 6.5.2010

Author

Contents

Foreword	3
List of symbols and abbreviations.....	6
1 Introduction.....	9
2 WRSs and their mechanical relieving	11
2.1 Introduction to WRSs	11
2.2 On the conditions/treatments that relieve WRSs in NPP components	12
2.2.1 Irradiation effects	12
2.2.2 Thermal effects	13
2.2.3 Mechanical load effects.....	13
3 On the selection of suitable WRS assumptions for structural integrity analyses...	15
3.1 Applicability of current notable WRS definitions for numerical simulations ...	15
3.2 Comparison of current notable WRS definitions	17
3.2.1 Input data considerations.....	17
3.2.2 WRS definition comparison results	20
4 Procedures to assess WRS relaxation in NPP Components under operation	26
4.1 Purpose and scope of literature study.....	26
4.2 Results of the performed literature study	28
5 Uncertainties and probabilistic aspects concerning assessing WRS distributions	41
5.1 Uncertainties concerning measured WRS distributions	41
5.2 Probabilistic methods to define WRS distributions	42
5.2.1 Least-squares technique.....	43
5.2.2 Bayesian statistical approach.....	43
5.2.3 Spatial Bayesian approach	44
5.2.4 Spatial deconvolution approach.....	44
5.2.5 Heuristic method	44
5.2.6 Fuzzy-set approach	47
5.2.7 Goodness of fit technique	49
5.3 Treatment of WRSs in probabilistic PRAISE analysis code	50
5.3.1 Introduction	50
5.3.2 Residual stresses.....	50
5.4 Treatment of WRSs in some other notable probabilistic crack growth analysis codes	53
5.4.1 PRO-LOCA.....	53
5.4.2 ProSACC	54
5.4.3 PASCAL-SP.....	55
6 Numerical modelling of WRSs and their relaxation.....	57

6.1	Examined weld, initial WRSs, considered loads and other relevant input data	57
6.2	Numerical heat transfer and stress/strain simulations.....	59
6.3	Analysis results from the viewpoint of WRS relaxation	61
7	Discussion and suggestions for further research.....	67
8	Conclusions.....	72
	References	74
	Appendix 1: Summary of input data parameters necessary for RS relaxation assessment procedures	81

List of symbols and abbreviations

Note that for clarity the parameters and variables concerning the WRS relaxation assessment procedure formulas and equations are presented only in the associated compilation tables in this study, see Chapter 4. Otherwise all symbols and abbreviations concerning this report are presented here.

Latin symbols

A	Experimental scaling constant in spatial Bayesian approach
a_g	Normalised constants describing the ratios between the weights in heuristic method
b_j	Constants in linear function for stress measurement data in heuristic method
B	Background signal in spatial Bayesian approach
$C_{\alpha,j}$	binary α -cut combinations in fuzzy-set approach
D_k	Independent stress measurements in least-squares technique
$e(x)$	Random error function in heuristic method
f	adjustment factor in WinPRAISE
$f(y)$	Analytical model in spatial Bayesian approach
F_k	Analytical prediction corresponding to independent stress measurements in least-squares technique
$H(y)$	Instrumental resolution function in spatial Bayesian approach
ID	Inner diameter
m	Number of experimental data items in heuristic method
N	Number of load cycles
N	Number of independent stress measurements
N	Number of fuzzy material parameters in fuzzy-set approach
$N_{c/\alpha}$	number of combinations per α -cut in fuzzy-set approach
OD	Outer diameter
p	Pressure
p_{\max}	Maximum pressure value
p_{\min}	Minimum pressure value
r_{ij}	Correlation coefficient of stress between i th and j th point (neighbouring points) in PASCAL-SP
R	Stress ratio
R_k^2	Relative squared differences
S_i	Weld residual stress in pipe component wall thickness direction at i th point in PASCAL-SP
S_i^{ave}	Average weld residual stress in pipe component wall thickness direction at i th point in PASCAL-SP
SS_1	Difference between measured stress data and best-fit data in goodness of fit technique
SS_2	Difference between measured stress data and mean value of all measured stresses in goodness of fit technique
t	Time
t_{wall}	Component wall thickness
T	Temperature

$T_i(x)$	Linearly independent basis functions in heuristic method
w_g	Relative weights in heuristic method
X	Quantity of interest consisting of several measurements
X	Free parameters of the computation model
X_c	Weld residual stress distribution distance parameter in PRO-LOCA
X_i	Fuzzy material parameters in fuzzy-set approach
X_0^L	Left end of the range of variation of fuzzy material parameters in fuzzy-set approach
X_0^R	Right end of the range of variation of fuzzy material parameters in fuzzy-set approach
$X_{1.0}^{L,R}$	Nominal value of fuzzy material parameters in fuzzy-set approach
y_k	Position of measurement in spatial Bayesian approach
y	Linear function for stress measurement data in heuristic method
y_i	Measured values for weld residual stress in heuristic method
\hat{y}_i	Values for weld residual stress to be fitted in heuristic method
Z	Random number following a standard normal distribution in PASCAL-SP

Greek symbols

α_{HT}	Heat transfer coefficient
$\Delta\sigma$	Total stress load range
ϕ	Outer diameter
$\mu(X)$	Membership function (possibility distribution) in fuzzy-set approach
σ	Weld residual stress field in fuzzy-set approach
σ_a	Applied stress amplitude
σ_e	von Mises equivalent stress
σ_g	Data group specific variance in heuristic method
σ_h	Hydrostatic stress
σ_i	Standard deviation of weld residual stress in PASCAL-SP
σ_k	Estimated error in least-squares technique
σ_{max}	Load cycle specific maximum stress value
σ_{min}	Load cycle specific minimum stress value
σ^R	Weld residual stress
σ^{rs}	Residual stress at surface
$\sigma_{WRS,AXIAL}$	Maximum remaining axial weld residual stress
σ_y	Yield stress, yield strength
σ_1	Maximum principal tensile stress
σ^2	Overall variance in heuristic method

Abbreviations

API	American Petroleum Institute
ASME	American Society of Mechanical Engineers
BG	BeräkningsGrupp
BS	British Standard
BWR	Boiling water reactor

EFPY	Effective full power year
FEA	Finite element analysis
FEM	Finite element method
IGSCC	Intergranular stress corrosion cracking
IHSI	Heating stress improvement
IWM	Fraunhofer-Institut für Werkstoffmechanik
JAEA	Japan Atomic Energy Agency
LBB	Leak-before-break
LC	Load cycle
LCS	Load cycle sequence
LLNL	Lawrence Livermore National laboratory
LOCA	Loss-of-coolant-accident
LWR	Light water reactor
MIG	Metal inert gas welding
MSIP	Mechanical stress improvement process
NPP	Nuclear power plant
ORNL	Oak Ridge National Laboratory
PFM	Probabilistic fracture mechanics
PNNL	Pacific Northwest National Laboratory
PWHT	Post weld heat treatment
PWR	Pressurised water reactor
PWSCC	Primary water stress corrosion cracking
RPV	Reactor pressure vessel
RS	Residual stress
SAW	Submerged arc welding
SCC	Stress corrosion cracking
SINTAP	Structural Integrity Assessment Procedures for European Industry
SMAW	Shielded metal arc welding
SO	Start of operation
SS	Stainless steel
SSM	Strål Säkerhets Myndigheten (Swedish Radiation Safety Authority)
TIG	Tungsten inert gas welding
TVO	Teollisuuden Voima Oyj
USNRC	U.S. Nuclear Regulatory Commission
VSR	Vibratory stress relief
VTT	Technical Research Centre of Finland
VYR	State Nuclear Waste Management Fund (Valtion Ydinjätehuoltorahasto)
WCL	Weld centre line
WOL	Weld offset line
WRS	Weld residual stress

1 Introduction

Firstly, this report presents a literature study concerning computation procedures for the relaxation of the welding process induced residual stresses in steel components. The applicability of the covered procedures for Nuclear power plant (NPP) components under operation is also discussed. Secondly, the performed numerical simulations concerning WRS distributions and their behaviour under cyclic loading are presented, as well as are uncertainties and probabilistic aspects associated with assessing WRS distributions.

This study represents the results concerning the third year, i.e. 2009, of a research project spanning four years, i.e. 2007 – 2010. A literature study concerning various commonly used WRS definition procedures was carried out in the first project year in 2007, see ref. [1]. In that study seven different WRS definition procedures were presented, reviewed and compared against each other for a representative set of application examples concerning NPP reactor circuit piping welds. During the second project year 2008 it was studied with numerical simulations how the WRSs alter over the years in plant operation in primary circuit component welds due to various typical/anticipated transient load cases. The target of application was from a Finnish Boiling Water Reactor (BWR) unit. With such stress results, it was then examined what is their impact to the corresponding simulated crack growth rates. In the latter analyses a fracture mechanics based analysis tool was used.

The present study continues the work of the previous parts of the project. Here the emphasis is on a literature study concerning various WRS relaxation assessment procedures for NPP component welds. Also numerical simulations of WRS distributions were carried out with the same FEM model as was used in 2008, i.e. that consisting of a safe-end connecting to a nozzle and pipe. The scope of the analyses was extended so that here it was examined how the WRS distributions in the safe-end/pipe joint weld region behave under constant cyclic loading. Several load cycle sequences with different load amplitudes covering loading conditions ranging from moderate to relatively severe were considered. Based on obtained FEM simulation results analytical expressions for assessment of WRS relaxation were formed. Also uncertainties and probabilistic aspects of WRS distributions are considered in this study.

As compared to the work plan, due to time resource limitations one topic was postponed to be covered in the next part of the project. This topic concerns for crack growth analysis procedures a parametric study in which it is clarified based on existing world-wide and/or TVO crack data, what should the WRS distributions be like, so that the crack growth analysis results would correspond to existing crack data. Here it is assumed that the available material and process condition specifically constant crack growth formula parameters are defined realistically/correctly. Analysis code VTTBESIT, which is based on fracture mechanics and is partly developed at VTT, will be used in the involved crack growth analyses. Also, applicable existing crack data for these analyses remains to be obtained. The challenge here is to find such data which includes also the duration of the crack growth process, starting from a relatively early stage (sufficiently close to nucleation) up to the time of detection.

After this introductory chapter, the conditions/treatments that can relax the relatively high WRSs are described in Chapter 2. These conditions/treatments include irradiation effects, thermal effects and mechanical load effects.

Chapter 3 concerns the selection of the suitable WRS definition procedures for structural integrity analyses. Applicability of commonly used WRS definition procedures for numerical simulations is discussed first. Comparison of seven commonly used WRS definitions as applied for a representative selection of NPP piping components is presented then. One purpose for this is to have a starting point for WRS relaxation simulations, which are covered further in the study. Namely, the approach for obtaining the WRS distribution data used in the simulations is presented here.

Chapter 4 presents the discovered residual stress relaxation assessment procedures. These are the main results of this study. Altogether 25 different WRS relaxation assessment procedures were found as a result of an extensive survey covering a great number of sources of information, including the major technical scientific journals, with tracing of cited references in each new article as it was obtained, as well as conference papers, academic theses, dissertations, handbooks and technical reports, both from libraries in paper format and from Internet databases.

Chapter 5 describes the uncertainties and probabilistic aspects of WRS distributions. The uncertainties concerning WRS distribution definitions are discussed first. Next a selection of currently applied probabilistic methods to define the WRS distributions is presented. The treatment of WRSs in some notable current probabilistic crack growth analysis codes is described then.

The above mentioned FEM simulations of WRSs in the safe-end/pipe joint weld region are described in Chapter 6. This includes describing the needed analysis input data and the FEM model, and presenting the analysis results. The analyses cover eight loading histories, each including a constant amplitude load cycle sequence, and together spanning a representative range of loading conditions. Here are also presented the analytical expressions for the assessment of WRS relaxation, as developed within this study.

Chapter 7 presents discussion and suggestions for further research.

Finally, conclusions concerning the whole study are presented in Chapter 8.

2 WRSs and their mechanical relieving

2.1 Introduction to WRSs

Assessment of the structural integrity of critical components and structures in NPPs is of remarkable importance for safe operation. When assessing the structural integrity of a component, both the loading and the load-carrying capacity are determined. The WRSs are included in the analysis on either the loading or capacity side, depending on the design strategy.

Since WRSs with various magnitudes and distributions are present in virtually all structurally engineered components, there is a demand for accurate assessment of the WRS distributions, especially in critical components. The residual stress distributions present in a structure are the result of the manufacturing history and the elastic-plastic properties of the structure. The former referring to the mechanical and thermal processes executed during the whole production sequence and the latter to the elastic-plastic behaviour of the structure. Because the elastic-plastic properties influence the severity and distribution of the WRSs, it follows that a structure comprised of several materials will experience the development of the WRSs in a completely different way than one made of a single material.

Depending on the importance of the WRSs, different approaches have been introduced for the assessment of the structural integrity. In structures where the effect of the WRSs on the performance is limited or small, the assessment of the WRSs is of less importance. On the other hand, in the structures where their integrity is of remarkable importance for their reliability, such as NPP primary circuit components, a thorough and accurate assessment of the WRS state is of primary concern. NPPs are typically concerned with manufacturing and managing components which are strongly regulated by national and/or international technical guidelines, standards and design codes to ensure reliable operation.

WRSs are defined as static mechanical stresses that are present in a thermodynamically (and mechanically) closed system of equilibrium. In a more general way, WRSs are mechanical stresses that exist in a component without any external applied mechanical or thermal loads. A direct consequence of the definition is that all internal forces and moments resulting from the WRSs of a system are in mechanical equilibrium. The size of the considered system determines the type of the WRSs that are assessable.

Another consequence of the above mentioned definition is that the internal stresses induced by thermal transients are outside the scope of the WRSs, as they do not represent closed systems. Such load transients are typical for uneven cooling during heat treatments and thermal in-service loads. However, the thermal transients can relax WRSs, when the yield strength is exceeded locally and plastic flow occurs.

The mechanical properties that govern the formation of WRSs are primarily the modulus of elasticity and the strain hardening coefficient. For a work hardening material the WRSs are completely different than for a work softening one. Thus, a mismatch in strain hardening capabilities in adjoining materials, with otherwise similar elastic properties, induces local plastic deformation in the weaker material.

Manufacturing of welded structures in NPPs is carried out with traditional methods for which there is considerable welding experience. The methods are shielded metal arc welding (SMAW), tungsten inert gas welding (TIG) and submerged arc welding (SAW). However, metal inert gas welding (MIG) is generally not used due to a higher risk for lack of fusion. Manufacturing of clad structures is a time consuming process, and therefore it is mostly done with SAW. Other methods have also been used, though less frequently. Butt welding of pipes, on the other hand, is made with TIG.

Regardless of the welding method used, the material properties of the welds and the structural materials affect the formation and distribution of WRSs. The resulting WRS state in a welded component is determined by welding related parameters and geometrical constraints. The former refers to the local shrinkage, quench and phase transformations resulting from the localised thermal cycle. The latter is dealt with through the unbalance in material properties of dissimilar metal welds, and the constraining effect of the surrounding structure.

The components of primary interest in NPPs often have a bi-metallic or dissimilar metal structure, where the mechanical properties of the joined materials are different, and thus add to the formation of the WRSs. However, in most cases NPP primary circuit welds are similar, i.e. same materials are joined in a weld.

2.2 On the conditions/treatments that relieve WRSs in NPP components

In the assessment of the WRS distributions in NPP components, the possible relaxation of them by post processing or during service operation is necessary to be taken into account.

Before considering computation procedures for the relaxation of the WRSs in NPP components, the conditions/treatments that relieve WRSs are first described briefly. Thus one gains a better understanding of the physical reality which WRS relaxation computation procedures attempt to capture.

It is a generally known fact that there are three primary sources for WRS redistribution or relaxation. These are described in the following.

2.2.1 Irradiation effects

The first source of WRS relaxation is related to irradiation effects, which have been studied for several stainless steels and nickel-base alloys. The results showed that exposure to a high neutron fluency level corresponding to over ten Effective Full Power Years (EFPY) causes the WRSs to relax by 30 % [13].

However, in practise irradiation is not used to relax the WRSs in components. Besides NPP reactor pressure vessel (RPV) and its internals, the scale of irradiation to other metallic NPP components is so low, that its effects to physical/material properties are practically negligible [14].

2.2.2 Thermal effects

The second source of WRS relaxation is related to thermal effects. It is well known that prolonged holding or operating times at elevated temperatures cause WRSs to relax. If a specimen of pure metal is annealed at a temperature of 50 % of its melting or solidus temperature, and then cooled down to room temperature, almost total relaxation of the residual stresses arising from forming, machining, heat treatment or joining operations can be achieved. The necessary annealing time depends essentially on the specimen dimensions and the material state. Residual stress relaxation by annealing is brought about by thermally activated processes, for which the annealing temperature and the annealing time are interchangeable within certain limits [47]. In order to achieve comparable residual stress relaxation at a lower annealing temperature, the annealing time must be increased correspondingly. Thermal residual stress relaxation is fundamentally affected by the residual stress state itself and by the material state [15, 16].

At the BWR operating temperature of 286 °C the time dependent relaxation of WRSs due to creep is of very moderate scale. Even though the operating temperature of a Pressurised Water Reactor (PWR) is approximately 50 °C higher than that of a BWR, the thermal relaxation effects still remain small. Relaxation of the WRSs requires higher temperatures, where the yield strength drops below the WRS and plastic flow occurs.

A controlled reduction in the magnitude of the WRSs is obtained when applying a post weld heat treatment (PWHT) to the component. The treatment time and temperature are primarily determined by the involved alloys [17]. Besides complete PWHT, also annealing at approximately 450 °C, which has been done for many NPP components, has an impact on the WRSs. The effect is caused by reduction in tensile WRS at the elevated temperature.

2.2.3 Mechanical load effects

The third source of WRS relaxation is associated with static or cyclic mechanical load applied to the component to cause local plastic yielding, which redistributes/relaxes the residual stresses. In case of static loading the relaxation occurs when a critical loading value is exceeded and a directed dislocation movement converts the elastic strain associated with the macro residual stress into micro plastic strain. Whereas in case of cyclic loading it is the critical stress amplitude that is to be exceeded and the dislocation movement leading to relaxation progresses cyclically but is otherwise the same as for static load.

Concerning cyclic loading, many studies have shown that the effect of macro residual stresses decreases with increasing stress amplitude and growing number of cycles as a result of residual stress relaxation, see e.g. refs. [15, 16]. This is illustrated in Figure 2.2.3-1 for quenched and tempered AISI 4140 steel specimen in a shot-peened condition that has undergone a push/pull fatigue test. More specifically, this figure shows the altering of the shot-peening induced residual stresses at the surface, σ^s [MPa], as a function of the number of cycles, N [-]. The residual stress values are strongly reduced in the first cycle. After that a stress range specific linear dependency between the residual stresses and the number of load cycles prevails. Repeated cyclic loading can also cause gradual changes in the residual stresses over time, even if no single fatigue cycle induces local yielding [19].

The above mentioned shot-peening is a surface treatment, thus affecting mainly/only the residual stresses in the component surface layers. With this treatment it is attempted to create a beneficial compressive residual stress distribution to the component surface layers, leading

e.g. to prolonged fatigue life [20, 21, 22]. As compared to shot-peening vibratory stress relief (VSR) introduces energy into the whole of the metallic component by means of vibrations. The applied vibration energy reorganizes the crystalline atomic structure, relieving residual stresses and stabilizing the piece, without distortion [23, 24, 25, 26]. Based on the weight of the piece, the VSR method introduces into it high amplitude and low frequency vibrations for a given period of time, typically within the scale of tens of minutes. This relieves residual stresses without distortion or alteration of tensile strength, yield point or resistance to fatigue, and the static equilibrium is restored. The most efficient vibrations are the resonant ones, because in the resonance frequency vibrations stresses are better distributed, if compared with sub-resonant frequency.

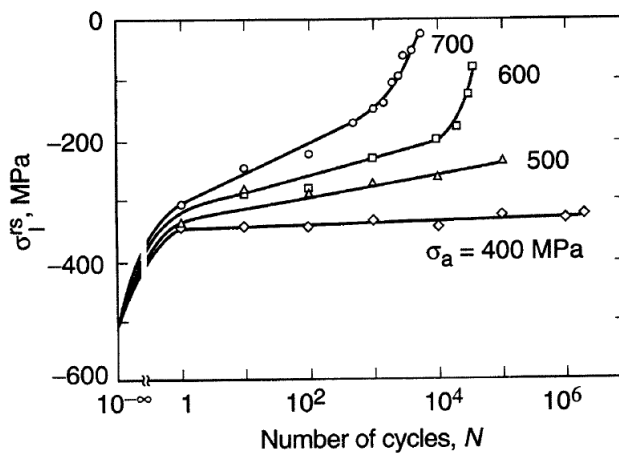


Figure 2.2.3-1. For quenched and tempered AISI 4140 steel specimen in a shot-peened condition that has undergone a push/pull fatigue test, the altering of residual stresses at the surface, σ^{fs} [MPa], as a function of the number of cycles, N [-], for a selection of applied stress amplitudes σ_a [MPa], see ref. [18].

3 On the selection of suitable WRS assumptions for structural integrity analyses

Based on the measurement data from experiments concerning the relaxation of the WRSs, analysis models have been developed to capture this effect. In addition to collection of and discussion concerning analytical WRS relaxation computation procedures, one object in this study is to examine with numerical simulations how repeated mechanical loads affect the local WRS maximum and overall levels.

To have a starting point for WRS relaxation simulations, the as-welded state WRSs need to be assessed first. Those are obtained from the selection of the current notable WRS definition procedures for steel components covered in ref. [1]. In the following, the applicability of these WRS assumptions for numerical simulations is assessed first. Then they are compared against each other by applying them to a set of representative NPP piping components. In this connection also the input data treatment approaches of these definition procedures are briefly described and compared against each other. The results from the WRS assumption application comparisons presented then are a revision of the corresponding ones presented in ref. [1]. The motivation to carry out this revision was to provide a more practical set of as-welded state WRS distribution examples and starting points than the more parametric WRS assumption application examples in ref. [1]. Namely, the WRS distribution definitions found from the fitness-for-service procedure collections and handbooks almost invariably base their formulas to material yield strength, and separate formula sets are typically given for austenitic and ferritic steels. In ref. [1] one value for material yield strength was selected as a starting point, corresponding more to an austenitic stainless steel, and it was used as such as part of the input data when applying WRS distribution formulas both for austenitic and ferritic steels. In the present study two actual NPP piping component materials are chosen, being an austenitic stainless steel and a ferritic steel, and in the ensuing WRS distribution formula applications their material yield strengths are also used with recommended correction factors, where necessary. Furthermore, the limitations of use of the covered WRS distribution definitions, a subject which was mainly omitted in the application examples in ref. [1], are taken fully into account here.

3.1 Applicability of current notable WRS definitions for numerical simulations

The WRS procedures considered here are: the ASME recommendations [2, 3], the British Standard BS 7910: 1999 [4], the R6 Method, Revision 4 [5], the SSM handbook [6], the SINTAP Procedure [7, 8], the API 579 Procedure [9] and the FITNET Procedure [10]. The covered WRS type here is as-welded state. The SSM handbook [6] is an updated and expanded version of the earlier SAQ handbook [11], which was used in ref. [1]. Otherwise the same WRS definition procedures were covered here as in ref. [1].

The WRS definitions in the mentioned procedures are based both on the available experimental data and FEM analysis results. In some older ones of the mentioned WRS procedures, uniform distributions have conservatively been defined to WRSs for some cases

due to lack of data, e.g. those given for parallel to weld for austenitic stainless steel for pipe-to-pipe welds in ASME recommendations [2, 3].

The published experimental WRS data have a substantial scatter. Consequently the defined WRS distributions have been developed as tensile upper bound solutions based on the data. However, according to [86, 87, 88, 89], this approach not only lacks consistency for the same type of joints and welding parameters, but can either significantly overestimate the WRS level in some cases, or underestimate it in others.

Over the last decade or so, WRSs have received increasing attention in the pressure vessel and piping research community. The driving force for this interest can be attributed to the fact that application of modern structural integrity assessment procedures for defective welded components, e.g., the British Standard BS 7910: 1999 [4], R6 Method, Revision 4 [5], SINTAP Procedure [7, 8], API 579 Procedure [9] and FITNET Procedure [10], require considerably more input data on the WRS state to give a more realistic assessment. The conventional approach for characterising a WRS profile has been to adopt a tensile upper bound solution, as mentioned above. All WRS procedures covered here base their definitions on material yield strength, so that typically the maximum tensile WRS values are of the scale of yield strength in and near the inner weld surface. The variation of the yield stress values within the typical operational temperature range in light water reactor (LWR) NPP piping systems, being approximately from 20 to 330 °C, is of the scale of 10 %. According to most of the covered WRS assumption procedures, for austenitic NPP piping stainless steels (SSs) the stress values at 1.0 % strain should be used for yield strength, whereas for corresponding ferritic steels the stress values at 0.2 % strain should be used, respectively.

The mentioned seven WRS definition procedures provide a range of approaches to define the WRS distributions. In older WRS procedures, such as ASME recommendations [2, 3], only one approach in the form of a few simple functions is given, whereas in the more recent WRS procedures, such as R6 Method Rev. 4 [5] and FITNET Procedure [10], a selection of levels for defining WRSs are presented, ranging from coarse level 1 definitions giving single values, to level 2 with WRS definitions as analytical functions, to subtle and computationally laborious level 3 approaches, requiring e.g. the use of advanced non-linear 3D FEM analysis tools. Depending on the needed accuracy and available resources, one can choose which WRS procedure and level to apply. In general, the WRS distributions are defined in all of the mentioned seven procedures also (or only) with analytic functions, such as polynomials and exponent function. On the behalf of the more recent WRS assumption procedures, these correspond to level 2 definitions. Separate definitions are typically given for austenitic and ferritic steels, weld types and weld wall thickness ranges. Also, overall validity ranges are given in most procedures for WRS definitions, as a function of e.g. weld wall thickness and yield strength.

One unfortunate departure from realism in case of some of the more recent WRS assumption procedures, e.g. R6 Method Rev. 4, API 579 and FITNET, is that in the transverse to weld direction the WRSs are mostly not self-balancing. While making local crack growth calculations with a fracture mechanics based analysis tool this feature may not pose remarkable problems, but in case of corresponding 3D FEM analyses it is quite the other way around, as in order to achieve equilibrium FEM automatically modifies the WRSs towards self-balanced distributions over the component model walls, and thus the original WRS distributions are not maintained.

In the light of the present WRS assumption application results for cases concerning austenitic SS, only ASME recommendations and SINTAP procedure in all cases, and SSM handbook in

most cases, give WRS distributions that are self-balancing in the transverse to weld direction. Of them the least over conservative WRS assumption procedure appears to be SINTAP. As for the corresponding analysis results for cases concerning ferritic steel, for Small and Large cross-sections SSM handbook gives self-balancing WRS distributions, whereas for Medium cross-section only SINTAP procedure gives a self-balancing WRS distribution, respectively.

3.2 Comparison of current notable WRS definitions

3.2.1 Input data considerations

Geometry, materials and loads

In this study the WRS distributions are calculated with the above mentioned seven procedures for the same representative small, medium and large NPP reactor circuit pipe cross-sections in a Finnish BWR unit as in ref. [1]. The dimensions of these pipes are:

- Small pipe; outer diameter = 60 mm, wall thickness = 4.0 mm,
- Medium pipe; outer diameter = 170 mm, wall thickness = 11.0 mm,
- Large pipe; outer diameter = 510 mm, wall thickness = 26.0 mm.

For these three pipe sizes the WRS distributions through wall are calculated in both perpendicular and parallel to weld directions. The covered weld condition in the calculations is as-welded state.

The considered materials are austenitic stainless steel SS 2353, which corresponds to steel TP 316L according to U.S. standards, and ferritic steel SS 2301, which corresponds to steel ASTM 405 according to U.S. standards.

Table 3.2.1-1. Some relevant material property values of austenitic stainless steel SS 2353 as a function of temperature [12].

Temperature [°C]	Young's modulus [GPa]	Yield strength [MPa]	Tensile strength [MPa]
20	198	210	515
286	176	125	412
Temperature [°C]	Coefficient of thermal expansion [$10^{-6}/K$]	Thermal conductivity [W/mK]	Specific heat [J/kgK]
20	16.5	13.5	440.0
286	18.0	17.4	537.2

Table 3.2.1-2. Some relevant material property values of ferritic steel SS 2301 as a function of temperature [12].

Temperature [°C]	Young's modulus [GPa]	Yield strength [MPa]	Tensile strength [MPa]
20	225	250	540
286	204	184	540
Temperature [°C]	Coefficient of thermal expansion [$10^{-6}/K$]	Thermal conductivity [W/mK]	Specific heat [J/kgK]
20	11.0	23.5	460.0
286	11.4	25.3	557.2

In the two tables above the yield strength corresponds to the stress value at strain of 0.2 % in the stress-strain curve. As the stress values at strain of 1.0 % are not available, first approximation approaches recommended in the WRS procedure documentations to obtain them were resorted to.

Due to often lacking more specific weld material data a commonly followed approach to use the material property data of the adjacent base material for the structural integrity analyses of the weld as well is also followed here.

The pressure and temperature are set to 7.0 MPa and 286 °C in all calculations, corresponding to normal operation conditions in Finnish BWR NPP units. The evenly through wall distributed axial and circumferential stress components corresponding to pressure were calculated with analytical expressions for thin walled cylindrical shells.

Treatment of yield strength according to covered WRS definition procedures

The treatment of material yield strength according to the covered WRS definition procedures is described here in more detail. This is because all other WRS definition procedures covered here besides the ASME recommendations [2, 3] base their WRS formulas to the material yield strength. To clarify the issue more, this means that the yield strength linearly scales the WRS values calculated with these formulas. For instance, increasing the used yield strength value with a factor of two would provide the same effect to the resulting WRS distribution values. Corresponding decrease effect results when using lower yield strength value. The treatment and selection of yield strength values holds importance also in regard of considered temperature, as yield strengths of various steel types are all temperature dependent. Examples of this are the yield strength data for the selected austenitic and ferritic steels as presented in Tables 3.2.1-1 and 3.2.1-2. When comparing yield strength values at room temperature 20 °C and normal operation temperature of 286 °C, for the selected austenitic steel the value at the latter temperature is 59.4 % of that in the former temperature, whereas for the selected ferritic steel this ratio is 73.4 %, respectively.

According to the covered WRS definition formulas the treatment of material yield strength, as obtained from the results of uniaxial tests or applicable material standards, is as follows:

- ASME recommendations [2, 3]; yield strength not included in the WRS formulas,
- the British Standard BS 7910: 1999 [4];
 - both in WRS formulas for austenitic and ferritic steels the stress to be used as yield strength is that corresponding to 0.2 % strain,
 - concerning the associated temperature range when selecting the yield strength value to be used, no information is given regarding what temperature it is assumed to correspond to,
- the R6 Method, Revision 4 [5];
 - in WRS formulas for ferritic steels the stress to be used as yield strength is that corresponding to 0.2 % strain,
 - in WRS formulas for austenitic steels the stress to be used as yield strength is that corresponding to 1.0 % strain, and if no actual stress-strain data is available it is assumed that as a first approximation 1.5 times the stress corresponding to 0.2 % strain can be used as that for the stress corresponding to 1.0 % strain,
 - concerning the associated temperature range when selecting the yield strength value to be used, it is assumed to correspond to room temperature,

- the SSM handbook [6];
 - for ferritic steels the stress to be used as yield strength in WRS formulas is that corresponding to 0.2 % strain,
 - for austenitic steels the stress to be used as yield strength in WRS formulas is that corresponding to 1.0 % strain, and if no actual stress-strain data is available, as a first approximation 1.3 times the stress corresponding to 0.2 % strain can be used as that for the stress corresponding to 1.0 % strain,
 - concerning the associated temperature range when selecting the yield strength value to be used, it is assumed to correspond to each temperature in the material temperature history, as caused by the analysis case in question,
- the SINTAP Procedure [7, 8];
 - in WRS formulas the stress to be used as yield strength for ferritic steels is that corresponding to 0.2 % strain,
 - in WRS formulas the stress to be used as yield strength for austenitic steels is that corresponding to 1.0 % strain, and if no actual stress-strain data is available, as a first approximation 1.5 times the stress corresponding to 0.2 % strain can be used as that for the stress corresponding to 1.0 % strain,
 - concerning the associated temperature range when selecting the yield strength value to be used, it is assumed to correspond to that temperature in which it reaches the maximum value over the temperature history of the analysis case in question,
- the API 579 Procedure [9];
 - for both ferritic and austenitic steels the stress to be used as yield strength in WRS formulas is the sum of that corresponding to 0.2 % strain and 69 MPa,
 - concerning the associated temperature range when selecting the yield strength value to be used, it is assumed to correspond to each temperature in the material temperature history, as caused by the analysis case in question,
- the FITNET Procedure [10];
 - in WRS formulas for ferritic steels the stress to be used as yield strength is that corresponding to 0.2 % strain,
 - in WRS formulas for austenitic steels the stress to be used as yield strength is that corresponding to 1.0 % strain, and if no actual stress-strain data is available it is assumed that as a first approximation 1.5 times the stress corresponding to 0.2 % strain can be used as that for the stress corresponding to 1.0 % strain,
 - concerning the associated temperature range when selecting the yield strength value to be used, it is assumed to correspond to room temperature.

The main reason for selecting the yield strength value for austenitic steels as the stress corresponding to 1.0 % strain is the relatively large work hardening part of the stress-strain curves associated with this material type. Typically the tensile strength for austenitic steels is of the scale of two times higher than the stress corresponding to the 0.2 % strain. Whereas in case of ferritic steels, typically the work hardening part of the stress-strain curves associated with this material type is relatively moderate, so that there is a somewhat distinctive difference in the path of the stress-strain curve before and after approximately 0.2 % strain point.

Validity ranges for as-welded state residual stresses for steels

The validity ranges of application concerning the as-welded state WRS assumptions for steels vary between the covered procedures, and not all of them give specific information concerning this issue in the associated documentations.

To begin with the WRS distribution assumptions given in the ASME recommendations [2, 3], their use is limited to austenitic SS welds. Also, no validity range limitations concerning the wall thickness are given.

For the WRS distribution assumptions in the British Standard BS 7910: 1999 [4], R6 Method, Revision 4 [5], SINTAP Procedure [7, 8] and FITNET Procedure [10], their validity range of use is given in Table 3.4-1 in the following.

Table 3.4-1. Validity ranges for as-welded WRS definitions for piping component profiles. For WRS distributions in the R6 Method, Revision 4 [5] and FITNET Procedure [10] these limitations concern only ferritic steels, whereas for the British Standard BS 7910: 1999 [4] and SINTAP Procedure [7, 8] they concern both austenitic and ferritic steels.

Geometry	Thickness [mm]	Yield strength [MPa]	Electrical heat input per unit length [kJ/mm]
Pipe circumferential butt welds	9 - 84	225 - 780	0.35 - 1.9

As for the WRS distribution assumptions in the API 579 Procedure [9], it is mentioned that they apply as such both to welded joints located in equipment that has been in-service, as well as to new constructions. Also, a distinction is not made concerning the material of construction. The WRS assumptions in API 579 are mainly intended for welds associated with base materials of ferritic steel. However, it is currently assumed that stainless steel welds can be assessed with equal accuracy using these WRS distribution equations. No validity range limitations concerning the wall thickness are given.

As for the WRS distribution assumptions in the SSM handbook [6], the following information concerning their range of applicability is given. The WRS distributions are recommendations based on numerical investigations on austenitic stainless steel pipes. They are valid for a inner radius to thickness ratio of approximately 8 but can conservatively be used for profiles with higher value for this ratio. The validity range of heat input relative to the pipe thickness is from 75 to 101 MJ/m². The validity range concerning wall thickness is up to 40 mm, and for pipe wall thickness greater than this the WRS recommendations should be conservative.

Also, for the time being the SSM handbook [6] is the only one of the covered WRS definition procedures that provides WRS distributions for a selection of dissimilar weld types as well. These are applicable to e.g. dissimilar welds connecting ferritic RPV nozzles to safe-ends of stainless steel.

3.2.2 WRS definition comparison results

The comparison of the covered WRS definitions, namely those in the ASME recommendations [2, 3], the British Standard BS 7910: 1999 [4], the R6 Method, Revision 4 [5], the SSM handbook [6], the SINTAP Procedure [7, 8], the API 579 Procedure [9] and the

FITNET Procedure [10], for a representative selection of NPP piping welds is described in this section.

WRSs defined with the above mentioned seven procedures were calculated for three pipe sizes in this study, which are presented in Section 3.2.1. These sizes were taken to correspond to representative small, medium and large pipes in Finnish BWR NPP piping systems, respectively, and they were provided by a representative from TVO [27], which is gratefully acknowledged. The considered two NPP piping materials are austenitic stainless steel SS 2353, and ferritic steel SS 2301, as mentioned earlier. For both of these materials the needed material property data are presented in Section 3.2.1. As full stress-strain curves for the considered materials were not available, the earlier mentioned treatments for yield strength values were resorted to. Also the earlier mentioned procedure specific validity ranges for WRS assumptions were taken into account here.

For the three considered pipe sizes the as-welded state WRS distributions through wall were calculated in both perpendicular and parallel to weld directions. The results are presented in the following Figures 3.2.2-1 to 3.2.2-6. These results are an update to those presented in ref. [1], as mentioned earlier. In the result figures, t_{wall} [mm] in the horizontal axis is the radial coordinate through pipe wall with origin on the inner surface. In the figure legends, “Au” in the end of WRS procedure name means that the curve in question is for austenitic stainless steel SS 2353, correspondingly “Fe” in the end of procedure name means that the curve in question is for ferritic steel SS 2301. Also, the presented computation results correspond to WRS distributions through the weld centre line.

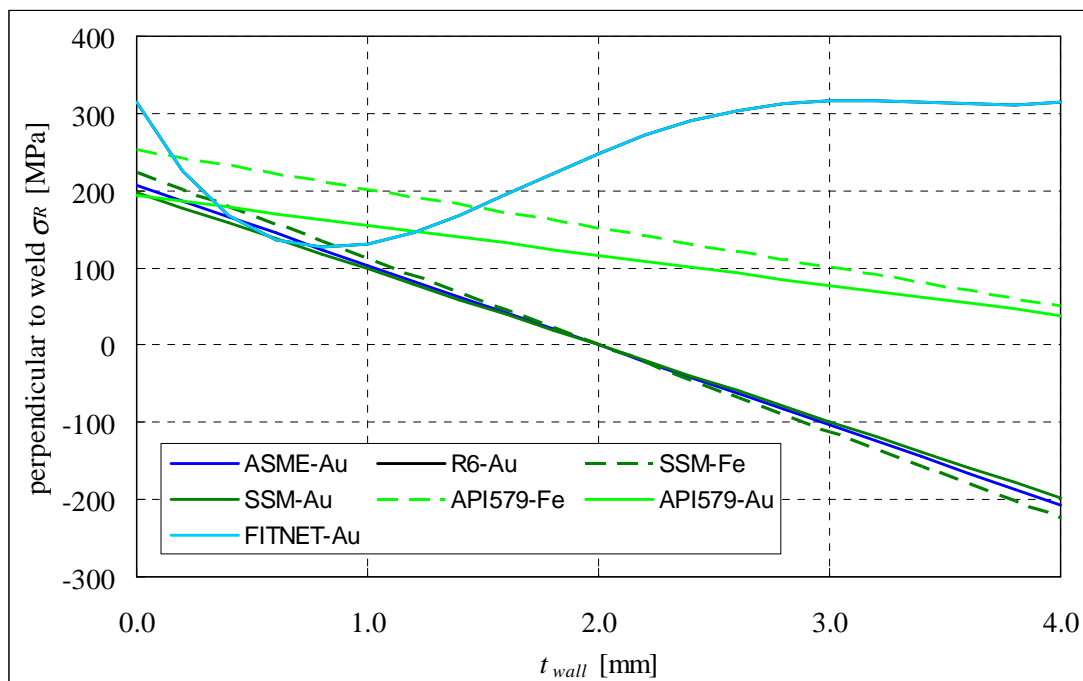


Figure 3.2.2-1. As-welded state WRS distributions in weld centre line and perpendicular to weld for the Small pipe, calculated with the seven covered WRS procedures. Here for FITNET, R6 Rev. 4, BS 7910: 1999 and API 579 procedures, low heat input was conservatively used. Here the wall thickness was not within the covered validity range in case of some/all WRS formulas of FITNET, R6 Rev. 4, BS 7910: 1999 and SINTAP procedures.

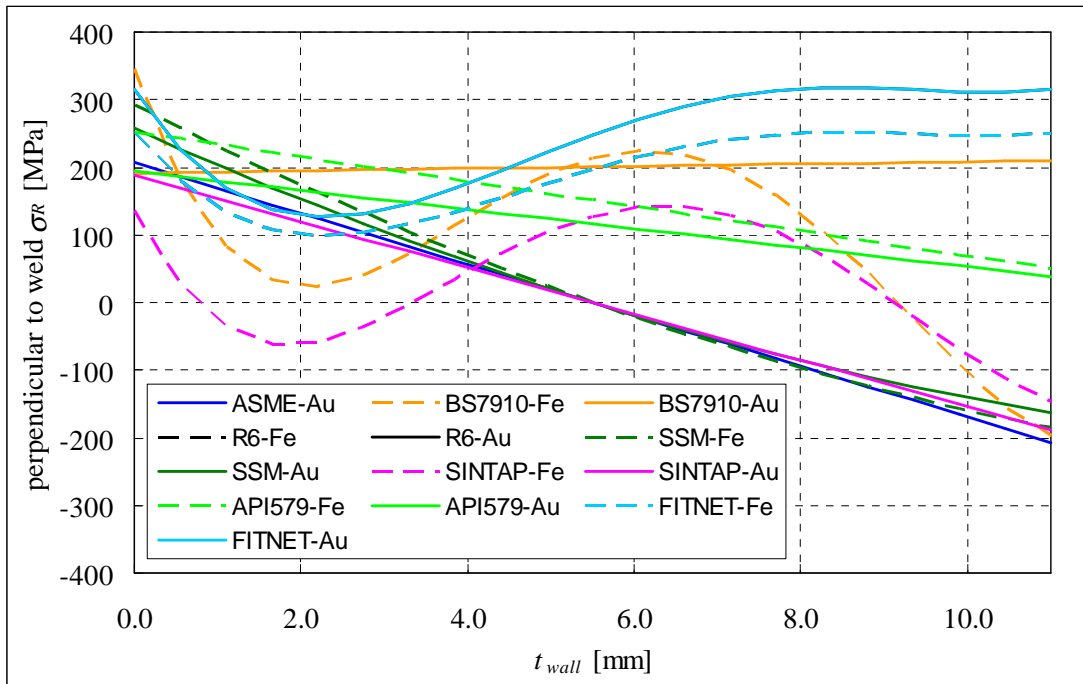


Figure 3.2.2-2. As-welded state WRS distributions in weld centre line and perpendicular to weld for the Medium pipe, calculated with the seven covered WRS procedures. Here for FITNET, R6 Rev. 4, BS 7910: 1999 and API 579 procedures, low heat input was conservatively used.

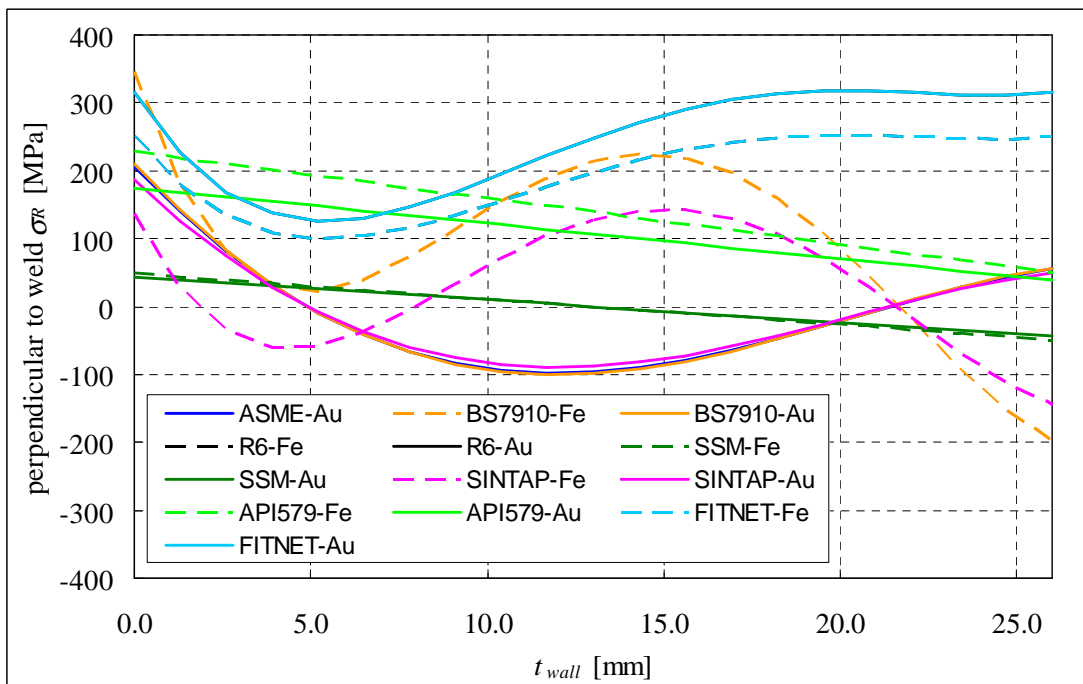


Figure 3.2.2-3. As-welded state WRS distributions in weld centre line and perpendicular to weld for the Large pipe, calculated with the seven covered WRS procedures. Here for FITNET, R6 Rev. 4, BS 7910: 1999 and API 579 procedures, low heat input was conservatively used.

conservatively used.

Concerning the discussion of the results in the following it should be kept in mind that in the considered temperature of 286 °C the 0.2 % strain yield strengths for the considered austenitic stainless steel and ferritic steel are 125 and 184 MPa, respectively.

As can be seen from Figures 3.2.2-1 to 3.2.2-3, the WRS distributions through wall and perpendicular to weld in as-welded state, as calculated for the three examined pipe sizes with the covered WRS definition procedures, differ quite much from each other. Near and in the inner surface the WRS values vary approximately between 50 to 350 MPa of tension, where the highest values are given by the R6 Method, Revision 4 [5] and FITNET Procedure [10]. Correspondingly, the lowest WRS values are mostly given there by the SSM handbook [6] and SINTAP Procedure [7, 8], respectively. Also elsewhere within the weld wall and in the outer surface the R6 Method, Revision 4 [5] and FITNET Procedure [10] give the highest WRS values, staying through wall clearly in tension, whereas in case of all other WRS procedure definitions besides the API 579 Procedure [9] the WRS distributions turn to compression, reaching its maximum at the outer surface. Thus in axial direction self-balancing WRS distributions are provided by these latter WRS definition procedures. In all cases the R6 Method, Revision 4 [5] and FITNET Procedure [10] give identical results. None of the covered WRS assumption procedures give values that exceed the material tensile strength, so realism is not violated.

As more than 90 % of the piping crack cases have been oriented circumferentially, see e.g. ref. [98], it is these perpendicular to weld WRSs that play a prominent role in piping component crack growth considerations.

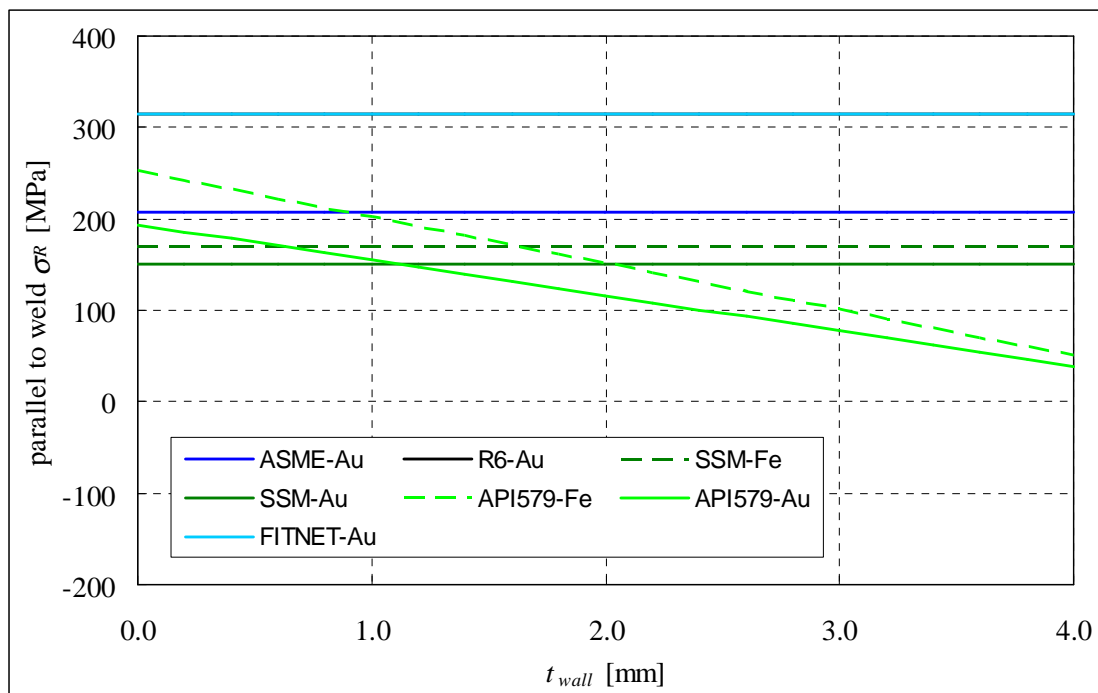


Figure 3.2.2-4. As-welded state WRS distributions in weld centre line and parallel to weld for the Small pipe, calculated with the seven covered WRS procedures. Here the wall thickness was not within the covered validity range in case of some/all WRS formulas of FITNET, R6 Rev. 4, BS 7910: 1999 and SINTAP procedures.

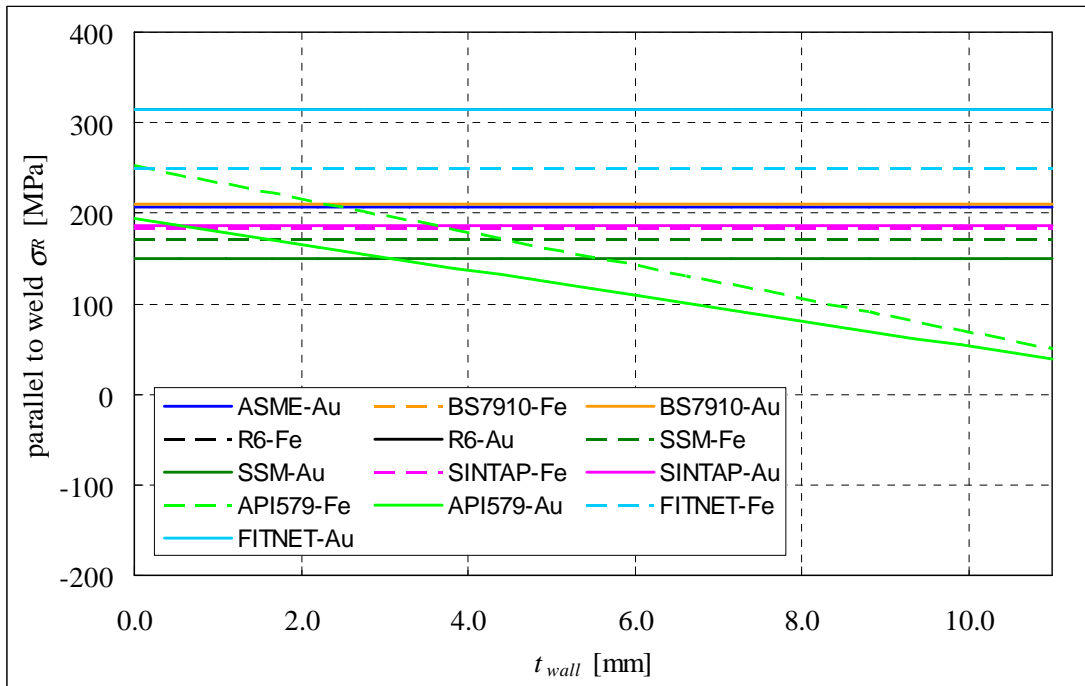


Figure 3.2.2-5. As-welded state WRS distributions in weld centre line and parallel to weld for the Medium pipe, calculated with the seven covered WRS procedures.

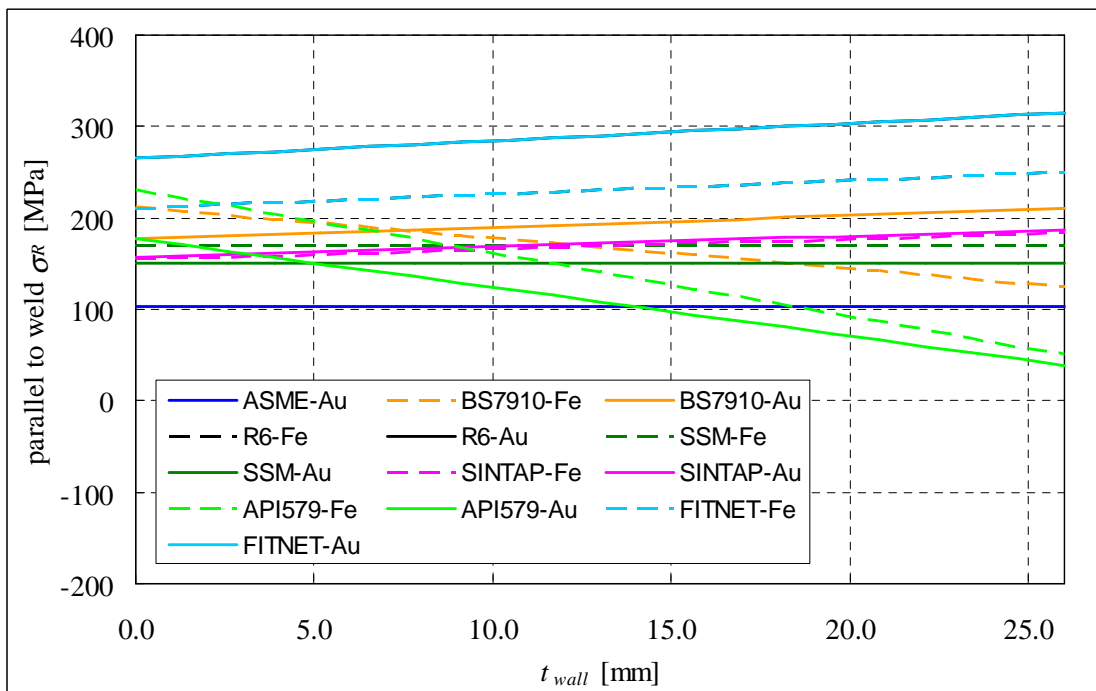


Figure 3.2.2-6. As-welded state WRS distributions in weld centre line and parallel to weld for the Large pipe, calculated with seven different WRS procedures.

Concerning the discussion of the results in the following it should be kept in mind that in the considered temperature of 286 °C the 0.2 % strain yield strengths for the considered austenitic stainless steel and ferritic steel are 125 and 184 MPa, respectively.

As can be seen from Figures 3.2.2-4 to 3.2.2-6, the WRS distributions through wall and parallel to weld in as-welded state, as calculated for the three examined pipe sizes with the covered WRS definition procedures, again differ quite much from each other. Near and in the inner surface the WRS values vary approximately between 100 to 320 MPa of tension, where the highest values are again given by the R6 Method, Revision 4 [5] and FITNET Procedure [10]. Correspondingly, the lowest WRS values are mostly given there by the SSM handbook [6] and SINTAP Procedure [7, 8], respectively. Also elsewhere within the weld wall and in the outer surface the R6 Method, Revision 4 [5] and FITNET Procedure [10] give the highest WRS values. All parallel to weld WRS distributions stay through wall clearly in tension, interestingly only the API 579 Procedure [9] gives WRS distributions that decrease towards the outer surface. In all cases the R6 Method, Revision 4 [5] and FITNET Procedure [10] give identical results. None of the covered WRS assumption procedures give values that exceed the material tensile strength, so realism is not violated.

In the light of the presented application example results, some more general conclusions can be drawn. Apparently the main reason for the R6 Method, Revision 4 [5] and the FITNET Procedure [10] for giving in all cases the highest WRS values is that concerning the associated WRS formulas they require material yield strength value in room temperature to be used. In the temperature of normal BWR operation, yield strength values are considerably lower than those in the room temperature, as described earlier. All other WRS procedure definitions allow the use of yield strength to be considered in the temperature of the analysis case in question. The upper bound approach in forming the WRS definitions applied in most of the covered WRS procedures also considerably adds to the conservative nature of the resulting WRS distributions. This shows especially in case of the British Standard BS 7910: 1999 [4], R6 Method, Revision 4 [5], API 579 Procedure [9] and FITNET Procedure [10], which generally do not give self-balancing WRS distributions in the transverse to weld direction, which is not realistic. Moreover, in the documentations of the R6 Method, Revision 4 [5] and FITNET Procedure [10] it is clearly mentioned that the resulting transverse to weld WRSs may not be, or are not in all cases, self-balancing.

4 Procedures to assess WRS relaxation in NPP Components under operation

This chapter presents the results of the literature study part of this work. When considering the conditions/treatments causing WRS relaxation, which were briefly described in section 2.2, it is mainly the mechanical load effects that the WRS relaxation models attempt to capture. This broadly divides to relaxation due to static mechanical loads and cyclic loads. Thermal effects are important for WRS relaxation too, but they begin to have more pronounced effect mainly in temperatures higher than those encountered in the LWR environments. However, cyclic thermal stresses due to temperature fluctuation are an exception, and it is necessary in most cases to take them into account. Whereas when considering creep for steels, it becomes a matter of technical concern when the operating temperature exceeds about 40 % of the absolute melting temperature of the material, see e.g. refs. [28, 29]. The melting range of SSs varies from approximately 1400 to 1450 °C, while the melting point of ferritic steels is approximately 1540 °C, see e.g. refs. [30, 31]. Thus the threshold temperature for creep to start to affect is for austenitic SSs at lowest approximately 560 °C, and for ferritic steels approximately 615 °C, respectively. Considering irradiation effects to the WRS, of the load bearing NPP components it is the RPV where they have an effect that needs to be taken into account. Outside the RPV the effect of irradiation to load bearing components is negligible.

The structure of this chapter is such that the purpose and scope of the performed literature study are described first. Then the results of the literature study are presented, together with some remarks concerning the compiled WRS relaxation assessment procedures.

4.1 Purpose and scope of literature study

In the following is presented a literature survey of the current understanding concerning residual stress relaxation in metallic components. The survey focuses on the computational residual stress relaxation assessment procedures/models. This includes redistribution and relaxation due to static mechanical load, repeated cyclic loads, fluctuating thermal loads as well as the combination of the latter two loading types. However, residual stress (RS) relaxation due to crack growth is not considered here.

Besides the set of WRS definition application examples presented in Section 3.2, relatively little attention is paid here to the detailed analysis of initial RS states (especially for life enhancement methods that involve substantial changes to the material state) and to the experimental methods used to measure RSs. Both of these topics are large and complex, and were judged to be beyond the scope of the present investigations. Here the RSs both on surface layers and within wall are considered.

The literature survey resulted with a few hundred RS relaxation associated references. However, larger part of them concern various mechanical means and methods of relaxing RSs and less such references were found that also contain any RS relaxation modelling procedures. Computer searches concerning the major technical scientific journals and other significant publication databases were employed widely, in addition to the tracing of cited references in each new article as it was obtained. The literature search was limited to English

language journal articles, conference papers, academic theses, dissertations, handbooks and technical reports that are available to the general public. Articles in other languages as well as academic theses dissertations and technical reports with limited circulation were included only in a few occasions. All found references containing any RS relaxation modelling approach are covered in this survey.

This literature survey is not a definitive critical review. However, reasonable effort was provided to evaluate the relative merits of the different explanations and models proposed. On the other hand, the technical scope of the covered issue was too broad and the available resources too limited to very thoroughly explore every single discovered RS relaxation assessment model. However, those models that after first screening looked to be promising ones concerning the applicability to NPP components, are planned to be examined and evaluated in more detail in the next part of the project. Which is an issue with a variety of aspects to be considered, as most of the found RS relaxation assessment models are developed for other than NPP environments, e.g. for aircraft, vehicle, conventional machinery and offshore structures/components.

The main Internet literature sources/databases not freely available that were used in this study include:

- Science Direct;
 - contains more than 2500 scientific journals and almost ten million articles at early 2010,
 - contains scientific journals in four main categories; Physical Sciences and Engineering, Life Sciences, Health Sciences, and Social Sciences and Humanities,
 - the category mainly containing literature concerning RSs is Physical Sciences and Engineering, and it contains scientific journals in nine sub-categories; Chemical Engineering, Chemistry, Computer Science, Earth and Planetary Sciences, Energy, Engineering, Materials Science, Mathematics, and Physics and Astronomy,
 - more than ten journals containing RS related/associated articles were found,
 - => more than one hundred RS related/associated articles were obtained.

- Compendex/Engineering village;
 - contains more references than Science Direct,
 - does not contain actual articles,
 - => was not used very much as each article/reference had to be obtained from another source, most often purchased,
 - => some tens of RS related/associated articles were obtained.

- ETDEWEB;
 - the name stands for; ETDE World Energy Base,
 - ETDEWEB is produced by the member countries of the Energy Technology Data Exchange (ETDE), an international agreement under the International Energy Agency (IEA),
 - contains over 4246000 literature references and more than 261000 full text documents at early 2010,
 - includes information on energy R&D; energy policy and planning; basic sciences (e.g., physics, chemistry and biomedical) and materials research; the environmental impact of energy production and use, including climate change;

energy conservation; nuclear (e.g., reactors, isotopes, waste management); coal and fossil fuels; renewable energy technologies (e.g., solar, wind, biomass, geothermal, hydro).

4.2 Results of the performed literature study

In this section are presented the results of the performed literature study concerning RS relaxation assessment procedures. This is displayed in the form of three tables, see Table 4.2-1, 4.2-2 and 4.2-3. Then follows a summary of the covered RS relaxation assessment procedures, as presented in Table 4.2-4, showing procedure specifically the necessary input data parameters.

Of all the found residual stress relaxation assessment procedures concerning metallic components, those 25 cases are included here that were deemed to be applicable to NPP components to any extent. This meaning that it appears that the scope of application of various RS relaxation assessment procedures varies substantially, but that even those that show to have even the slightest capability to be applicable to NPP component welds were included here as well. Brief descriptions of the main characteristics of the procedures are given. In addition to the relaxation assessment procedure equations/formulas, also mentioned are the original reference/authors, target of application, required input data, parameters to be fitted, range of applicability and the covered phenomena.

The RS relaxation assessment procedures presented in the following are divided to three categories according to characteristics of the stress relaxing physical phenomena they cover. Within these categories the RS relaxation assessment procedures are presented in chronological order together with some remarks providing background. The mentioned three categories are:

- Mechanical residual stress relaxation; Relaxation of macroscopic residual stresses as well as work hardening can occur with increasing applied stress amplitude and number of load cycles during cyclic deformation at temperatures below creep region, see e.g. ref. [47]. See RS relaxation assessment procedures in Table 4.2-1.
- Thermal residual stress relaxation; Residual stress relaxation at elevated temperatures is caused by thermally activated processes, e.g. creep, see e.g. ref. [47]. Dislocation movement, rearrangement as well as annihilation occur at elevated temperatures and cause the relaxation process. See RS relaxation assessment procedures in Table 4.2-2.
- Thermomechanical residual stress relaxation; Recently, more advanced applications consider cyclic loading at elevated temperatures. Under such conditions mechanical and thermal residual stress relaxations may occur simultaneously. However at present not much information concerning thermomechanical residual stress relaxation exist, see e.g. refs. [59, 60, 61]. Some authors report that under isothermal fatigue loading, thermomechanical residual stress relaxation should be in principle separated into two parts: mechanical and thermal. Nevertheless, thermomechanical residual stress relaxation phenomena are still not completely clear, hence they need to be examined further. See RS relaxation assessment procedures in Table 4.2-3.

Table 4.2-1. Results of the performed literature study concerning mechanical residual stress relaxation assessment procedures, together with brief descriptions of their main characteristics. Here RS means residual stress.

WRS relaxation model formulas and equations	Author(s), ref., year	Target of application	Required input data	Parameters to be fitted	Range of applicability	Considered phenomena
$\frac{\sigma_{mN}}{\sigma_{m1}} = \frac{\sigma_y - \sigma_a}{\sigma_{m1}} - \left(\frac{\sigma_a}{\sigma_y}\right)^b \cdot \log N$ <p style="text-align: right;">(RS Relaxation Eq. 1)</p>	Morrow, Sinclair, [32], 1958	fatigue tests of SAE 4340	σ_{m1} ; mean stress at 1 st cycle, σ_a ; stress amplitude, σ_y ; yield stress, N ; number of load cycles	b ; material and strain range dependent	experimental results support model for; number of load cycles $N < 10^6$	mean RS relaxation due to cyclic mechanical loads
$\sigma^{rs} = \sigma^{rs}(N=1) - \mu \cdot \lg N$ <p style="text-align: right;">(RS Relaxation Eq. 2)</p>	Morrow, Ross, Sinclair, [51], 1960	metallic materials	$\sigma^{rs}(N=1)$; RS value after first load cycle, N ; number of load cycles	μ ; material specific slope parameter linearly dependent on stress amplitude	model covers mainly RS relaxation of metallic materials due to cyclic loading, is valid for number of load cycles $N > 1$	RS relaxation due to mechanical cyclic loading
$\sigma_{RS} = \sigma_{R0} \cdot \exp\left[\frac{-\alpha \cdot N \cdot \Delta \varepsilon_a \cdot \Delta \sigma_a}{\sigma_y}\right]$ <p style="text-align: right;">(RS Relaxation Eq. 3)</p>	Impellizzeri, [48], 1970	notched test specimens of aluminium alloys 7075-T6 and MIL-A-8866	σ_{R0} ; initial RS, σ_y ; yield stress, N ; number of load cycles, $\Delta \varepsilon_a$, $\Delta \sigma_a$; applied strain and stress range at notch root, respectively	α ; material specific empirically determined constant of proportionality, independent of geometry	model combines theoretical concepts and empirical relationships and as such cannot be used with a great deal of confidence for materials, specimen configurations or loading spectra substantially different from those investigated	RS relaxation at notch root due to cyclic mechanical loads

Table 4.2-1. Results of the performed literature study concerning mechanical residual stress relaxation assessment procedures, together with brief descriptions of their main characteristics. Here RS means residual stress. Continued from the previous page.

WRS relaxation model formulas and equations	Author(s), ref., year	Target of application	Required input data	Parameters to be fitted	Range of applicability	Considered phenomena
$\sigma_N^{re} = A + m \cdot \lg N$ <p style="text-align: right;">(RS Relaxation Eq. 4)</p>	Kodama, [35], 1972	shot-peened mild steel specimens	N ; number of load cycles	A, m ; material and stress amplitude dependent	experimental results support model only after first load cycle	surface RS relaxation due to cyclic mechanical loads
$\frac{\sigma_R + K_T \cdot s_m}{\sigma_{R0} + K_T \cdot s_m} = - \frac{\ln[N/(N+K)]}{\ln(1+K)},$ $K = K(\sigma_{rms}, \varepsilon_{rms}, K_T, \sigma_y, C)$ <p style="text-align: right;">(RS Relaxation Eq. 5)</p>	Rotvel, [52], 1972	carbon steel, corresponding to SAE 1064	σ_{R0} ; initial RS, K_T ; notch factor, s_m ; mean nominal stress, σ_{rms} , ε_{rms} ; local root mean square averaged stress and strain, σ_y ; yield stress, C ; clipping ratio, N ; number of load cycles	K ; material specific parameter dependent on mean square averaged stress and strain, notch factor, yield stress and clipping ratio	model arguably applicable for RS relaxation of metallic materials	RS relaxation due to mechanical cyclic loading
$\sigma_{mN} = \sigma_{m1} \cdot (N)^B$ <p style="text-align: right;">(RS Relaxation Eq. 6)</p>	Jhansale, Topper, [33], 1973	ductile structural metals, mild steels	σ_{m1} ; mean stress at 1 st cycle, N ; number of load cycles	B ; material softening and strain range dependent	model is based on experimental observations, covers at least RS relaxation of considered materials	mean RS relaxation due to cyclic mechanical loads
$\sigma_R = -K_T \cdot S_{OL} \cdot \exp\left[\left(\frac{N}{N_{EP}}\right) \cdot \ln(0.1)\right],$ $N_{EP} = C / \left[(K_T \cdot S_{max})^m \cdot (K_T \cdot S_{mean})^n \right],$ $N_{EP} \text{ is equilibrium period}$ <p style="text-align: right;">(RS Relaxation Eq. 7)</p>	Potter, [58], 1973	notched coupons of 2024-T4 aluminum alloy	K_T ; elastic stress concentration factor, S_{OL} ; difference between max working stress and overload stress, N ; number of load cycles, S_{max} , S_{mean} ; max nominal and mean stress	C ; material specific proportionality constant, m, n ; loading level specific constants defining relative contributions	model covers mean stress relaxation of aluminium, arguably also other metallic materials	RS relaxation in notches due to mechanical cyclic loading

Table 4.2-1. Results of the performed literature study concerning mechanical residual stress relaxation assessment procedures, together with brief descriptions of their main characteristics. Here RS means residual stress. Continued from the previous page.

WRS relaxation model formulas and equations	Author(s), ref., year	Target of application	Required input data	Parameters to be fitted	Range of applicability	Considered phenomena
$B = 8.5 \cdot 10^{-2} \cdot \left(1 - \frac{\Delta \varepsilon}{\Delta \varepsilon_{th}} \right),$ $\frac{\Delta \varepsilon_{th}}{2} = \exp[-8.41 + 5.36 \cdot 10^{-3} \cdot (\text{HB})]$ <p style="text-align: center;">(RS Relaxation Eq. 8)</p>	Landgraf, Chernenkoff, [34], 1988	ductile structural metals, mild steels	$\Delta \varepsilon$; total strain range, $\Delta \varepsilon_{th}$; threshold strain range for mean stress relaxation, HB; Brinell hardness	B ; this is the B in Jhansale & Topper model [33]	empirical model, covers at least RS relaxation of considered materials	mean RS relaxation due to cyclic mechanical loads
<p>1st load cycle; $\sigma_R' = E \cdot (\varepsilon - \varepsilon_{\min})$; $\varepsilon + \varepsilon_R \leq \varepsilon_y$, and $\sigma_R' = \sigma_y - E \cdot (\varepsilon_{\max} - \varepsilon_{\min})$; $\varepsilon + \varepsilon_R > \varepsilon_y$, other considered load cycles; $\sigma_R' = A + B \cdot \lg N$; $1 \leq N \leq 10^4$</p> <p style="text-align: center;">(RS Relaxation Eq. 9)</p>	Takanashi, Kamata, Iida, [46], 2000	pipe welds, as fabricated with normal and pure iron wire, base material being 500 MPa class high strength steel of 20 mm thickness	E ; elastic modulus, ε_R ; strain corresponding to initial RS, ε_y ; strain at yield, ε_{\max} and ε_{\min} ; cycle specific maximum and minimum strains, σ_y ; yield strength, N ; number of load cycles	A, B ; weld material and loading range specific fitted constants; given in [46] for two weld materials & loading ranges	model covers pipe component welds, only longitudinal RSs considered as in tests [46] transverse RSs did not notably change as a function of load cycles, model not valid for number of load cycles $N > 10^4$	relaxation of longitudinal RS (i.e. parallel to weld RS) due to cyclic mechanical loads
$\frac{\sigma_N^{re}}{ \sigma_0^{re} } = A \left[\frac{2 \cdot \sigma_a^2}{(1-R) \cdot (C_w \cdot \sigma_y)^2} \right]^m \cdot (N-1)^B - 1$ <p style="text-align: center;">(RS Relaxation Eq. 10)</p>	Zhuang, Halford, [36], 2001	wrought IN718 rectangular bar	σ_0^{re} ; initial RS, σ_a ; stress amplitude, σ_y ; yield stress, C_w ; degree of cold working, N ; number of load cycles, R ; loading ratio	A, m, B ; stress and strain response dependent constants	incorporates Bauschinger effect, elastic-plastic stress-strain relation and initial cold work effect	RS relaxation due to cyclic mechanical loads

Table 4.2-1. Results of the performed literature study concerning mechanical residual stress relaxation assessment procedures, together with brief descriptions of their main characteristics. Here RS means residual stress. Continued from the previous page.

WRS relaxation model formulas and equations	Author(s), ref., year	Target of application	Required input data	Parameters to be fitted	Range of applicability	Considered phenomena
$\sigma^{R,N} = \sigma^{R'} - B \cdot \exp(-C \cdot N)$ <p style="text-align: right;">(RS Relaxation Eq. 11)</p>	Smith, Farrahi, Zhu, McMahon, [42], 2001	forged shot-blasted bars of En15R steel	$\sigma^{R'}$; initial surface RS, N ; number of load cycles, results from FEM analyses with multilinear kinematic hardening model	B, C ; material specific constants fitted to FEM analysis results,	model arguably applicable to various metals, as compared to test results good correspondence for tensile load cycles, whereas too rapid RS relaxation for tensile-compressive load cycles	surface and to some extent bulk RS relaxation due to cyclic mechanical loads
$\frac{(\sigma_{res}^{ini} + \sigma_{app})}{\sigma_y} < 1;$ $\sigma_{res}^{relax} = \sigma_{res}^{ini} \cdot N^{-k},$ $\frac{(\sigma_{res}^{ini} + \sigma_{app})}{\sigma_y} \geq 1;$ $\sigma_{res}^{relax} = \sigma_{res}^{ini} \cdot \left\{ -1.6 \cdot \left[\frac{(\sigma_{res}^{ini} + \sigma_{app})}{\sigma_y} \right] + 2.6 \right\} \cdot N^{-k}$ <p style="text-align: right;">(RS Relaxation Eq. 12)</p>	Han, Kang, Shin, [38], 2001, Han, Lee, Shin, [39], 2002	weld joints with SUS-316 stainless steel and SM490B as base materials	σ_{app} ; applied stress, σ_y ; yield stress, σ_{res}^{ini} ; initial RS, N ; number of load cycles	Exponent k is material dependent, here fitted for SUS-316 the value is 0.004	model arguably applicable to several steel grades, gives non-conservative results for some large scale weld details	RS relaxation due to cyclic mechanical loads
$\sigma^{RS} = A(\sigma_a) - m(\sigma_a) \cdot \lg N$ <p style="text-align: right;">(RS Relaxation Eq. 13)</p>	Löhe, Vöhringer, [47], 2002	quenched and tempered AISI 4140 in shot-peened condition	N ; number of load cycles, experimental fatigue data for each stress amplitude	A, m ; determined for each stress amplitude, σ_a , from the experimental data in linear section of RS- N curves	mechanical surface RS relaxation of metallic materials, model valid for number of load cycles $N > 1$	mechanical surface RS relaxation due to cyclic loading in room temperature

Table 4.2-1. Results of the performed literature study concerning mechanical residual stress relaxation assessment procedures, together with brief descriptions of their main characteristics. Here RS means residual stress. Continued from the previous page.

WRS relaxation model formulas and equations	Author(s), ref., year	Target of application	Required input data	Parameters to be fitted	Range of applicability	Considered phenomena
$\sigma_R = \sigma_{Rini} \cdot \left[1 - k_1 \cdot \ln \left(\frac{S_{max} + \sigma_{Rini}}{\sigma_y} \right) \right] \cdot \exp[-k_2 \cdot (N - 1)];$ $(S_{max} + \sigma_{Rini}) \geq \sigma_y$ <p style="text-align: center;">(RS Relaxation Eq. 14)</p>	Goo, Yang, Seo, [45], 2005	weld notch root, base material JIS SM 490 A	σ_{Rini} ; initial RS, S_{max} ; local stress as caused by nominal stress S , N ; number of load cycles, σ_y ; yield stress, results from FEM analyses with elastic-plastic material model	k_1, k_2 ; material specific constants fitted to FEM analysis results	arguably welded metallic structures	RS relaxation due to cyclic mechanical loads
$\Delta\sigma = 1.05 \cdot 10^{-5} \cdot K \cdot E \cdot \sigma_d \cdot [1 - \exp(-1.13642 \cdot N / \sigma_d)]$ <p style="text-align: center;">(RS Relaxation Eq. 15)</p>	Rao, Wang, Chen, Ni, [37], 2007	steel 304L, as subjected to vibratory fatigue	K ; ratio of initial RS and yield stress, N ; number of load cycles, σ_d ; dynamic stress amplitude	E ; dynamic modulus corresponding to strain, dynamic stress amplitude and loading frequency	incorporates initial RS, dynamic stress amplitude and cyclic altering of dynamic modulus	RS relaxation due to cyclic mechanical loads
$\frac{(\sigma_{res}^{ini} + \sigma_{app})}{\sigma_y} < 1;$ $\frac{\sigma_{res}^{2cycles}}{\sigma_{res}^{ini}} = 1,$ $\frac{(\sigma_{res}^{ini} + \sigma_{app})}{\sigma_y} \geq 1;$ $\frac{\sigma_{res}^{after-max}}{\sigma_{res}^{ini}} = -1.1 \cdot \left[\frac{(\sigma_{res}^{ini} + \sigma_{app})}{\sigma_y} \right] + 2.1$ <p style="text-align: center;">(RS Relaxation Eq. 16)</p>	Li, Wan, Wang, Ji, [40], 2009	ship structural steel, weld hot spot	σ_{app} ; applied stress, σ_y ; yield stress, σ_{res}^{ini} ; initial RS	no parameters to be fitted, model possibly applicable for cyclic loads by using each computed $\sigma_{res}^{after-max}$ as σ_{res}^{ini} for next cycle	model arguably applicable to several steel grades	amount of relaxed RS at hot spot due to mechanical loads, possibly mean RS relaxation due to cyclic mechanical loads
$\Delta\sigma_R = (\sigma_{pk0} - \sigma_y) \cdot \left[1 - \exp \left(\frac{-4 \cdot \varepsilon_a \cdot N \cdot \theta_0}{\sigma_y} \right) \right]$ <p style="text-align: center;">(RS Relaxation Eq. 17)</p>	Kwofie, [41], 2009	metallic materials, as subjected to vibratory fatigue	σ_{pk0} ; initial peak stress, σ_y ; yield stress, ε_a ; cyclic strain amplitude, N ; number of load cycles	θ_0 ; initial slope of flow stress-strain curve	at least for metallic materials subjected to vibratory fatigue	RS relaxation due to cyclic mechanical loads

Table 4.2-1. Results of the performed literature study concerning mechanical residual stress relaxation assessment procedures, together with brief descriptions of their main characteristics. Here RS means residual stress. Continued from the previous page.

WRS relaxation model formulas and equations	Author(s), ref., year	Target of application	Required input data	Parameters to be fitted	Range of applicability	Considered phenomena
$\lg\left(\frac{\sigma_{mN}}{\sigma_{mi}}\right) = \left(\frac{1}{1-m}\right) \cdot \lg[N \cdot B \cdot E \cdot (m-1) \cdot \sigma_{mi}^{m-1} + 1],$ <p>for $m \neq 1$</p> <p style="text-align: right;">(RS Relaxation Eq. 18)</p>	Arcari, De Vita, Dowling, [54], 2009	high strength aluminum alloys, 7475-T651, 7075-T6511, and 7249-T76511	σ_{mi} ; initial mean stress, N ; number of load cycles, E ; elastic modulus	B ; material specific coefficient, m ; material specific exponent	model covers mean stress relaxation of metallic materials	mean stress relaxation due to mechanical cyclic loading

Table 4.2-2. Results of the performed literature study concerning thermal residual stress relaxation assessment procedures, together with brief descriptions of their main characteristics. Here RS means residual stress.

WRS relaxation model formulas and equations	Author(s), ref., year	Target of application	Required input data	Parameters to be fitted	Range of applicability	Considered phenomena
$\frac{\sigma}{\sigma_0} = \exp(-k \cdot t^p)$ <p style="text-align: center;">(RS Relaxation Eq. 19)</p>	Rovinskiy, Lutsau, [55], 1957, Borzdyka, Getsov, [56], 1972	RPV base material and cladding of WWER-440 and WWER-1000 type reactors	σ_0 ; initial stress, t ; time	k ; temperature dependent material specific constant, p ; temperature dependent material specific exponent	model covers thermal RS relaxation of metallic materials	stress relaxation due to thermal creep
$\frac{\sigma^{RS}(T, t)}{\sigma_0^{RS}} = \exp[-(A \cdot t)^m],$ $A = C \cdot \exp(-\Delta H/k \cdot T)$ <p style="text-align: center;">(RS Relaxation Eq. 20)</p>	Vöhringer, [43], 1983	metallic materials in general	σ_0^{RS} ; RS before annealing, T ; temperature, t ; time, C ; velocity constant, ΔH ; activation enthalpy, k ; Boltzmann constant	m ; exponent dependent on relaxation mechanism	thermal RS relaxation of metallic materials	RS relaxation due to thermal annealing
$\sigma_e(t) = [\sigma_e(0)^{-(n-1)} + \lambda \cdot (n-1) \cdot K \cdot E_T \cdot t]^{-1/(n-1)},$ $\lambda = 1 \text{ for uniaxial case,}$ $\lambda = \frac{3}{2} \sqrt{\left[(1+\nu) + \frac{1}{3} \cdot (1-2 \cdot \nu) \cdot \frac{\sigma_e(0)}{S_D(0)} \cdot \xi \right]}$ for multiaxial case, $\xi = 1 / [0.8 + 1.3 \cdot (\sigma_H(0) / \sigma_e(0))^2]$ for steel materials <p style="text-align: center;">(RS Relaxation Eq. 21)</p>	Sandström, Malén, Otterberg, [44], 1983	Pipe of ferritic RPV steel A533B with wall thickness of 130 mm and containing a weld	$\sigma_e(0)$; initial equivalent stress, E_T ; elastic modulus, t ; time, ν ; Poisson coefficient, $S_D(0)$; initial stress deviator in the considered direction, $\sigma_H(0)$; initial hydrostatic stress	K ; material specific constant, n ; material specific exponent	model covers only thermal RS relaxation, arguably applicable to several steel materials	thermal RS relaxation as a function of time
$\dot{\epsilon}_p = A \cdot (\sigma_m^{rs})^n \cdot \exp(-\Delta H_N/k \cdot T),$ where $\dot{\epsilon}_p$ is plastic strain rate <p style="text-align: center;">(RS Relaxation Eq. 22)</p>	Viereck, Löhe, Vöhringer, Macherauch, [50], 1991	shot-peened AISI4140 steel as quenched and tempered	σ_m^{rs} ; average value of RSs within regarded time interval, ΔH_N ; activation enthalpy, k ; Boltzmann constant, T ; considered temperature	A ; material specific velocity constant, n ; material specific Norton equation exponent	model covers only thermal RS relaxation, arguably applicable to several steel grades	thermal RS relaxation as a function of time

Table 4.2-2. Results of the performed literature study concerning thermal residual stress relaxation assessment procedures, together with brief descriptions of their main characteristics. Here RS means residual stress. Continued from the previous page.

WRS relaxation model formulas and equations	Author(s), ref., year	Target of application	Required input data	Parameters to be fitted	Range of applicability	Considered phenomena
$\sigma = \sigma_0 \cdot \left[\frac{1}{1 + C \cdot E \cdot (n-1) \cdot \sigma_0^{n-1} \cdot t} \right]^{1/(n-1)}$ <p style="text-align: center;">(RS Relaxation Eq. 23)</p>	Webster, Ainsworth, [53], 1994	notched compact tension specimens of Type 316H austenitic stainless steel at 550 °C	σ_0 ; initial stress, t ; time, E ; elastic modulus	C ; temperature dependent material constant, n ; power-law stress exponent	model covers thermal RS relaxation of metallic materials	stress relaxation due to thermal creep
$\frac{\sigma^{RS}(T, t)}{\sigma_0^{RS}} = \exp[-(A \cdot t)^D],$ $A = C \cdot \exp\left\{ \frac{\Delta H_{A1} + \Delta H_{A2} \cdot \exp[-(T - T_s)^2/a]}{k \cdot T} \right\},$ $D = m_1 + m_2 \cdot \exp[-(T - T_s)^2/a]$ <p style="text-align: center;">(RS Relaxation Eq. 24)</p>	Hoffmeister, Schulze, Wanner, Hessert, [49], 2008	Ni based shot-peened superalloy IN718, which is a turbine component material	σ_0^{RS} ; RS before annealing, T ; temperature, t ; time, C ; velocity constant, ΔH_{A1} , ΔH_{A2} ; activation enthalpy values corresponding to temperatures T_1 , T_2 , k ; Boltzmann constant, T_s ; temperature corresponding to anomaly in Vöhringer model [43] exponent m	m_1 , m_2 ; exponent values dependent on relaxation mechanism, a ; parameter governing the transition between two different parameter zones, i.e. regular and anomaly	thermal RS relaxation of metallic materials, model is a modification of Vöhringer model [43] to incorporate temperature dependency for exponent m	RS relaxation due to thermal annealing

Table 4.2-3. Results of the performed literature study concerning thermomechanical residual stress relaxation assessment procedures, together with brief descriptions of their main characteristics. Here RS means residual stress.

WRS relaxation model formulas and equations	Author(s), ref., year	Target of application	Required input data	Parameters to be fitted	Range of applicability	Considered phenomena
$ \dot{\alpha} = -\frac{\Psi}{E_r} \cdot \left(1 - \frac{G-H}{R}\right),$ <p>$\dot{\alpha}$ is rate of uniaxial stress relaxation, for clarity purposes only 1D model is presented here, instead of the more general and complex 3D model that is also given in the source ref.</p> <p style="text-align: right;">(RS Relaxation Eq. 25)</p>	Kwangsoo, [57], 2009	metallic materials in general	H ; kinematic stress, G ; back stress,	Ψ ; material specific constant, E_r ; material specific inelastic modulus that is based on total strain, R ; material specific scalar concerning isotropic hardening	this elastic visco- plastic model is of general type covering both thermal effects and those caused by cyclic loading, however includes several material specific parameters to be fitted	stress relaxation due to both mechanical cyclic loading and thermal creep

Table 4.2-4. A summary of the input data parameters concerning the covered RS relaxation assessment equations. Equation numbers are used here, for actual equations, see Tables 4.2-1, 4.2-2 and 4.2-3.

Input data parameter name, symbol	RS relaxation model equation number																								
	1	2	3	4	5	6	7	8	9	10	11	12	13	14	15	16	17	18	19	20	21	22	23	24	25
initial mean stress, σ_{mi} , σ_{m1}	X					X												X							
initial residual stress, σ_{R0}			X	X						X	X	X		X	X	X				X				X	
residual stress value after first load cycle $\sigma^{rs} (N = 1)$		X																							
initial peak stress, σ_{pk0}																		X							
applied stress, σ_{app}																	X								
mean nominal stress, S_m					X																				
max mean stress, S_{mean}							X																		
max nominal stress, S_{max}							X																		
local stress as caused by nominal stress, S_{max}														X											
extraction of max and overload stress, S_{OL}							X																		
dynamic stress amplitude, σ_d															X										
applied stress range, $\Delta\sigma_a$	X	X								X	X														
applied strain range, $\Delta\epsilon_a$			X					X										X							
local root mean square averaged stress, σ_{rms}					X																				
local root mean square averaged strain, ϵ_{rms}				X																					
loading ratio, R										X															
strain corresponding to initial residual stress, ϵ_R									X																
cycle specific maximum strain, ϵ_{max}									X																
cycle specific minimum strain, ϵ_{min}									X																
threshold strain range for mean stress relaxation, $\Delta\epsilon_{th}$								X																	
initial slope of flow stress-strain curve, θ_0																		X							
number of load cycles, N	X	X	X	X	X	X	X	X	X	X	X	X	X	X	X	X	X	X	X						
yield stress, σ_y	X	X	X					X	X	X	X	X	X	X	X	X	X								
strain at yield, ϵ_y								X																	
elastic modulus, E								X										X		X		X			
dynamic modulus corresponding to load & stress, E															X										
material dependent parameter(s)			X		X	X				X	X		X					X		X	X	X		X	
material & stress range dependent parameter(s)		X	X			X	X					X													
material & strain range dependent parameter(s)	X						X																		
material & strain & stress dependent parameter(s)				X																					
strain & stress dependent parameter(s)										X															
elastic stress concentration factor, K_T					X	X																			
clipping ratio, C				X																					
degree of cold working, C_w										X															
stress & strain field results from FEM analyses											X			X											
fatigue test data for each stress amplitude													X												
initial stress, σ_0																			X				X		
initial equivalent stress, $\sigma_e(0)$																				X					
initial direction specific stress deviator, $S_D(0)$																				X					
initial hydrostatic stress, $\sigma_H(0)$																				X					
kinematic stress, H																									X
back stress, G																									X
plastic strain rate, $d\epsilon_p/dt$																					X				

Table 4.2-4. Continued from the previous page. A summary of the input data parameters concerning the covered RS relaxation assessment equations. Equation numbers are used here, for actual equations, see Tables 4.2-1, 4.2-2 and 4.2-3.

Input data parameter name, symbol	RS relaxation model equation number																								
	1	2	3	4	5	6	7	8	9	10	11	12	13	14	15	16	17	18	19	20	21	22	23	24	25
temperature, T																				X		X		X	
anomaly temperature, T_s																								X	
time, t																			X	X	X		X		
material specific inelastic modulus, E_t																									X
Poisson coefficient, ν																					X				
Boltzmann constant, k																				X		X		X	
material & temperature dependent parameter(s)																			X						
relaxation mechanism dependent parameter(s)																				X				X	
velocity constant, C																				X		X			
activation enthalpy, ΔH																				X		X		X	
transition parameter between behaviour zones, a																								X	

In the following are some remarks concerning the presented RS relaxation assessment procedures.

As can be seen, most of the collected RS relaxation assessment procedures consider mechanical cyclic loading as the covered loading phenomena. This is quite as expected, as in general RS relaxation procedures have been mainly developed to applications associated with repeating load cycles and relatively moderate altering of temperatures, such as vehicle and machinery components. Much less were found RS relaxation assessment procedures that consider thermal loading as the covered loading phenomena. These are mainly developed for assessment of effects of thermal annealing and creep to RS distributions in components. Only one thermomechanical RS relaxation procedure was found. This is assumed to be due to challenges in both measuring as well as computationally assessing such joint effects to RS relaxation, as only quite recently have there been available the means to these, e.g. numerical analysis codes with coupled analysis capabilities and computers with enough memory capacity and process efficiency to enable to perform the analysis runs with reasonable effort.

However, due to resource limitations, it is possible that not all RS relaxation assessment procedures applicable to NPP components were found within the available time frame, and thus the presented procedure compilation might not be an exhausting one. Still, it among other data combines those in the most recently published RS relaxation associated bibliography studies, so it is not very likely that any relevant RS relaxation assessment procedure is missing.

The adopted categorisation of the RS relaxation assessment procedures was selected by the author of this work. Other categorisation systems could be envisaged as well, e.g. such that are in more detail based on the various treatments that can cause the RS relaxation, such as welding, machining, PWHT, and shot-peening, or such that depict the scope of RS relaxation in question, such as surface RS relaxation and mean RS relaxation. However, as here the scope is to consider NPP component welds and the loading phenomena they are actually and/or anticipated to be exposed to under operation, the adopted categorisation system was deemed to be the most applicable one for this purpose.

The adopted categorisation of the RS relaxation assessment procedures was selected by the author of this work. Other categorisation systems could be envisaged as well, e.g. such that are in more detail based on the various treatments that can cause the RS relaxation, such as welding, machining, PWHT, and shot-peening, or such that depict the scope of RS relaxation in question, such as surface RS relaxation and mean RS relaxation. However, as here the scope is to consider NPP component welds and the loading phenomena they are actually and/or anticipated to be exposed to under operation, the adopted categorisation system was deemed to be the most applicable one for this purpose.

As was implicitly mentioned above, not all of the covered RS relaxation assessment procedures consider specifically welds, but also selected details in the base material side, such as surfaces, notches, geometry details with relatively small radius of curvature and local holes, or regular and continuous geometries as well. However, as the physical events that can cause RS relaxing are by and large the same for most metallic materials, especially concerning various steel grades, the presented RS relaxation assessment procedures are assumed to be applicable to NPP steel component weld materials as well.

Also, several of the presented RS relaxation assessment procedures are mainly developed for assessing the gradual relaxation of intentionally induced surface RSs that have been obtained with various surface treatments, such as shot-peening, which typically create a compressive surface RS distribution, which in turn prolongs the fatigue life of the component. As all such RS relaxation procedures include material specifically adjustable parameters, they can presumably be fitted so that they are applicable to through thickness RS relaxation assessments of NPP component welds as well.

All in all, each of the covered RS relaxation procedures here contain material and/or temperature range dependent parameters that need to be fitted to sufficiently large amount of accurate enough data. Also required are data concerning the initial RS state. If measured RS data are not available, the initial RS distribution has to be assessed somehow, e.g. using such alternatives from the WRS definition procedures covered in Chapter 3 that give reasonably conservative and in transverse to weld direction self-balancing RS values. For the time being it appears that only advanced numerical analysis codes with coupled analysis capabilities, e.g. certain finite element analysis (FEA) codes, enable to perform analyses that at the same time take into account all possible relevant physical RS relaxation phenomena.

5 Uncertainties and probabilistic aspects concerning assessing WRS distributions

The uncertainties and probabilistic aspects concerning assessing WRS distributions are considered in this chapter. This includes describing uncertainties concerning measured WRS distributions, and probabilistic methods to assess WRS distributions. Also the treatment of WRSs in some most notable current probabilistic crack growth analysis codes are briefly described, most notably those implemented in probabilistic fracture mechanics (PFM) based code PRAISE.

5.1 Uncertainties concerning measured WRS distributions

Typically the available RS data contains measurement uncertainties, which vary from technique to technique. Generally the main uncertainties in RS measurement can be categorised according to ref. [62] as:

- (1) Technique specific – inherent uncertainties associated with the different techniques, volume/area averaging as well as operator expertise etc.
- (2) Material specific – highly textured, non-uniform microstructures, accurate mechanical and physical property data.
- (3) Component/geometry specific – dissimilar materials, duplex structures, complex geometries, stabilities of RS state, geometric effects, removal of materials etc.

Three commonly used techniques nowadays to measure WRS distributions are:

- Neutron diffraction method,
- Deep hole drilling method, and
- Contour method.

These three methods display different features of uncertainty which are briefly described below.

Concerning the Neutron diffraction method, the sources of uncertainty are associated with the positioning error, diffracting peak position uncertainty, variability of material within component and stress free reference uncertainty. The typical uncertainty in terms of the stress for surface and through wall measurement is between 20 to 40 MPa [62].

Concerning the Deep hole drilling method, the technique suffers from limited strain sensitivity and potential errors and uncertainties related to the dimensions of the hole (diameter, concentricity, profile, depth etc), surface roughness, flatness, and specimen preparation. The typical uncertainty in terms of the stress for surface measurement (within 0.5 mm from the surface) is between 50 to 100 MPa, but may be higher with fine increments and low strain gauge readings close to the surface [62].

Concerning the Contour method, the main factors of uncertainty that should be taken into account are the plasticity during cutting, i.e. the cutting error, the roughness of cut or out-of-plane cutting (e.g. due to insufficient clamping), and the determination of RS at the surface in the subsequent analysis. The typical uncertainty in terms of the stress for surface

measurement (within 0.5 mm from the surface) is approximately 50 MPa, depending on the geometry of the material. Whereas the typical uncertainty in terms of stress for through wall measurement is slightly lower than the surface measurement, being approximately 40 MPa [62].

In general, errors in measuring WRSs are often classified as systematic or random [63, 65]. Systematic error is usually caused by factors that systematically affect measurement such as the use of the instrument (e.g. miscalibration and specimen alignment), inaccurate values for elastic modulus and Poisson coefficient, and the type of stress analysis used in fitting the data (use of different fitting techniques, algorithm and software). Systematic errors may also arise from the use of a different assumption model in deriving stresses from the measured quantities. Random error is caused by factors that randomly affect measurements. It can be estimated for a particular measuring device by repeating the measurements many times. This kind of error reflects both human and technical incapability to perform the same measurement in exactly the same way several times to obtain exactly the same answer. Practically, it is very difficult to account for unknown systematic and random errors while analysing stress data; particularly when dealing with historical data. However, where stress data are obtained using different measurement techniques, results may need to be corrected to remove any known systematic errors, for example by recalculating stresses using the same stress assumption models.

The published experimental as-welded state WRS data have a substantial scatter. Consequently the WRS distributions defined in the commonly used fitness-for-service procedures have been developed as tensile upper bound solutions based on the data. However, according to [86, 87, 88, 89], this approach not only lacks consistency for the same type of joints and welding parameters, but can either significantly overestimate the WRS values in some cases, or underestimate them in others.

As the relaxation of the WRSs during NPP operation is an issue that has thus far received quite limited attention, it was no surprise that no documentation specifically concerning quantification of its uncertainties were found available. It can be estimated, however, that the sources of uncertainty associated with defining the as-welded state WRSs do not decrease in quantity when moving on to using any of the WRS relaxation assessment procedures covered here. This is an issue that appears to require further research. At least one can perform sensitivity analyses with the WRS relaxation assessment procedures e.g. to see what is the model response for altering its primary variables within their assessed realistic regions of variation. More specifically this could be realised so that the uncertainties quantified as variation in basic material properties, such as elastic modulus and yield strength, would be taken fully into account when assessing the values for the material specific fitting parameters in the WRS relaxation assessment procedures, thus obtaining a range of values for them, which would then be further used when computing the model response. In this connection also the relatively strong temperature dependency of most of the material properties is necessary to be taken into account. At the same time some variation should be given for initial WRS distribution, which is also needed among input data when using most of the WRS relaxation assessment procedures covered here.

5.2 Probabilistic methods to define WRS distributions

The number of continuous reliability distributions available which empirically describe the scatter of test data is considerable. Commonly used distribution functions include e.g.

exponential, polynomial, normal, log-normal and Weibull distributions. Also several data fitting procedures exist, such as least-squares technique, regression analysis and maximum likelihood method, from all of which a number of variations have been developed. However, here the scope is limited to such distribution functions and fitting procedures that have been used when assessing WRS distributions.

A number of probabilistic/statistical methods to define WRS distributions have been developed. All of them are based on the underlying WRS data, which have been obtained from laboratory experiments and/or FEA results. A representative selection of the most useful ones of these procedures, covering both earlier and more recent examples is described in the following.

Statistics are commonly used to best estimate a quantity X of interest consisting of several measurements. For WRSs, estimating the best stress value based on a number of independently measured stresses can be achieved by calculating the stress mean at each measurement location or by fitting an analytical model that reasonably represents the measured data at all locations [66].

It is important to emphasize that the analytical model to be fitted in the statistical treatment must reasonably well represent the associated experimental data and preferably have the least number of free parameters.

Here mainly both conventional and Bayesian statistical techniques are considered. The latter approach uses probability distributions for both the measured data and the free parameters in analytical models used to fitting the data. In contrast, conventional statistical techniques only consider the probability distributions of experimental data. In addition the Bayesian approach can incorporate sources of prior information about measurements and this allows analysts to include their personal judgments in the analysis [63].

5.2.1 Least-squares technique

Arguably the most widely used method to fit an analytical model to experimental data is the least-squares technique [66]. Suppose that we have N independent stress measurements D_k and their unknown error bars σ_k . The least-squares technique optimises the model free parameters by minimising the X^2 function defined as [64]:

$$X^2 = \sum_{k=1}^N \left(\frac{F_k - D_k}{\sigma_k} \right)^2 = \sum_{k=1}^N R_k^2 \quad (5.2.1-1)$$

where values F_k are the analytical predictions and R_k^2 are the relative squared differences.

5.2.2 Bayesian statistical approach

The Bayesian method uses the probability distributions of both measured data and the free parameters defined in analytical model [67, 68]. The Bayesian method defines a probability distribution of the free parameters from which those parameters can be optimised. Such a method can incorporate sources of prior information about measurements allowing analysts to include their personal judgments in the analysis. Suppose that the noise of N independent

stress measurements (D_k, σ_{0k}) from various laboratories can reasonably well be represented as a Gaussian process and the measured data contain individual members with uncertainties larger than the stated error bars, σ_k , the Bayesian analysis leads to the following posterior probability [63, 66]:

$$\ln[\text{probability}(X/D_k, I)] = \text{constant} + \sum_{k=1}^N \ln \left[\frac{1 - \exp(-R_k^2/2)}{R_k^2} \right] \quad (5.2.2-1)$$

where X represents the free parameters of the model and values R_k^2 are defined as in equation (5.2.1-1). This technique provides a method of analysing data from the different laboratories that is less constrained and more robust than a traditional least-squares fit. The other advantage of this approach is that the estimated mean is far less affected by outliers than the traditional mean value [68]. Thus it is very effective in dealing with data of relatively poor accuracy, especially when there are relatively few data points.

5.2.3 Spatial Bayesian approach

The measured stresses are influenced by the spatial resolution of the measurement technique and it is desirable to account for this in statistical treatments of data. This can be dealt with using two different approaches. The first approach is to add the effect of spatial resolution which exists in the experimental data to the analytical model, by smearing it with the instrumental resolution function $H(y)$. This results in the construction of a new analytical model F_k , defined as [63]:

$$F_k = A \cdot \int f(y) \cdot H(y_k - y) dy + B \quad (5.2.3-1)$$

where A is an experimental scaling constant that may be proportional to the amount of time for which the experiment was conducted [67], $f(y)$ is the analytical model, B is the background signal and y_k is the position of measurement. F_k in equation (5.2.1-1) is then replaced by the new analytical model defined here in equation (5.2.3-1). This ensures that both the theoretical and measured data have the same spatial resolution effect.

5.2.4 Spatial deconvolution approach

The second spatial approach is to remove the effect of spatial resolution from the measured data by deconvolving the measurements with the instrumental resolution function. Deconvolution, which is the inverse of convolution, allows the reconstruction of the original stress profile (by removing spatial resolution effect). This approach requires measurements to be uniformly sampled [63].

5.2.5 Heuristic method

The heuristic method for statistical analysis of WRSs is based on a combination of the weighted least-squares method and the application of expert judgement [62]. Thus it is a specific example of Bayesian statistical analysis methods. The least-squares method allows a model of the WRS profile to be determined as a linear combination of the basis functions; the

expert knowledge gives the flexibility of applying expert judgement to determine the weights from the observed scatter in the WRS data.

In WRS data analysis, a heuristic method is based the following assumptions [62]:

- (1) The measurement data may be arranged in groups with expert judgement being used to assess the relative weights of each different group. The relative weights are used to reflect the scatter of the data where more than one measurement techniques are employed. For example, it may be judged that one technique deserves a weight twice as large as another.
- (2) The measurement data for the same weld type and measurement technique can be arranged in groups. The determination of the weights is then equivalent to the determination of the weights of each group.
- (3) The measurement data is assumed to be homoscedastic (i.e. with constant variance) within each group.

The above assumptions have been incorporated into a generalised weighted least-square method. In this method, the measurement data for stress can be expressed as a linear function of:

$$y = b_0 + b_1 \cdot T_1(x) + \dots + b_{n-1} \cdot T_{n-1}(x) + e(x) \quad (5.2.5-1)$$

where $T_i(x)$ are linearly independent basis functions and $e(x)$ is a random error function. The coefficients, b_j , $j = 0, \dots, n-1$, are constants that cannot be determined exactly but can be estimated by the least-square method. The best estimates for the coefficients b_j can be shown to be those for which the following function has a global minimum:

$$\phi = \sum_{i=1}^m w_i \cdot [y_i - b_0 - b_1 \cdot T_1(x_i) - \dots - b_{n-1} \cdot T_{n-1}(x_i)]^2 \quad (5.2.5-2)$$

where m is the number of experimental data items, (x_i, y_i) represent the measured normalised through-wall position and stress, and w_i is a weight assigned to each data item.

In heuristic fitting method, instead of assigning weight to each observation, the weight is assigned to each group of data, and thus equation (5.2.5-2) becomes:

$$\begin{aligned} \phi = & \sum_{i=1}^m w_1 \cdot [y_i - b_0 - b_1 \cdot T_1(x_i) - \dots - b_{n-1} \cdot T_{n-1}(x_i)]^2 + \\ & + \sum_{i=1}^m w_2 \cdot [y_j - b_0 - b_1 \cdot T_1(x_j) - \dots - b_{n-1} \cdot T_{n-1}(x_j)]^2 + \dots \\ & \dots + \sum_{i=1}^m w_g \cdot [y_k - b_0 - b_1 \cdot T_1(x_k) - \dots - b_{n-1} \cdot T_{n-1}(x_k)]^2 \end{aligned} \quad (5.2.5-3)$$

where $m_1 + m_2 + \dots + m_g = m$. The variance σ_g for each group of data is assumed to be proportional to an overall variance σ^2 that describes how the data is scattered about the mean curve:

$$\sigma_g^2 = a_g \cdot \sigma^2 \quad (5.2.5-4)$$

The overall variance σ^2 is related the relative weights w_g by:

$$w_g = 1/(a_g \cdot \sigma^2) \quad (5.2.5-5)$$

where values a_g are constants chosen to describe the ratios between the weights and are normalised such that:

$$\sum_g a_g = 1 \quad (5.2.5-6)$$

The overall variance can be calculated by assuming a uniform weight value (1, for example) for all data:

$$\sigma^2 = \frac{1}{\nu} \cdot \sum_{i=1}^N w_i \cdot (y_i - \hat{y}_i)^2 \quad (5.2.5-7)$$

where y_i is the measured value for WRS which is known, and \hat{y}_i is the value to be fitted. The parameter ν is the degree of freedom. The values of \hat{y}_i can be calculated by the least-square method using the uniform weights value. Once the values of \hat{y}_i are determined, the values for σ^2 can be calculated using equation (5.2.5-7), and the values of w_g can then be obtained using equation (5.2.5-5) where a_g is determined by the expert knowledge.

Applying equation (5.2.5-3) with relative weights w_g , the new values for \hat{y}_i are obtained, and the upper bound residual stress curve can then be determined to a pre-determined confidence level.

In the following are some remarks concerning the uncertainty and relative weights associated with the heuristic method [62]. The measurement uncertainty is related to the relative weights through constants a_g , as seen in equations (5.2.5-5) and (5.2.5-6). The values of a_g are weight ratios among different data sets. In other words, it presents the relative magnitude of uncertainties among these data sets when different measurement techniques are employed. Once the relative magnitudes of measurement uncertainty are known, the relative weights can be obtained from equation (5.2.5-5).

To obtain the relative weights, expert knowledge on measurement uncertainties is required. However, difficulties arise in obtaining expert knowledge. This is mainly due to:

- (1) Measurement uncertainty of WRS varies considerably depending on the technique used and on the component/material type measured.
- (2) It is difficult to obtain comprehensive, complete data of measurement uncertainties from experts as every expert only has experience on specific measurement techniques or material type and may not be familiar with all the measurement techniques. The use of incomplete data could result in large errors in determining the upper bound stress profile.

The results in ref. [62] show that with the heuristic method, it is possible to obtain less conservative WRS profile to a known confidence level.

5.2.6 Fuzzy-set approach

A more advanced probabilistic method to define WRS distributions is the fuzzy-set approach. In ref. [69] this approach has been used together with FEA simulations of the fusion welding processes to quantify the effect of uncertainty in material properties to the corresponding uncertainty/variability in WRS distributions. Due to scarcity of experimental data and the limitations of measurement technology, many of the material parameters involved in the kinetic laws concerning the metallurgical transformations cannot be determined/estimated with sufficient accuracy/repeatability. In the study presented in ref. [69] it is considered that in the welding process the nature of the uncertainty in material properties is non-stochastic (e.g. uncertainty arising from imprecision or fuzziness). Thus the fuzzy-set approach is suggested to be more appropriate for modelling such uncertainty [69, 70]. The results of the mentioned study are the upper and lower bounds (i.e. envelopes) for the WRS distributions as functions of the variability (uncertainty) in material parameters.

For simulating the fusion welding processes, the following FEA procedure was used [69]. The strains and strain rates encountered during welding are typically small, and therefore the heat resulting from the inelastic work is negligible as compared to the heat input from the welding arc [71]. Thus, an uncoupled thermo-mechanical analysis is performed. Temperature history is obtained first from the heat transfer analysis, and subsequently it is input to the stress-strain analysis. In the latter analysis, an elastic-plastic material model with nonlinear kinematic hardening and temperature dependent material properties is adopted. In both the heat transfer and stress-strain analyses, the metallurgical transformations that occur during the entire weld thermal cycle are taken into account. The associated mathematical modelling includes metallurgical transformations, thermal model for heat incorporated from the welding arc as well as temperature field history in the weld material, and constitutive model for depicting stress-strain relationship.

The steps of the fuzzy-set analysis are briefly described in the following. Uncertainty due to imprecision (i.e. variability or fuzziness) in any material parameter X is introduced by specifying a membership function (possibility distribution) $\mu(X)$. It is assumed in ref. [69] that the membership functions of all fuzzy parameters are triangular as shown schematically in Figure 5.2.6-1. The WRS distributions are functions of the material parameters, and hence are treated as fuzzy functions. The analysis aims at constructing the possibility distributions of the fuzzy WRSs by using the so-called Vertex method to numerically implement the extension principle.

In the Vertex method, the membership functions of all fuzzy material parameters X_i ($i = 1, 2, \dots, N$) are discretized using several so-called α -cuts. An α -cut of a fuzzy variable X denotes the interval $[X_\alpha^L, X_\alpha^R]$ in which the possibility of X is at least equal to α , see Figure 5.2.6-1. Thus, $[X_0^L, X_0^R]$ refers to the range of variation of X and $X_{1,0}^{L,R}$ denotes the nominal value of X , which does not necessarily bisect the range of variation. Upon discretizing the membership functions, different binary combinations are formed by the left and right end points of the α -cut intervals for all fuzzy parameters. The number of combinations per α -cut $N_{c/\alpha}$ is:

$$N_{c/\alpha} = \begin{cases} 2^N & \text{for } 0 \leq \alpha < 1 \\ 1 & \text{for } \alpha = 1 \end{cases} \quad (5.2.6-1)$$

where N is the number of fuzzy material parameters.

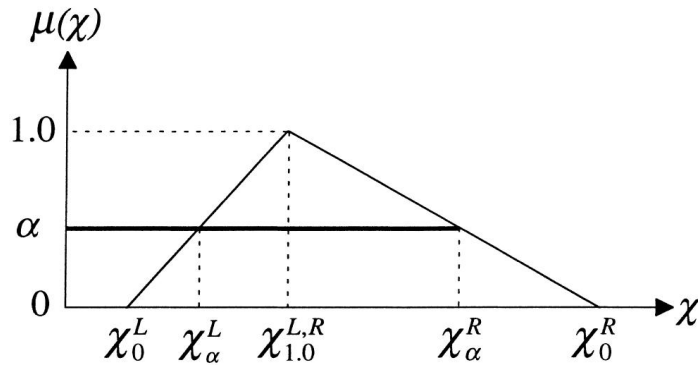


Figure 5.2.6-1. Triangular membership functions for the fuzzy (uncertain) material parameters.

For brevity, the binary combinations are referred to henceforth as $C_{\alpha,j}$ where $j = 1, 2, \dots, N_{c/\alpha}$. Also, the WRS field $\sigma = \sigma(X_1, X_2, \dots, X_N)$ is written in the abbreviated form $\sigma = \sigma(C_{\alpha,j})$. For a given α -cut, the corresponding interval in σ is obtained from the relation:

$$[\sigma_{\alpha}^L, \sigma_{\alpha}^R] = \left[\min_{|\omega,j} \{ \sigma(C_{\omega,j}) \}, \max_{|\omega,j} \{ \sigma(C_{\omega,j}) \} \right], \quad \omega \geq \alpha, \quad j = 1, 2, \dots, N_{c/\alpha} \quad (5.2.6-2)$$

The possibility distributions $\mu(\sigma)$ can thus be constructed by applying equation (5.2.6-2) to a sweep of α -cuts at different possibility levels ranging from 0 to 1. Accuracy of the constructed distributions is directly proportional to the number of α -cuts employed. The range of variation of σ is given by the interval at $\alpha = 0$; i.e. $[\sigma_0^L, \sigma_0^R]$. The nominal value of the WRS field is that corresponding to the combination of the nominal values of all fuzzy material parameters, i.e. at $\alpha = 1$. It can be seen from equations (5.2.6-1) and (5.2.6-2) that the computational cost of the analysis is strongly dependent on the number of input fuzzy variables. It is therefore desirable to have only a small number of input fuzzy variables and/or make use of a rapid re-analysis technique to reduce the computational cost. A significant advantage of the fuzzy-set approach to modelling uncertainty is that it can be implemented in series with existing deterministic FEA codes in the form of a pre-processor and a post-processor.

The following example of results obtained with the above described fuzzy-set approach is presented in ref. [69]. Consider two straight and identical plates of mild steel, with length x width x thickness as 127 x 25.4 x 5.8 mm, with shorter ends joined plate-to-plate with butt-welding while the corresponding other ends of both beams are rigidly supported. As results from the FEA assisted computations, three stress quantities are chosen as examined WRS components. These quantities are the maximum principal tensile stress σ_1 , the von Mises equivalent stress σ_e , and the hydrostatic stress σ_h , respectively. Variations in the parallel to weld direction of the upper bounds, lower bounds, and nominal values of these WRS quantities are shown in Figure 5.2.6-2 for the root of the weld.

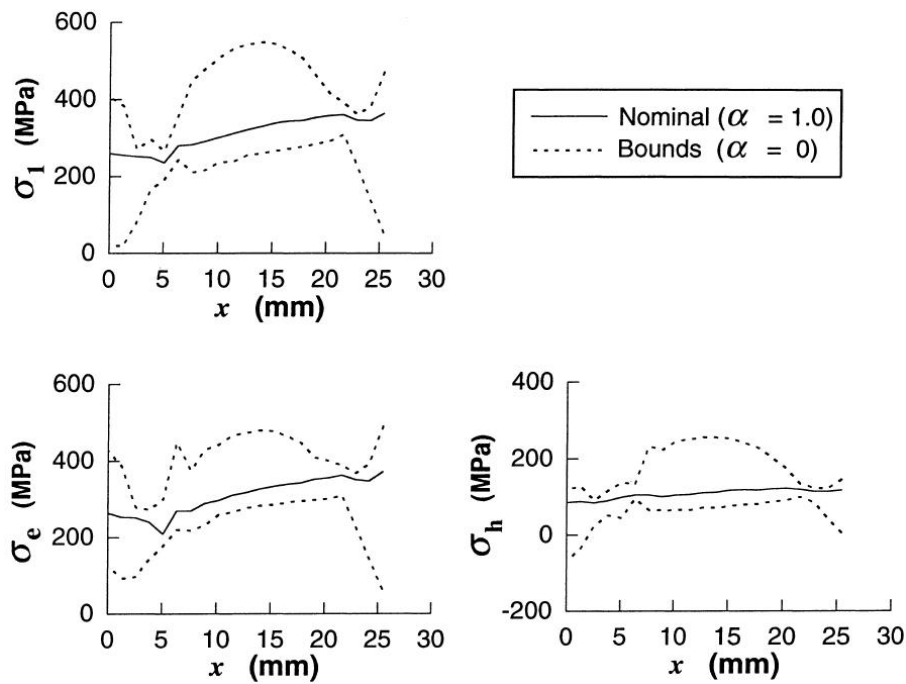


Figure 5.2.6-2. Envelopes of the RS distribution along the weld root for GMA welding of the HY-100 steel butt-welded plates [69].

5.2.7 Goodness of fit technique

The goodness of fit technique is not a probabilistic method to define WRS distributions, but instead a means to assess the accuracy/quality of an already developed WRS distribution. The performance of the predicted stresses in fitting the measurements can be evaluated e.g. using the R^2 quantitative goodness of fit technique [72]. Values close to 1 indicate good fits and correspondingly values close to 0 mean poor fits. The value of R^2 is calculated from the sum of squared difference between the measured stress data and the best-fit data (SS_1), normalised to the squared difference between the measured stress data and the mean value of all measured stresses (SS_2), as follows:

$$R^2 = 1 - \frac{SS_1}{SS_2} \tag{5.2.7-1}$$

When the value of R^2 equals zero the predictions fit the data no better than a straight line. The value of R^2 can sometimes be negative when the fit is worse than a horizontal line. Using the R^2 goodness of fit technique, it has been found that in general there is a reasonable agreement between the predicted and measured WRSs [66]. This agreement is better in the axial direction compared with the hoop direction and better in thick pipes compared to thin pipe welds.

5.3 Treatment of WRSs in probabilistic PRAISE analysis code

5.3.1 Introduction

PRAISE is a PFM based analysis code for estimating probabilities of leaks and breaks in NPP cooling piping. The code was originally developed at Lawrence Livermore National laboratory (LLNL) for the assessment of seismic events on the failure probability of pressurized water reactor (PWR) piping. PRAISE is an acronym for Piping Reliability Analysis Including Seismic Events [73]. The original version of PRAISE considered only fatigue induced crack growth, a more recent version called PC-PRAISE includes also a probabilistic treatment of stress corrosion cracking (SCC) [74]. The latest version of the code is named as WinPRAISE, which is a Windows version of the PC-PRAISE code.

PC-PRAISE considers the initiation and growth of crack-like defects in piping welds. The cumulative crack growth probability can be computed up to 40 years. The initiation analyses are based on the results of laboratory studies and field observations in austenitic piping material operating under BWR conditions. The considerable scatter in such results is quantified and incorporated into a probabilistic model. The crack growth analysis is based on deterministic fracture mechanics principles, in which some of the inputs, such as initial crack size and applied stresses, are considered to be random variables. Monte Carlo simulation, with stratified sampling on initial crack size is used to generate weld reliability results [74].

5.3.2 Residual stresses

The RSs can be input to WinPRAISE using one of the altogether seven options, both deterministic and random. In fatigue they only influence the crack growth through the R ratio.

Deterministically defined residual stresses

The RSs can be deterministically defined by an axisymmetric linear through wall variation (which will not be necessarily self-equilibrating).

Random distribution of residual stresses in large austenitic lines (OD > 20 inches)

The distribution was obtained by curve fitting to experimental values. These data suggest that axial stresses are axisymmetric and self-equilibrating. Line size adjustments were made to RSs in order to improve the agreement between the code predictions and field data. In the case of large pipes the RSs (and stress intensity factors) are multiplied by a factor of 0.15. In WinPRAISE, the user can define a multiplier to these RSs. This multiplier is applied to the stresses along with the benchmarking factor. Pre-defined values of this multiplier are 1, 0.5 and 0.25 for the “High”, “Medium” and “Low” level, respectively. This distribution is considered also applicable to ferritic piping.

Random distribution of residual stresses in small and intermediate austenitic lines

It was found that the RSs in these lines vary through the wall thickness as well as around the circumference. At a given angular location, the stress on the inside surface is sampled from a normal distribution having a positive mean (tensile stress). At the OD the stress is sampled from the same normal distribution, although the mean in this case is negative (compressive stress). Further, the stress is assumed to vary linearly through the wall between the values sampled from the appropriate distributions. For these lines, the benchmarking factor introduced in order to improve the agreement between the code predictions and field data is 0.20. In WinPRAISE, the user can define a multiplier to these RSs. This multiplier is applied to the stresses along with the benchmarking factor. Predefined values of this multiplier are 1, 0.5 and 0.25 for the “High”, “Medium” and “Low” level respectively. This distribution is considered also applicable to ferritic piping.

Residual stress following remedial treatment

The WinPRAISE code provides capabilities for treating the effects of using procedures to obtain a more favourable RS distribution, such as Induction Heating Stress Improvement (IHSI) or the Mechanical Stress Improvement Process (MSIP). Experimental data suggest that these stresses can be adequately described as axisymmetric with a linear through wall gradient. The stresses at the ID follow a normal distribution whose mean and standard deviation should be defined by the user. The stresses at the OD are obtained by imposing the self-equilibrium condition.

Decreased WRS distributions as compared to ASME recommendations

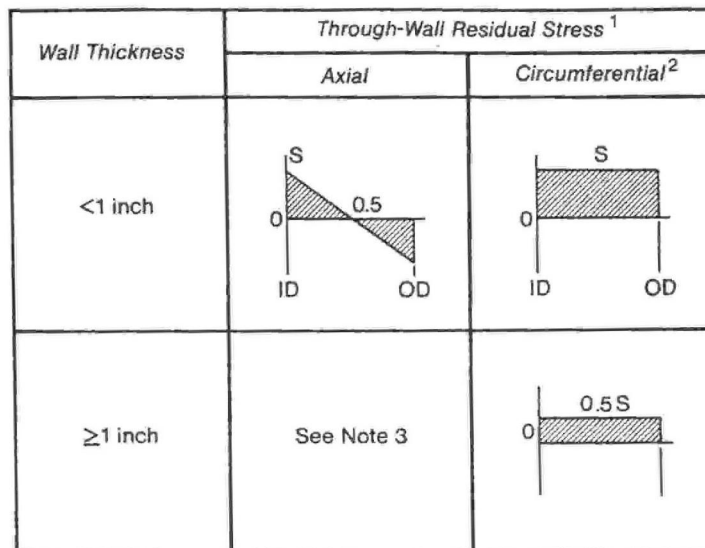
Perhaps the most commonly used definitions for WRSs in NPP reactor circuit component welds are those recommended by the ASME code Section XI Task Group for Piping Flaw Evaluation [2, 75]. These recommendations apply only for austenitic stainless steel pipe-to-pipe welds in as-welded state. Both axial and circumferential WRS components through the pipe wall in weld centre-line are considered, see Figure 5.3.2-1. How WRSs even out in perpendicular to weld direction is not explained. Considering Figure 5.3.2-1, “a” is radial coordinate through pipe wall thickness with origin at the inner surface, and $S = 30$ ksi corresponds to 206.8 MPa in SI units.

Sensitivity studies were performed to determine the components of the developed PFM model that could be adjusted by reasonable amounts to improve the agreement between calculated and observed piping behaviour. It was found that adjustments to the WRSs were most effective in improving agreement. Adjustments were made for each of the three ranges of pipe sizes, and good agreement was obtained [76].

In the SCC analyses it is necessary to consider the WRS distributions in full, and it is also assumed that this degradation mechanism is mainly active under the operational state, in which static conditions the NPPs reside most of their lifetime. Further, as the WRS values in large pipes (OD > 20 inches) are according to the ASME recommendations [2, 75] dependent on the WRS value in the inner pipe component surface, it is appropriate to assume that it corresponds to the material yield stress in the operational temperature. For instance, for the austenitic stainless steel SS 2353 considered in Section 3.2 the yield stress at operational temperature of 286 °C of the Finnish BWR units is 125 MPa [12].

Now it is possible to compute according to PRAISE approach [76] some decreased WRS values as compared to ASME recommendations [2, 75] for large (OD > 20 inches), intermediate (OD = 10 to 20 inches) and small (OD = 4 to 10 inches) lines of austenitic stainless steel, as follows:

- Large lines; inner surface; $t_{wall} \geq 1$ inch; axial WRS = $0.15 \cdot 125 = 19$ MPa, and when $t_{wall} < 1$ inch; axial WRS = $0.15 \cdot 207 = 31$ MPa,
- Intermediate lines; inner surface; $t_{wall} \geq 1$ inch; axial WRS = $0.2 \cdot 125 = 25$ MPa, and when $t_{wall} < 1$ inch; axial WRS = $0.2 \cdot 207 = 41$ MPa,
- Small lines; inner surface; $t_{wall} < 1$ inch; axial WRS = $0.2 \cdot 207 = 41$ MPa,
- Large lines; inner surface; $t_{wall} \geq 1$ inch; circumferential WRS = $0.15 \cdot 0.5 \cdot 207 = 15$ MPa, and when $t_{wall} < 1$ inch; circumferential WRS = $0.15 \cdot 207 = 31$ MPa,
- Intermediate lines; inner surface; $t_{wall} \geq 1$ inch; circumferential WRS = $0.2 \cdot 0.5 \cdot 207 = 21$ MPa, and when $t_{wall} < 1$ inch; circumferential WRS = $0.2 \cdot 207 = 41$ MPa,
- Small lines; inner surface; $t_{wall} < 1$ inch; circumferential WRS = $0.2 \cdot 207 = 41$ MPa.



¹ S = 30 ksi

² Considerable variation with weld heat input.

³ $\sigma = \sigma_i [1.0 - 6.91 (a/t) + 8.69 (a/t)^2 - 0.48 (a/t)^3 - 2.03 (a/t)^4]$

σ_i = stress at inner surface ($a = 0$)

Figure 5.3.2-1. Recommended axial and circumferential WRS distributions for austenitic stainless steel pipe welds [2, 75]. Here ID stands for inner diameter, i.e. inner surface, and OD for outer diameter, i.e. outer surface.

However, the relatively remarkable adjustments to WRS distributions as described above exceeded the estimate bounds of the uncertainties in the WRS levels. Therefore the material experts at Pacific Northwest National Laboratory (PNNL) revisited the prior calibrations by adjusting the effects of plant loading/unloading cycles in addition to adjusting the WRS levels [77].

The local WRSs at the inside surface of small and intermediate pipes are treated as being normally distributed. The through thickness distributions of WRSs are assumed to be linear variations between local values sampled for the inner and outer surfaces. For small pipes, the mean value of WRS at the inner surface was 168 MPa with a standard deviation of 100 MPa.

The independently sampled WRS at the outside surface was 168 MPa with a standard deviation of 98 MPa. For the intermediate pipe, the inner surface WRS had a mean value of 64 MPa and a standard deviation of 98 MPa. The independently sampled WRS at the outer surface of the intermediate pipe had a mean value of 64 MPa with a standard deviation of 98 MPa [77].

According to the results obtained by PNNL [77], for the above mentioned three pipe sizes indicate that for WRS adjustment factor, f , a value of $f = 0.75$ gives good agreement between predicted and observed leak probabilities.

Thus according to the most recent results obtained by PNNL [77] the decreased WRS values as compared to ASME recommendations [2, 75] for large, intermediate and small lines of austenitic stainless steel are as follows:

- All three line sizes; inner surface; $t_{wall} \geq 1$ inch; axial WRS = $0.75 \cdot 125 = 94$ MPa, and when $t_{wall} < 1$ inch; axial WRS = $0.75 \cdot 207 = 155$ MPa,
- All three line sizes; inner surface; $t_{wall} \geq 1$ inch; circumferential WRS = $0.75 \cdot 0.5 \cdot 206 = 77$ MPa, and when $t_{wall} < 1$ inch; circumferential WRS = $0.75 \cdot 207 = 155$ MPa.

5.4 Treatment of WRSs in some other notable probabilistic crack growth analysis codes

Concerning the treatment of WRS distributions in NPP components, the probabilistic analysis codes covered in this section are PRO-LOCA [79], ProSACC [6] and PASCAL-SP [80]. Other notable current probabilistic analysis codes applicable for NPP components, such as PRODIGAL [81] and STRUREL [82, 83] were excluded here, as they do not contain any useful procedures for treatment of WRS distributions.

5.4.1 PRO-LOCA

The PFM based PRO-LOCA analysis code has been developed for the prediction of break probabilities for loss-of-coolant-accidents (LOCAs) in NPP piping systems. In brief the background of PRO-LOCA is that in 2003 the USNRC began its development [78] with the intention to adopt and apply advances in fracture mechanics models, and thereby to provide the successor to the PRAISE code. Like PRAISE, the PRO-LOCA code addresses the failure mechanisms associated with both pre-existing cracks and service induced cracks. Both fatigue and intergranular SCC (IGSCC) are addressed. In addition, PRO-LOCA can also predict failure probabilities for primary water SCC (PWSCC). Other improved capabilities are in the areas of leak rate predictions and the prediction of critical/unstable crack sizes. PRO-LOCA has also incorporated an improved basis for simulating WRS distributions.

In prior versions of PRO-LOCA, WRS distributions that were geometry specific were included. The through thickness WRS values from FEAs were normalised against the material yield strength. The code sampled on yield strength to simulate the variability of the WRS values. Even though this may capture the material variability in the WRSs, it does not capture other variabilities such as those concerning welding parameters and analysis assumptions. In the recent version of PRO-LOCA, the user can provide a WRS distribution input as described in Figure 5.4.1-1. In this case, the user provides as input a distribution of ID WRS, and a distribution of distance parameter X_c . In this context, X_c is defined in the radial pipe cross-section coordinate direction as the distance between the inner surface and the location within

the wall where WRS crosses through zero. The code then calculates a 3rd order polynomial distribution that balances through the wall thickness. For the time being the scope of this approach does not include WRS distributions of repair welds [79].

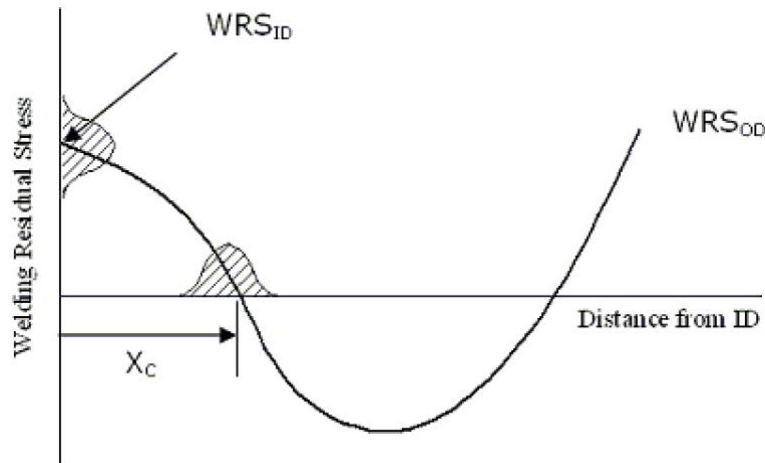


Figure 5.4.1-1. WRS distributions in PRO-LOCA [79].

5.4.2 ProSACC

The Swedish analysis code ProSACC, which stands for Probabilistic Safety Assessment of Components with Cracks, has been developed for probabilistic assessment of crack growth due to SCC and fatigue. The analysis code also has an option which enables the assessment of cracks according to the 1995 edition of the ASME Boiler and Pressure Vessel Code, Section XI, Appendices A, C and H, for assessment of cracks in ferritic pressure vessels, austenitic piping and ferritic piping, respectively. The probabilistic assessments with ProSACC are based on the R6 Method only [6].

Within the PFM based computation procedure of ProSACC analysis code, several parameters are treated as random parameters [6]. As for stresses these include:

- Primary stresses,
- Secondary stresses.

The WRS distributions belong to the category of secondary stresses. In ProSACC the random parameters are treated as not being correlated with one another. The random parameters can follow a normal, log-normal, Weibull or exponential distribution. For all of these distributions the user needs to provide the necessary mean value and standard deviation data.

The scope of the associated guidelines for estimation of WRSs in steel components due to welding given in ref. [6] is deterministic, with no quantification of the uncertainty associated with the WRSs nor suggestions concerning how to expand the scope of their assessment to probabilistic.

There is also another Swedish analysis code, ProLBB, intended for probabilistic examinations of NPP components. More specifically this analysis code has been developed as a complement to the demonstration of leak-before-break (LBB) and also to help to identify the

key parameters that influence the resulting leakage and failure probabilities [85]. As the probabilistic LBB approach of ProLBB was implemented using the calculation engine from the analysis code ProSACC [6], it is assumed that it provides the same treatment capabilities to the WRS distributions as ProSACC does.

5.4.3 PASCAL-SP

The PFM based PASCAL-SP analysis code has been developed by Japan Atomic Energy Agency (JAEA) for the prediction of failure probabilities of NPP piping components due to SCC [80]. PASCAL-SP uses Monte Carlo simulation and includes a simplified probabilistic model for defining WRS distributions. This model is based on FEM analysis results, which have then been applied to the PFM based failure probability analysis procedure of the analysis code.

A WRS database is used to determine the WRS distributions in the PASCAL-SP. The database consists of results from parametric FEM analyses covering a representative range of heat input levels and welding speeds, based on welding experiments. The 108 cases of parametric FEM analyses with a 2D axisymmetric model were performed for 250A piping [84]. It is assumed that the uncertainty of WRS at a point in or near welding joint follows a normal distribution. The statistics in the form of average and standard deviation of WRS at each point and correlation coefficient between nearest neighbouring points in piping thickness direction are introduced to determine the WRS distribution, see Figure 5.4.3-1. The standard deviation represents the uncertainties and the correlation coefficient means the tendency of fluctuations associated with increase and decrease of WRS. The values of the average, standard deviation and the correlation coefficient are estimated using the results from the parametric FEAs. The WRS distribution in piping thickness direction for each sampling calculation is evaluated in PASCAL-SP as follows, see also Figure 5.4.3-2. At first, the WRS following a normal distribution at each point is determined based on the data in the database. The following equation is used to determine the stress S_j [MPa] at each point in pipe component wall thickness direction:

$$S_j = \sigma_j \cdot \left(C_i + Z \cdot \sqrt{1 - r_{ij}^2} \right) + S_j^{ave} \quad (5.4.3-1a)$$

and:

$$C_i = \frac{r_{ij} \cdot (S_i - S_i^{ave})}{\sigma_i} \quad (5.4.3-1b)$$

where S_i [MPa] is the WRS at the i th point, S_i^{ave} [MPa] is average stress, σ_i [MPa] is the standard deviation of the WRS, r_{ij} [-] is the correlation coefficient of stress between i th and j th point (neighbouring points) in pipe component wall thickness direction, and Z [-] is a random number following a standard normal distribution. Secondly, a fourth order polynomial expression in pipe component wall thickness direction is determined according to the least-squares method using the stress S_j . The polynomial coefficients are used for the calculation of stress intensity factor values, as based on influence function method. Using the calculated stress intensity factor values, crack growth rate is determined according to SCC growth rate diagram as prescribed in the JSME FFS code. By repeating the procedures above, the uncertainties of residual stress distribution are evaluated.

The scatter of the WRS values is calculated as follows:

$$\text{Scatter} = \frac{S_i - S_i^{ave}}{\sigma_i} \tag{5.4.3-2}$$

The standard deviation of WRS at a point in the database, see Figure 5.4.3-1, represents uncertainty at that point. The difference of the standard deviation at each point corresponds to the extent of uncertainty.

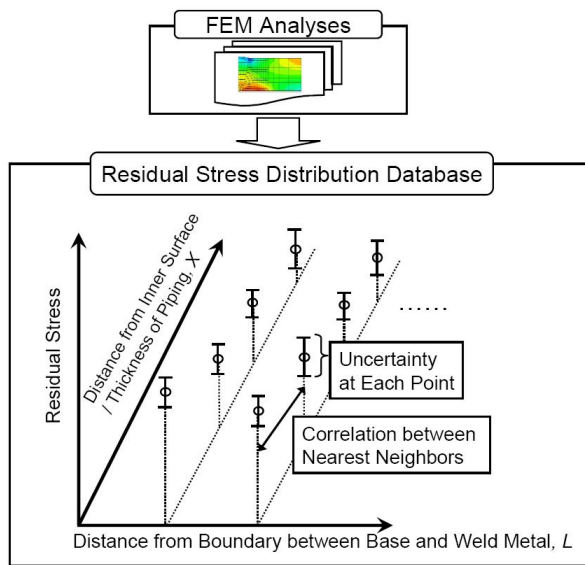


Figure 5.4.3-1. Contents of WRS distribution database [80].

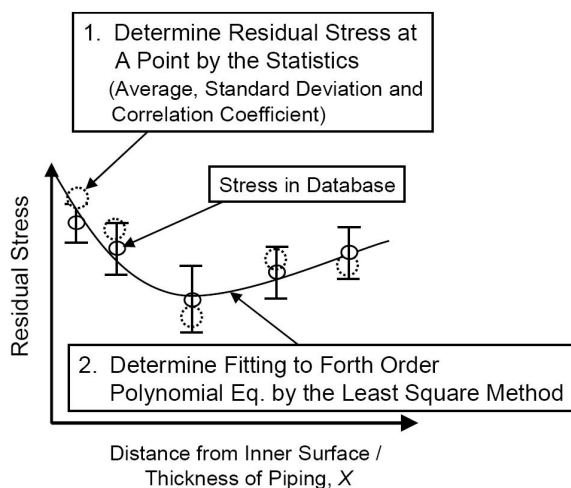


Figure 5.4.3-2. Probabilistic model for WRS distributions [80].

6 Numerical modelling of WRSs and their relaxation

The NPP primary circuit components analysed here are a safe-end connecting to a nozzle and pipe, resembling those that connect the feed water system to the Reactor Pressure Vessel (RPV) in BWR units. In particular, it is examined how to simulate with FEM the WRS distributions and their behaviour for a number of different constant amplitude load cycle sequences in the safe-end/pipe weld joint. The as-welded state WRS distribution for this weld is assumed according to SINTAP procedure [7]. The main background documents for the presented numerical simulations are refs. [90, 91], in particular the latter one.

6.1 Examined weld, initial WRSs, considered loads and other relevant input data

The general geometry of the analysed NPP component assembly is presented in Figure 6.1-1 in the following. The relevant numerical geometry, material, WRS and loading input data values are presented in Table 6.1-1 and Table 6.1-2, respectively. The types of the considered materials are for nozzle; ferritic steel, for base metals of safe-end and pipe; austenitic stainless steel, and for the examined safe-end/pipe joint weld material same properties are assumed as for the associated base materials. As detailed analysis input data concerning the considered NPP components are presented in the associated research reports [90, 91], they are presented here only briefly.

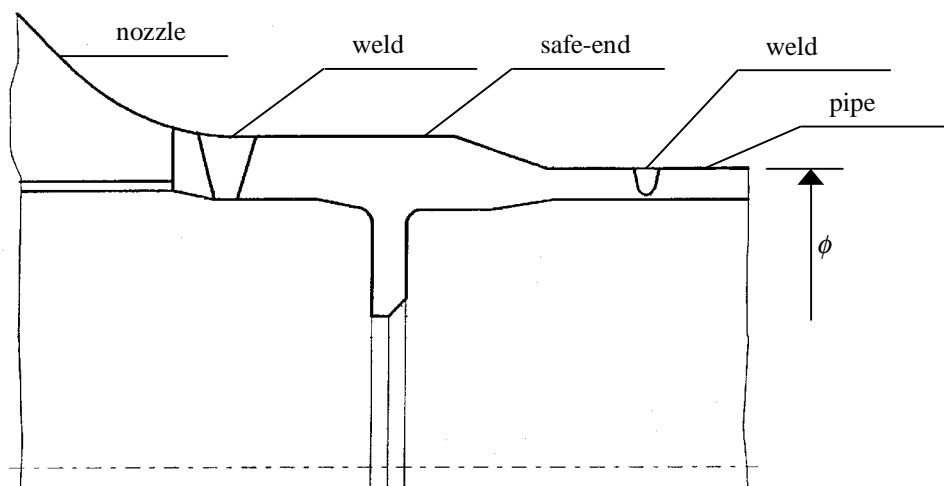


Figure 6.1-1. The overall geometry of the safe-end connecting to a nozzle and pipe, resembling those that connect the feed water system to the RPV in BWR units; horizontal section of the components at the level of their common symmetry axis. The outer diameter ϕ is of the scale of a few hundred mm.

Table 6.1-1. Geometry, material and WRS input data for numerical simulations concerning the safe-end/pipe joint weld, here weld material properties are taken as to correspond those of the austenitic SS safe-end material. The material property data values are from ref. [92].

Geometry & Material Property Data		WRS Data	
Outer diameter [mm]	a few hundreds	WRS definition procedure	SINTAP
Wall thickness [mm]	~ 16	WRS direction	axial
Yield strength at 20/286 °C [MPa]	241/220 (*)	WRS, inner surface at 20/286 °C [MPa]	269/245
Tensile strength at 20/286 °C [MPa]	586/586	WRS, outer surface at 20/286 °C [MPa]	-269/-245
Young's modulus at 20/286 °C [GPa]	214/199	Variation of WRS between inner/outer surface	linear

(*) These yield strength values correspond to 0.2 % strain.

The main cyclic loading used here, see Table 6.1-2, was applied in the form of even stress distribution over the pipe end cross-section surface, i.e. load sequence specifically it varies only as a function of time. The direction of the stress loading is axial, i.e. parallel to the common symmetry axis of the considered components. Also inner pressure was a cyclically altering load parameter here. Altogether eight different load cycle sequences were prepared. They all are constant amplitude load sequences with linear altering of the loading parameter values within the respective loading ranges. The rising and decreasing load cycle parts are separated with parts of static loading conditions having the same duration as the neighbouring altering parts. All prepared load cycles end up to the same loading conditions as they start with. The prepared load cycle sequences cover a representative range of stress amplitudes from moderate up to relatively severe loading conditions.

Table 6.1-2. Load cycle sequence (LCS) data for numerical simulations concerning the safe-end/pipe joint weld. The cyclic loads are: even stress distribution perpendicular to the weld and acting over the pipe end cross-section surface, and inner pressure. Here σ_{min} and σ_{max} denote minimum and maximum axial stress loads, whereas p_{min} and p_{max} denote minimum and maximum inner pressure loads, respectively, and LC means a single load cycle.

LCS No.	σ_{max} [MPa]	σ_{min} [MPa]	$R = \sigma_{min}/\sigma_{max}$	p_{max}/p_{min} [bar]	Temperature [°C]
1	150	0	0	70.0/1.0	286
2	100	0	0	70.0/1.0	286
3	50	0	0	70.0/1.0	286
4	25	0	0	70.0/1.0	286
5	150	-150	-1	70.0/1.0	286
6	100	-100	-1	70.0/1.0	286
7	50	-50	-1	70.0/1.0	286
8	25	-25	-1	70.0/1.0	286
LC Rising/Decreasing/Static Part Durations [s]					100/100/100
LC Duration [s]					400
No. of LCs in LCS					10 x 5

The loading events considered in the heat transfer and the stress/strain simulations were applied as load histories, the total duration of each of which being 60000 s. Also, the dead weights of the analysed components were considered, based on their dimensions and material densities. Each considered load history started with the loading of the WRSs, during which event no other mechanical loads were present and the overall temperature was kept at 20 C°.

Following that, the pressure and temperature were elevated to the values corresponding to the operational conditions, those being for the considered BWR environment pressure of 70 bar and temperature of 286 °C, respectively. This was realised with a load event called here Start of operation (SO), resembling typical plant load transient Cold start-up. For all considered load histories these first two load events were exactly the same. Then followed the load history specific LCS, ending itself and at the same time the considered load history to steady state. Altogether eight load histories were covered, and consequently eight separate FEM analyses were performed. A diagram showing in principal the two types of prepared LCs is presented in Figure 6.1-2 in the following. For both types a set of five LCs are shown in the Figure 6.1-2, corresponding to the performed FEM analyses where the covered LCSs were composed of step assemblies with ten of LC sets in each.

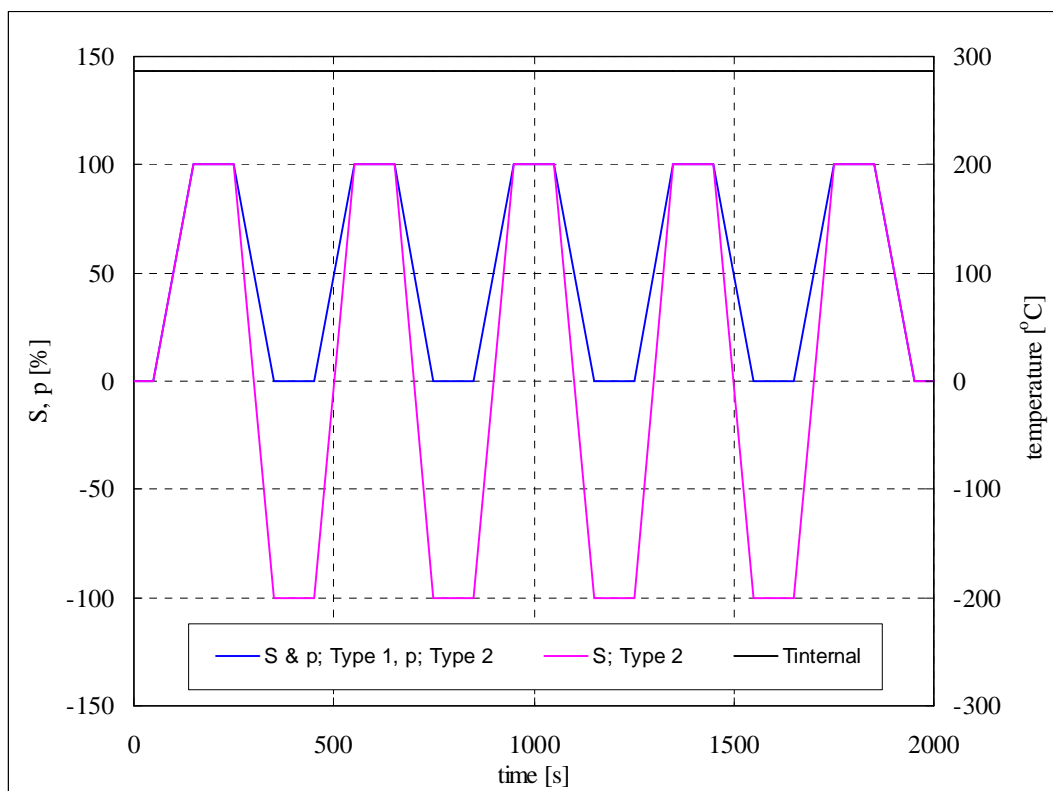


Figure 6.1-2. A diagram showing in principal the two types of prepared load cycles. Here S is axial stress at pipe end, p is internal pressure, Type 1 corresponds to LCSs from 1 to 4, and Type 2 corresponds to LCSs from 5 to 8, respectively. For S and p the shown values are percents of the respective LC specific maximum value, and when being on the negative side they correspond to compression. $T_{internal}$ is internal temperature.

6.2 Numerical heat transfer and stress/strain simulations

All heat transfer and stress/strain analyses were performed with FEM code Abaqus, version 6.8-2 [93, 94]. Concerning the analysis steps loading of WRSs and Start of operation that include both mechanical and temperature loads, they were performed as fully coupled. This means that the heat transfer and stress/strain solutions were obtained from the same analysis

run. As for analysis steps corresponding to analysis case specific load cycle sequences with altering mechanical loads but constant temperature, they were performed as static stress/strain analyses. To summarise, for each analysis run the first two steps were performed as fully coupled and the rest as static.

With Abaqus the time incrementation in a transient heat transfer analysis can be controlled directly by the user or automatically by the analysis code. Automatic time incrementation is generally preferred [94]. However, here due to the selected fully coupled analysis type, only user predetermined incrementation is allowed by the analysis code. This is carried out as a function of time, so that for each analysis step a suitable time increment is selected, i.e. these increments are analysis step specific. For analysis steps loading of WRSs and Start of operation, with corresponding durations of 3000 and 27000 s, the selected time increment for both was 50 s.

As for static analysis steps in the performed analyses, i.e. the load cycle sequences with total duration of 30000 s in each case, the maximum allowed time increment was 25 s. And as an ending criterion the analyses were continued keeping as static conditions those with which the last load cycle ended until the stress distributions had ceased altering, which took at maximum 1000 s, depending of the case.

As all considered loads, including WRS distributions, are symmetric in relation to geometry symmetry axis of the considered components, it sufficed to prepare an axisymmetric FEM model for the numerical simulations. The examined safe-end/pipe joint weld region of the prepared FEM model used in the simulations is shown in Figure 6.2-1, in the following.

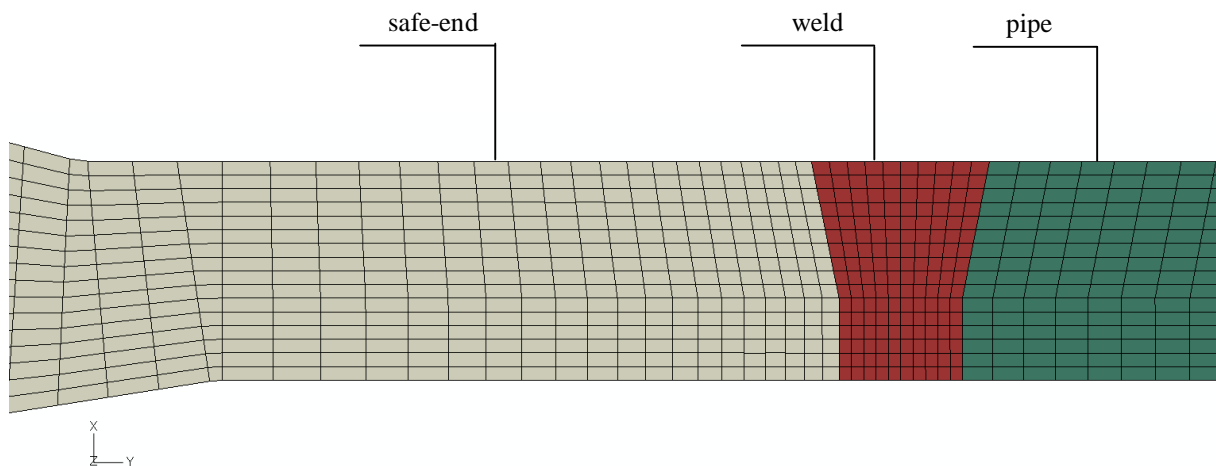


Figure 6.2-1. Detail of the element mesh of the axisymmetric FEM model of the examined safe-end/pipe joint weld, showing all involved material regions emphasised with different colours.

The thermal boundary conditions of the overall FEM model are such that for the outer surfaces and for the two cut-off sections with which the model was cut from the global structure, adiabatic boundary condition was applied, whereas for the inner surfaces, where heat will be exchanged between the water and the metal, the value of the heat transfer coefficient, α_{HT} , varied between 1000 and 70000 W/m²K.

In addition to the displacement boundary conditions caused by axial symmetry, those concerning the overall FEM model are such that for the safe-end side vertical cut-off surface, the horizontal displacements are set to zero, whereas the pipe side vertical cut-off surface is set to remain vertical and straight, but allowed to deform perpendicular to itself.

The axisymmetric FEM model was meshed with general purpose continuum elements. The selected element type from the Abaqus element library is CAX4RT, which is a 4-node rectangular bilinear displacement and temperature element, with reduced integration and hourglass control. Active degrees of freedom are the two displacements in the model plane, i.e. in the vertical (x -axis) and horizontal (y -axis, being here also the FEM model symmetry axis) directions, and temperature. The number of the nodes and elements in the whole model are 2836 and 2650, respectively.

The Oak Ridge National Laboratory (ORNL) has created a material model to describe the behaviour of austenitic SSs of types 304 and 316, see the Nuclear Standard NE F9-5T [95]. This model was used in the performed FEM analyses for the weld, safe-end and pipe materials, respectively. In this model the constitutive theory is uncoupled into a rate independent plasticity response and a rate dependent creep response, each of which is governed by a separate constitutive law. The plasticity theory uses a von Mises yield surface that can expand isotropically and translate kinematically in stress space. For kinematic work hardening, Ziegler's hardening rule [96] generalized to the non-isothermal case, is used in Abaqus [94]. The Nuclear standard NE F9-5T [95] provides for some coupling between the plasticity and creep responses by allowing prior creep strain to expand and translate the subsequent yield surface in stress space. For SSs of types 304 and 316, however, prior plasticity does not change the subsequent creep response.

To improve convergence in the FEM analyses, the line-search technique was used. With this technique one obtains a direction from an iterative procedure such as full and modified Newton-Raphson iteration [97]. The advantage in this technique is that by solving only a one-dimensional problem a better approximation is obtained. Then also the computation times of the analysis runs become shorter. Moreover, in some cases when it was not possible to achieve convergence with any other available means, it finally succeeded with the line-search technique.

It was deemed that 50 LCs in each prepared load history would suffice to show how the WRSs change/decrease as a function of LCs in the FEM simulations, if at all. This selected number of covered load cycles was also based on the computational feasibility, because as each load history was incorporated to a single analysis run, it was noticed in the preliminary analyses that the size of the output files soon became relatively large, i.e. of the scale of several GBs. With the selected number of analysis run specific load cycles the size of the output files and the analysis run durations stayed reasonable. Here a 2.0 GHz PC having two CPUs and 2.0 GB of RAM memory was used.

6.3 Analysis results from the viewpoint of WRS relaxation

In the following is a presentation concerning the heat transfer and stress/strain analysis results, mainly from the viewpoint of WRS relaxation. It was decided to limit the presentation here to concern only axial WRSs, as worldwide more than 90 % of the detected piping crack

cases have been oriented circumferentially, see e.g. ref. [98], and it is mainly the axial stresses that make such cracks grow.

More specifically, the WRS results obtained with FEM for the safe-end/pipe joint weld are examined in two sets of element mesh nodes, see Figure 6.3-1 in the following. In the through wall direction the spacing of the nodes is even for both node sets. As for the directions of the lines along which the nodes of the two examined node sets are located, the weld centre line (WCL) is vertical, whereas the weld offset line (WOL) tilts slightly from the vertical direction near the middle of the wall.

In the following is a brief description concerning the WRS simulation results in general:

- For LCS1 to LCS4, see Table 6.1-2, i.e. LCSs of Type 1 with $R = 0$; depending on the case, the WRSs ceased to change after 2 to 6 experienced LCs,
- For LCS5 to LCS8, see Table 6.1-2, i.e. LCSs of Type 2 with $R = -1$; depending on the case, the WRSs ceased to change after 2 to 5 experienced LCs,
- For all performed analyses the total stress exceeds the material yield strength in some regions of the component surfaces, i.e. in tension at inner surface and in compression at outer surface,
- For all performed analyses, the LCSs with larger stress load range decreased maximum WRS values more than those with smaller stress load range,
- For LCS1 to LCS4 in the weld centre line; the maximum WRS values in tension, which take place in node 30, decreased approximately from 28 to 60 %, depending on the case in question, whereas for maximum WRS values in compression, which take place in node 28, this decrease was negligible,
- For LCS5 to LCS8 in the weld centre line; the maximum WRS values in tension, which take place in node 30, decreased approximately from 22 to 48 %, depending on the case in question, whereas the maximum WRS values in compression, which take place in node 28, decreased approximately from 9 to 54 %, respectively,
- For all performed analyses in the weld centre line; within the wall the maximum WRS values both in tension and compression increased to some extent,
- For all performed analyses in the weld offset line; the maximum WRS values both in tension and compression decreased tens of percents both at inner & outer surface and slightly less so within wall,
- Note that despite the applied means to enhance convergence, analysis case LCS1 still diverged after 13th load cycle, while in the other seven cases the analysis runs converged through the considered load histories.

As within the scope of the performed numerical simulations the changing of the WRSs ceased relatively soon, in all cases in less than ten load cycles, it did not seem meaningful enough to examine further the behaviour of the WRSs in this respect. Instead, it was investigated in more detail how the WRSs alter as a function of applied stress range. Also, keeping in mind the result summary of the performed WRS relaxation procedure literature study, see Section 4.2, the altering of the considered load and stress response parameters was compared to the material yield strength, as it is mainly the part of the total stresses exceeding the yield strength that causes the WRSs to alter. Concerning the relaxation of the WRSs due to first load cycle as compared to that caused by the subsequent load cycles, it varied case specifically between approximately 50 and 80 % of the total WRS decrease. This is in line with what is described in many WRS relaxation assessment procedure source documents, see Section 4.2.

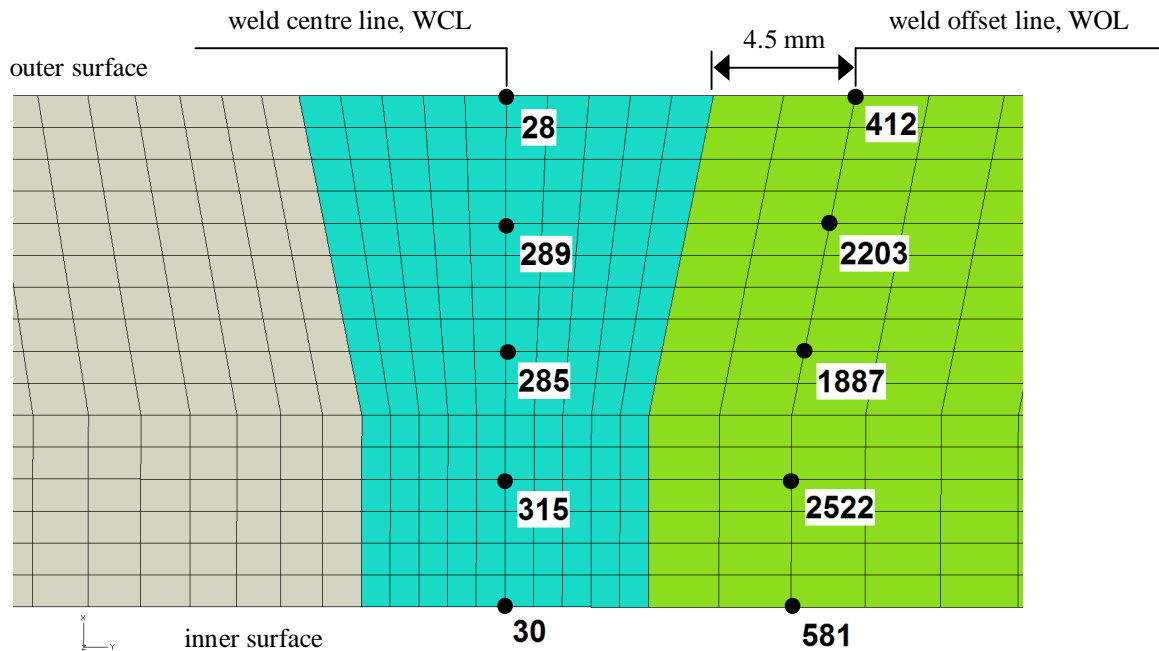


Figure 6.3-1. The node numbers of the two examined node sets in the safe-end/pipe joint weld element mesh region. Both sets are evenly spaced in the through wall direction, with the weld centre line being vertical, whereas the weld offset line tilts slightly near the middle of the wall.

In the following are presented the results of this investigation. Figure 6.3-2 presents for LCS1 to LCS4, i.e. LCSs of Type 1 with $R = 0$, the axial WRSs at the end of the considered load histories as a function of the part of the cyclic max total stresses perpendicular to weld exceeding the yield strength, with both axis parameters being divided by the yield strength. Also presented is a distribution that is linearly fitted to these results. Figure 6.3-3 presents the corresponding results for LCS5 to LCS8, i.e. LCSs of Type 2 with $R = -1$, again together with a fitted linear distribution. In Figure 6.3-3 the results are presented for two nodes, as corresponding to the locations of both maximum tension and compression, because unlike the results for LCSs of Type 1 as presented in Figure 6.4-2, with LCSs of Type 2 the total stresses exceed the yield strength also in compression, in addition to that in tension. The linear distribution was selected for fitting the mentioned results because due to the shapes of their distributions it was deemed to suit best for that purpose. Logarithmic fitting was not attempted here, even though a number of the covered WRS relaxation assessment procedures use that function to describe cyclically occurring WRS relaxing, because in those procedures the loading amplitude is assumed as constant, and possible WRS relaxation for relatively large number of load cycles is examined. Then, for comparison purposes Figure 6.3-4 presents only the two mentioned linearly fitted distributions.

In these three result figures the yield strength corresponding to 0.2 % strain is denoted as σ_y , whereas the part of the total cyclic max stresses exceeding the yield strength is denoted as $(\sigma_{total,max} - \sigma_y)$, respectively. It is also reminded that the results presented here were obtained for temperature of 286 °C, in other temperatures they would be to some extent different.

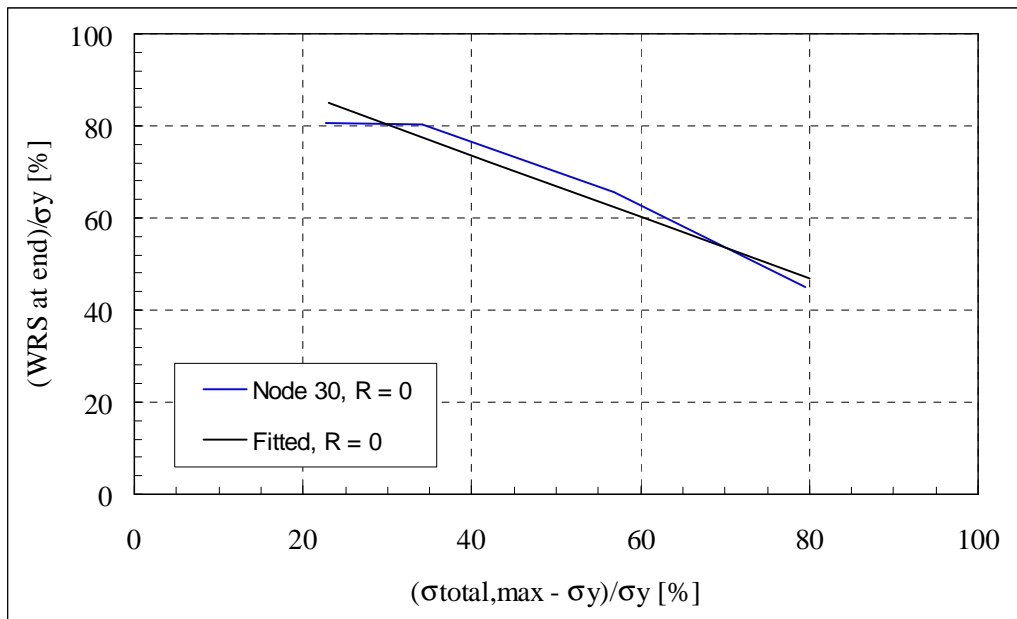


Figure 6.3-2. For LCS1 to LCS4 the axial WRSs at the end of the considered load histories as a function of the part of the cyclic max total stresses perpendicular to weld exceeding the yield strength corresponding to 0.2 % strain, with both axis parameters being divided by the yield strength. Also presented is a distribution that is linearly fitted to these results.

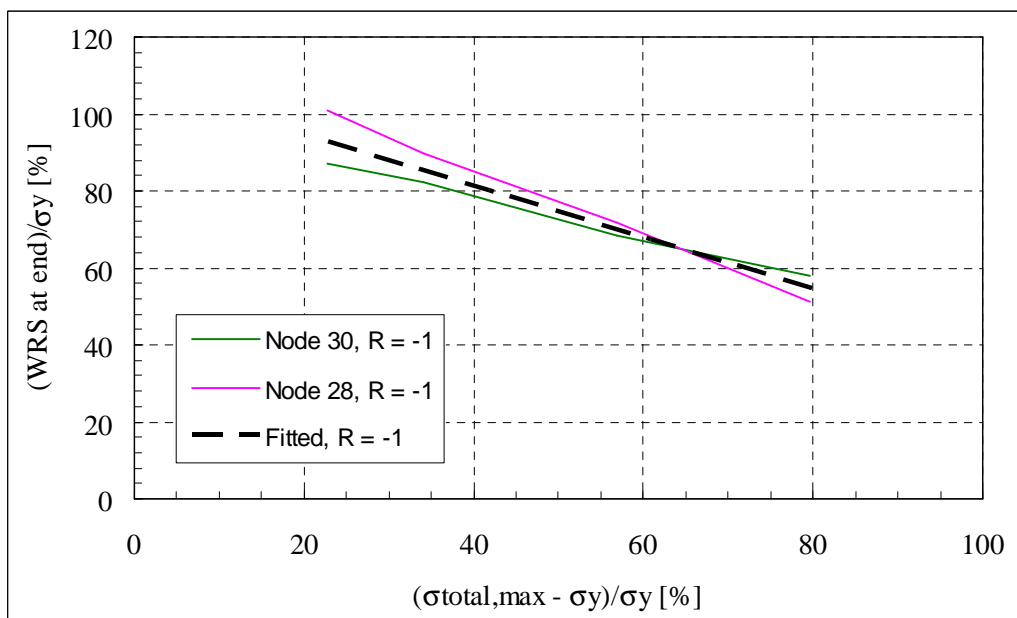


Figure 6.3-3. For LCS5 to LCS8 the axial WRSs at the end of the considered load histories as a function of the part of the cyclic max total stresses perpendicular to weld exceeding the yield strength corresponding to 0.2 % strain, with both axis parameters being divided by the yield strength. Also presented is a distribution that is linearly fitted to these results.

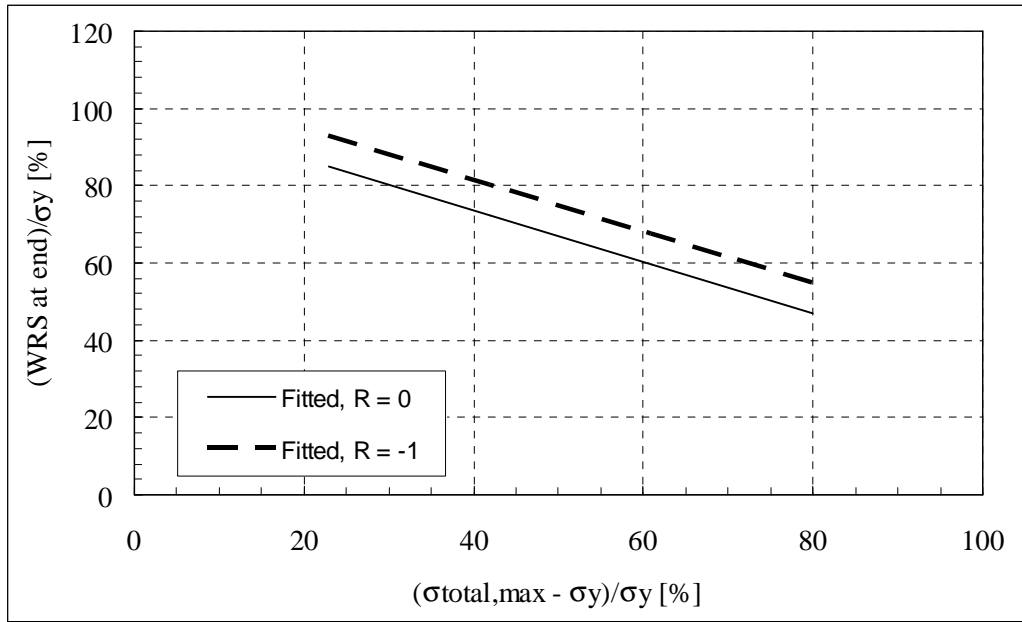


Figure 6.3-4. Separately both for LCS1 to LCS4 and LCS5 to LCS8, the linearly fitted distributions describing the axial WRSs at the end of the considered load histories as a function of the part of the cyclic max total stresses perpendicular to weld exceeding the yield strength corresponding to 0.2 % strain, with both axis parameters being divided by the yield strength.

The effect of the magnitude of the applied loading stress range to the decrease of the WRSs can clearly be seen from the mentioned three result figures. In addition, Figure 6.3-4 on its behalf shows that the stress ratio R also contributes to the altering of the WRSs, so that with $R = 0$ they decrease quite accurately with an offset of 8.0 % more than with $R = -1$, respectively.

The more detailed discussion concerning the WRS simulation results here is focused on result data from surface nodes. This is because in them the absolute values of the total stresses exceeded often the material yield strength during the covered cyclic loading histories. Whereas in inner nodes the experienced absolute values of the total stresses stayed mainly lower than the yield strength, and consequently in them the WRSs altered during loading histories very little, if at all.

The developed equations for the two linearly fitted distributions describing for the considered austenitic SS in the temperature of 286 °C the max axial WRSs at the end of the considered load histories LCS1 to LCS8 as a function of the applied total stress load range, are as follows:

$$\sigma_{\text{WRS,AXIAL}} = -\frac{2}{3} \cdot \sigma_{\text{total,max}} + \frac{20}{12} \cdot \sigma_y, \text{ for } R = 0, \quad (6.3-1)$$

$$\sigma_{\text{WRS,AXIAL}} = -\frac{2}{3} \cdot \sigma_{\text{total,max}} + \frac{21}{12} \cdot \sigma_y, \text{ for } R = -1, \quad (6.3-2)$$

and the validity range for both equation (6.3-1) and (6.3-2) is:

$$23 \leq \left(\frac{\sigma_{\text{total,max}} - \sigma_y}{\sigma_y} \right) \cdot 100 \leq 80,$$

where $\sigma_{\text{WRS,AXIAL}}$ [MPa] is the remaining max axial WRS, σ_y [MPa] is yield strength corresponding to 0.2 % strain, $\sigma_{\text{total,max}}$ [MPa] is cyclic max total axial stress value (i.e. sum of max value of applied cyclic stress load and initial WRS value), and R [MPa/MPa] is stress ratio, i.e. $\sigma_{\text{min}}/\sigma_{\text{max}}$, respectively.

As compared to relative units of WRS results presented in Figures 6.3-1 to 6.3-3, the equations (6.3-1) and (6.3-2) have been written straight for axial WRS values, so as to obtain more useful expressions for WRS decrease assessment purposes.

It could be argued, that for the results concerning LCS5 to LCS8, i.e. LCSs of Type 2 with $R = -1$, two separate linear distributions could be fitted, with one for maximum tensile axial WRSs (corresponding to Node 30) and the other for maximum compressive axial WRSs (corresponding to Node 28), respectively, see the red and green result curves in Figure 6.3-3. However, the material model used here is identical for tension and compression, and also the cyclic loading in this case is symmetrical, i.e. the absolute values of the maximum loading in tension and in compression are equal. Only the geometry of the model deviates from symmetry over the component wall, having here basically a cylindrical structure, and thus geometrical effect for the inner and outer surface differ to some extent. In addition, the wall thickness is not constant over the component model, as on the nozzle side it is more than twice thicker than on the pipe side. Thus it is considered that the approach followed here in forming the WRS decrease equations is appropriate and realistic enough.

The scope of the performed FEM analyses with cyclic loading was relatively limited, and so consequently is that of the fitted equations (6.3-1) and (6.3-2). However, the obtained results provide an example of an approach to derive analytical WRS relaxation equations for practical applications. Moreover, as the involved computational effort is reasonable, it is considered that the approach used here is technically feasible. Thus the scope of the WRS relaxation assessment equations could be widened to consider other temperatures and load amplitudes quite easily without the needed computational work becoming too resource demanding. Also, as it is FEM that is applied here, the presented approach could be well extended to other components having other materials and geometries as well. However, the thus obtained WRS relaxation equations should be to a sufficient extent verified against measurement data.

7 Discussion and suggestions for further research

According to experimental measurements and FEM analysis results the WRSs are typically relatively high in NPP component welds which are in as-welded state. Also, many NPP component welds have not been subject to any improvement treatment after manufacturing/installation, i.e. the welds remain in as-welded state. Thus it is of considerable importance to take the WRSs into account in the structural integrity analyses, e.g. crack growth sensitivity analyses. The residual stress distributions present in a structure are the result of the manufacturing history and the elastic-plastic properties of the structure. The former referring to the mechanical and thermal processes executed during the whole production sequence and the latter to the elastic-plastic behaviour of the structure.

The conditions/treatments that relieve residual stresses in NPP components include irradiation effects, thermal effects and mechanical load effects. In practise irradiation is not used to relax WRSs. Thus irradiation concerns mainly the RPV and its internals, as they are exposed to nuclear irradiation emanating from inside of the RPV, whereas its effect to other NPP systems and components is negligible. Thermal effects include annealing and PWHT, which are commonly used means to relieve the residual stresses. Also mechanical loads can relax the residual stresses, current techniques include e.g. shot-peening and vibratory stress relief.

Selection of suitable WRS distribution assumptions for structural integrity analyses is an issue requiring careful consideration. Several WRS definition procedures are currently available. Seven of those are compared in this study in the light of application examples for a representative set of NPP pipe components.

The main results of the performed literature study are the altogether 25 discovered residual stress (RS) relaxation assessment procedures. These were found as a result of an extensive survey covering a great number of sources of information, including the major technical scientific journals, with tracing of cited references in each new article as it was obtained, as well as conference papers, academic theses, dissertations, handbooks and technical reports, both from libraries in paper format and from Internet databases.

Brief descriptions of the main characteristics of the found WRS relaxation assessment procedures are given. In addition to the procedure equations/formulas, also mentioned are the original reference/authors, target of application, required input data, parameters to be fitted, range of applicability and the covered phenomena.

The found WRS relaxation procedures are divided to three categories according to characteristics of the stress relaxing physical phenomena they cover. The mentioned three categories and the numbers of the associated found RS relaxation procedures are:

- Mechanical residual stress relaxation; 18 procedures,
- Thermal residual stress relaxation; 6 procedures,
- Thermomechanical residual stress relaxation; 1 procedure.

Not all of the covered RS relaxation procedures consider specifically welds, but also selected details in the base material side, such as surfaces, notches, geometry details with relatively small radius of curvature and local holes, or regular and continuous geometries as well.

However, as the physical events that can cause RS relaxing are by and large the same for most metallic materials, especially concerning various steel grades, the presented RS relaxation procedures are assumed to be applicable to NPP steel component weld materials as well.

Also, several of the presented RS relaxation procedures are mainly developed for assessing the gradual relaxation of intentionally induced surface RSs that have been obtained with various surface treatments, such as shot-peening, which typically create a compressive surface RS distribution, which in turn increases the fatigue life of the component. As all such RS relaxation procedures include material specifically adjustable parameters, they can presumably be fitted so that they are applicable to through thickness RS relaxation assessments of NPP component welds as well.

Typically the available RS data contains measurement uncertainties, which vary from technique to technique. Generally the main uncertainties in RS measurement can be categorised according to ref. [61] to those that are technique specific, material specific, and component/geometry specific, respectively.

In general, errors in measuring WRSs are often classified as systematic or random [63, 65]. Systematic error is usually caused by factors that systematically affect measurement such as the use of the instrument (e.g. miscalibration and specimen alignment), inaccurate elastic modulus and Poisson coefficient, and the type of stress analysis used in fitting data (use of different fitting techniques, algorithm and software). Systematic errors may also arise from the use of a different assumption model in deriving stresses from the measured quantities. Random error is caused by factors that randomly affect measurements.

The published experimental as-welded state WRS data have a substantial scatter. Consequently the WRS distributions defined in the commonly used fitness-for-service procedures have been developed as tensile upper bound solutions based on the data. However, according to [86, 87, 88, 89], this approach not only lacks consistency for the same type of joints and welding parameters, but can either significantly overestimate the WRS level in some cases, or underestimate it in others.

As the relaxation of WRSs during plant operation is an issue that has thus far received quite limited attention, it was no surprise that no documentation specifically concerning quantification of its uncertainties were found available. It can be estimated, however, that the sources of uncertainty associated with defining the as-welded state WRSs do not decrease in quantity when moving on to using any of the WRS relaxation assessment procedures covered here. This is an issue that appears to require further research. At least one can perform sensitivity analyses with the WRS relaxation assessment procedures e.g. to see what is the model response for altering its primary variables within their assessed realistic regions of variation.

Concerning probabilistic methods to define WRS distributions, the following procedures are described in this study: least-squares technique, Bayesian statistical approach, spatial Bayesian approach, spatial deconvolution approach, heuristic method, fuzzy-set approach, and goodness of fit technique. Thus here mainly both conventional and Bayesian statistical techniques are considered. The latter approach uses probability distributions for both the measured data and the free parameters in analytical models used to fitting the data. In contrast, conventional statistical techniques only consider the probability distributions of experimental data. In addition the Bayesian approach can incorporate sources of prior information about measurements and this allows analysts to include their personal judgments in the analysis [63].

Also described in this study is the treatment of WRSs in some current notable probabilistic crack growth analysis codes. These PFM based codes are WinPRAISE [74], PRO-LOCA [79], ProSACC [6] and PASCAL-SP [80]. The WRSs can be input to WinPRAISE using one of the altogether seven options, which being both deterministic and random. The documentation [77] related to WinPRAISE also considers what should the WRS distributions be like, so that the crack growth analysis results would correspond to existing crack data. As compared to ASME recommendations [2, 75], according to the piping component test results obtained by PNNL [77], for WRS adjustment factor, f , a value of $f = 0.75$ gives good agreement between predicted and observed leak probabilities. In the PRO-LOCA, the WRSs are assumed to follow a 3rd order polynomial function through component wall. The associated probabilistic aspects are that the user can give as distributed the WRS at inner component surface as well as the location within the wall where the WRS changes from tension to compression. In ProSACC the distribution of WRSs can follow a normal, log-normal, Weibull or exponential distribution. For all of these distributions the user needs to provide the necessary mean value and standard deviation data. However, no recommendations concerning them are given, nor guidance from where such data could be obtained. PASCAL-SP includes a WRS distribution database that consists of results from parametric 2D axisymmetric FEM simulations for 250A pipe component. It is assumed that the uncertainty of WRS at a point in or near welding joint follows a normal distribution. The statistics in the form of average and standard deviation of WRS at each point and correlation coefficient between nearest neighbouring points in piping thickness direction, are introduced to determine the WRS distribution.

The numerical simulations of WRS distributions in this study were carried out with the same FEM model as was used in the previous part of the project, i.e. that consisting of a safe-end connecting to a nozzle and pipe, see ref. [90]. The scope of the analyses was extended so that here it was examined how the WRS distributions in the safe-end/pipe joint weld region behave under constant cyclic loading. A more detailed description of the performed simulations is presented in the associated analysis report [91].

The wall thickness in the region of the examined safe-end/pipe joint weld is 16 mm. The initial WRS values for the examined weld were assumed according to the as-welded state WRS distribution equations of the SINTAP procedure [7, 8]. In this case they vary in perpendicular to weld direction linearly from 245 MPa in the inner surface to -245 MPa in the outer surface, for temperature of 286 °C. Of the load types provided by Abaqus, the Body Force was selected for modelling WRSs in the safe-end/pipe joint weld region in the axisymmetric computation model. With this load type it is possible to set density forces to act on elements, or more specifically throughout their volumes, as the physical dimension this load type is N/m^3 . The heat transfer and stress/strain FEM analyses were performed with Abaqus version 6.8-2 [93, 94].

The performed analyses cover altogether eight loading histories, each being a constant amplitude load cycle sequence (LCS), and together spanning a representative range of loading conditions. This means that eight separate FEM analyses were carried out. The mentioned LCSs divide to two main types, with the axially oriented stress being the main cyclic load parameter. For the Type 1 the load range varies between 0 and 150 MPa, the stress ratio being in these cases 0. Whereas for the Type 2 the load range varies between -150 and 150 MPa, the stress ratio being in these cases -1, respectively. All prepared load histories include 50 load cycles, which was a sufficient number to show how the WRSs change/decrease as a function of LCs in the simulations, if at all.

The ORNL material model [95], specifically prepared to describe the behaviour of types 304 and 316 austenitic SSs, was used in the performed FEM analyses for the weld, safe-end and pipe materials. In this model the constitutive theory is uncoupled into a rate independent plasticity response and a rate dependent creep response, while the plasticity theory uses a von Mises yield surface that can expand isotropically and translate kinematically in stress space. For kinematic work hardening Ziegler's hardening rule [96], generalized to the non-isothermal case, is used in Abaqus [94]. To improve convergence in the FEM analyses, the line-search technique was used [97]. With this technique a better approximation is obtained, also the computation times of the analysis runs become shorter.

In the following is a brief description concerning the WRS simulation results:

- For all performed analyses the total stress exceeds the material yield strength in some regions of the component surfaces, i.e. in tension at inner surface and in compression at outer surface.
- For all performed analyses, the LCSs with larger stress load range decreased maximum WRS values more than those with smaller stress load range.
- For Type 1 load histories with stress ratio of 0; in the weld centre line the maximum WRS values in tension, which take place in inner surface, decreased approximately from 28 to 60 %, depending on the case in question, whereas for maximum WRS values in compression, which take place in outer surface, this decrease was negligible.
- For Type 2 load histories with stress ratio of -1; in the weld centre line the maximum WRS values in tension, which again take place in inner surface, decreased approximately from 22 to 48 %, depending on the case in question, whereas for maximum WRS values in compression, which again take place in outer surface, this decrease was approximately from 9 to 54 %, respectively.
- Concerning the relaxation of the WRSs due to first load cycle as compared to that caused by the subsequent load cycles, it varied case specifically between approximately 50 and 80 % of the total WRS decrease.
- For all performed analyses in the weld centre line; within the wall the maximum WRS values both in tension and compression increased to some extent.
- For all performed analyses in the offset line which is located approximately 4.5 mm to the base material side from the weld edge; the maximum WRS values both in tension and compression decreased tens of percents both at inner & outer surface and slightly less so within wall.

Based on the numerical WRS simulation results and within their scope, two analytical WRS relaxation assessment equations were also developed for the considered safe-end/pipe weld region in the temperature of 286 °C.

The scope of the WRS relaxation assessment equations could be widened to consider other temperatures and load amplitudes quite easily without the needed computational work becoming too resource demanding. Also, as it is FEM that is applied here, the presented approach could be well extended to components having other materials and geometries as well. However, the thus obtained WRS relaxation equations should be to a sufficient extent verified against measurement data.

Concerning cyclic loads, and keeping in mind that here only constant amplitude load cycle sequences were applied, it would be interesting to examine the model response for variable amplitude load cycle sequences as well. For instance, to see for the components analysed in this study whether such new results would fall between those obtained here for the constant

amplitude load cycles with stress ratio, R , as 0 and -1, or somewhere outside the region spanned by these results, and if so, then in what magnitude.

Here an axisymmetric FEM model was used in the fully coupled thermal-stress/strain analyses. The next step could be to use a suitably optimised global 3D FEM model in these analyses, or a coarser global 3D model in combination with a local but large enough and more densely meshed sub-model containing the region of interest, i.e. a weld. 3D modelling approach would also allow including bending loads.

One option to create local WRS distributions to a FEM model, which was due to work schedule limitations not attempted here, would be to use such values for the coefficient of thermal expansion in the weld region that the resulting stress field within the covered temperature range would match the desired WRS distribution. When using this approach the values of the coefficient of thermal expansion for the other material regions would be maintained in their original (i.e. correct) values or modified slightly.

Thermomechanical residual stress relaxation phenomena are still not completely clear, hence they need to be examined further.

As for crack growth analysis procedures, a parametric study is planned to be carried in which it is clarified based on existing world-wide and/or TVO crack data, what should the WRS distributions be like, so that the crack growth analysis results would correspond to existing crack data. Here it is assumed that the available material and process condition specifically constant crack growth formula parameters are defined realistically/correctly. Fracture mechanics based analysis code VTTBESIT, which is originally developed by Fraunhofer-Institut für Werkstoffmechanik (IWM) and further developed at VTT, will be used in the involved crack growth analyses. Also, applicable existing crack data for these analyses remains to be obtained. The challenge here is to find such data which includes also the duration of the crack growth process, starting from a relative early stage (sufficiently close to nucleation) up to the time of detection.

Also a set of computational examples for a representative selection of NPP component welds is planned. This will cover applicable WRS relaxation assessment procedures as well as as-welded state WRS definitions from commonly used fitness-for-service procedure handbooks. The set of computational examples will cover:

- application of WRS relaxation assessment procedures to NPP component welds,
- comparison of WRS distributions as obtained from experiments to those according to various WRS definition procedures,
- crack growth analyses with VTTBESIT for piping welds including WRSs.

Finally, the formation of the WRSs themselves could be examined via numerical simulations. Relevant guidance concerning this task will be provided e.g. in the next edition/revision of the R6 Method, see R5/R6 Newsletter [99]. Also this would necessitate the use of 3D FEM models, as manufacturing of circumferential (or any) weld is essentially a process taking place and causing effects three dimensionally.

8 Conclusions

One unfortunate departure from realism in case of some of the more recent WRS procedures, e.g. R6 Method Rev. 4, API 579 and FITNET, is that in the transverse to weld direction the WRSs are mostly not self-balancing. While making local crack growth calculations with a fracture mechanics based analysis tool this feature may not pose remarkable problems, but in case of corresponding 3D FEM analyses it is quite the other way around, as in order to achieve equilibrium FEM automatically modifies the WRSs towards self-balanced distributions over the component model walls, and thus the original WRS distributions are not maintained.

In the light of the obtained WRS application results for the considered Small, Medium and Large sized pipe components of austenitic SS, only ASME recommendations and SINTAP procedure in all cases, and SSM handbook in most cases, give WRS distributions that are self-balancing in the transverse to weld direction. Of them the least over conservative WRS procedure appears to be SINTAP. As for the corresponding analysis results for cases concerning ferritic steel, for Small and Large cross-sections SSM handbook gives self-balancing WRS distributions, whereas for Medium cross-section only SINTAP procedure gives a self-balancing WRS distribution, respectively.

According to the above mentioned and other commonly used WRS assumption procedures, if a weld has not been in any improvement treatment, such as PWHT, the WRSs will not alter in service from the considerably high values corresponding to the as-welded state. When considering NPPs that have been in operation for decades, this assumption does not appear exactly realistic. Thus one motivation to carry out a thorough literature survey concerning assessment procedures for altering/relaxing of WRSs in NPP components that have experienced decades worth of typical transient load cases and operational conditions in general, stems from this background. With such assessment procedures the unnecessarily added conservatism in many computational structural integrity analyses could hopefully be to some extent decreased, which would consequently lead to more realistic analysis results. For instance, the structural integrity analyses concerning SCC typically include using crack growth equations having material and environment specific constant parameters the values for which have been defined as upper bound solutions based on the underlying laboratory measurement data. The ensuing crack growth sensitivity analysis results obtained using such equation parameter values, as unfortunately no best estimate alternatives are presently available, already show faster crack growth than in reality has been experienced in the plants. As the effect of SCC is time dependent, it remarkably increases the already conservative computed crack growth rates when including to considered loads also conservatively defined WRS distributions and even letting them remain in their maximum i.e. as-welded state values through crack growth sensitivity analyses spanning several decades of plant operation.

The main results of this study are the altogether 25 discovered RS relaxation assessment procedures. These were found as a result of an extensive literature survey covering a great number of sources of information.

Most of the found RS relaxation procedures consider mechanical cyclic loading as the covered loading phenomena. This is quite as expected, as in general RS relaxation procedures have been mainly developed to applications associated with repeating load cycles and relatively small altering of temperatures, such as vehicle and machinery components. Much

less were found RS relaxation procedures that consider thermal loading as the covered loading phenomena. These are mainly developed for assessment of effects of annealing and creep range temperatures to RS distributions in components. Only one thermomechanical RS relaxation procedure was found.

All in all, each of the covered RS relaxation procedures here contain material and/or temperature range dependent parameters that need to be fitted to sufficiently large amount of accurate enough data. Also required are data concerning the initial RS state. If measured RS data are not available, the initial RS distribution has to be assessed somehow, e.g. using such alternatives from the WRS definition procedures covered in Chapter 3 that give reasonably conservative and in transverse to weld direction self-balancing RS values. For the time being it appears that only advanced numerical analysis codes with coupled analysis capabilities, e.g. advanced finite element analysis (FEA) codes, enable to perform analyses that at the same time take into account all possible relevant physical RS relaxation phenomena.

As within the scope of the performed numerical simulations the changing of the WRSs ceased relatively soon, in all cases in less than ten load cycles, it did not seem meaningful enough to examine further the behaviour of the WRSs in this respect. Instead, it was investigated in more detail how the WRSs alter as a function of the applied stress range. The linear distribution was selected for fitting the FEM results because due to the shapes of their distributions it was deemed to suit best for that purpose.

The developed analytical equations for the two linearly fitted distributions describing for the considered austenitic SS in the temperature of 286 °C the max axial WRSs at the end of the considered load histories as a function of the applied total stress load range, are as follows:

$$\sigma_{\text{WRS,AXIAL}} = -\frac{2}{3} \cdot \sigma_{\text{total,max}} + \frac{20}{12} \cdot \sigma_y, \quad \text{for } R = 0, \text{ and}$$

$$\sigma_{\text{WRS,AXIAL}} = -\frac{2}{3} \cdot \sigma_{\text{total,max}} + \frac{21}{12} \cdot \sigma_y, \quad \text{for } R = -1,$$

and the validity range for both equations is:

$$23 \leq \left(\frac{\sigma_{\text{total,max}} - \sigma_y}{\sigma_y} \right) \cdot 100 \leq 80,$$

where $\sigma_{\text{WRS,AXIAL}}$ [MPa] is the remaining max axial WRS, σ_y [MPa] is yield strength corresponding to 0.2 % strain, $\sigma_{\text{total,max}}$ [MPa] is cyclic max total axial stress value (i.e. sum of max value of applied cyclic stress load and initial WRS value), and R [MPa/MPa] is stress ratio, i.e. $\sigma_{\text{min}}/\sigma_{\text{max}}$, respectively, see equations (6.3-1) and (6.3-2) in Section 6.3.

The scope of the performed FEM analyses with cyclic loading was relatively limited, and so consequently is that of the developed fitted equations). However, the obtained results provide an example of an approach to derive analytical WRS relaxation equations for practical applications. Moreover, as the involved computational effort is reasonable, it is considered that the approach used here is technically feasible, and can thus be applied to components with other geometries, materials and experienced loads.

References

1. Cronvall, O. Review and Comparison of Welding Residual Stress Definitions, VTT Research report VTT-R-01415-08. Espoo, Finland, 2008. 102 p.
2. Section XI Task Group for Piping Flaw Evaluation, ASME Code. Evaluation of Flaws in Austenitic Steel Piping. Journal of Pressure Vessel Technology, Vol. 108, 1986. Pp. 352-366.
3. Shack, W., J. et al. Environmentally Assisted Cracking in Light Water Reactors: Annual Report, October 1981 – September 1982. NUREG/CR-3292, Washington D.C., U.S. Nuclear Regulatory Commission, June 1983.
4. British Standard BS 7910: 1999, Guide on methods for assessing the acceptability of flaws in fusion welded structures, 4th draft after public comment. England, 8 April, 1999.
5. R6 Method; Assessment of the Integrity of Structures containing Defects, Revision 4. 2004 update of 2001 edition. British Energy (BE).
6. Dillström, P. et al. 2008. A Combined Deterministic and Probabilistic Procedure for Safety Assessment of Components with Cracks – Handbook. SSM Research Report 2008:01, Swedish Radiation Safety Authority (Strålsäkerhetsmyndigheten, SSM). Stockholm, Sweden, 2008. 27+196 p.
7. SINTAP; Structural Integrity Assessment Procedures for European Industry; Final Procedure: November 1999. Project funded by the European Union (EU) under the Brite-Euram Programme: Project No. BE95-1426, Contract No. BRPR-CT95-0024.
8. Barthelemy, J., Y., Janosch, J., J. Structural Integrity Assessment Procedures for European Industry; SINTAP; Task 4; Compendium of Residual Stress Profiles; Final Report: 18.5.1999. Project funded by the European Union (EU) under the Brite-Euram Programme: Project No. BE95-1426, Contract No. BRPR-CT95-0024. 40+18 pages.
9. American Petroleum Institute (API). Recommended practice for fitness-for-service. API 579. Washington, DC, American Petroleum Institute, 2000.
10. FITNET Fitness-for-Service PROCEDURE – FINAL DRAFT MK7. Editor(s) Koçak, M. et al. European Fitness-for-Service Thematic Network – FITNET. Germany. 1.5.2006.
11. Andersson, P. et al. 1998. A Procedure for Safety Assessment of Components with Cracks – Handbook, 3rd revised edition. SAQ/FoU-Report 96/08, SAQ Kontroll AB. Stockholm, Sweden. 104 p.
12. ABB ATOM Materialhandboken – Normer och datablad för metalliska material. ABB Atom AB, 1999.
13. Danko, J. C. 1990. A Review of Weld Residual Stresses in Austenitic Stainless Steel Pipes. Recent Trends in Welding Science and Technology. Proceedings of 2nd International Conference, Gatlinburg, TN, 14-18 May 1989. Pp. 113-118.
14. Safety aspects of nuclear power plant ageing. Technical Report IAEA-TECDOC-540, International Atomic Energy Agency (IAEA), Vienna, Austria, January 1990. 200 p.
15. Vöhringer, O. In: Residual Stresses: Generation – Measurement – Valuation, Vol. 1. Editors: Macherauch, E., Hauk, V. DGM-Informationsgesellschaft, Oberursel, 1983. pp. 49-83.

16. Vöhringer, O. *Advances in Surface Treatments, Vol. 4, International Guidebook on Residual Stresses*. Editor: Niku-Lari, A., Pergamon Press, Oxford, 1987. pp. 367-396.
17. Hänninen, H., et al. Dissimilar metal weld joints and their performance in nuclear power plant and oil refinery conditions. VTT Research Notes 2347, Technical Research Centre of Finland (VTT), Espoo, Finland, June 2006. 208 p.
18. Schulze, V., Lang, K-H., Vöhringer, O., Macherauch, E. *Proceedings of International Conference on Shot Peening 6*. Editor: Champaign, J. San Francisco, USA, 1996. pp. 412-423.
19. McClung, R., C. A literature survey on the stability and significance of residual stresses during fatigue. *Fatigue & Fracture of Engineering Materials & Structures, Volume, 30 Issue 3, 2007*. pp. 173 - 205.
20. Schreiber, R. *Untersuchungen zum Dauerschwingverhalten des kugelgestrahlten Einsatzstahles 16 Mn Cr 5 in verschiedenen Wärmebehandlungszuständen*. Dissertation, Karlsruhe, Germany, 1976.
21. Wohlfahrt, H. *Kugelstrahlen und Dauerschwingverhalten*. 1st Conference on Shot Peening, Paris, France, September 1981. Pergamon Press Ltd.
22. Starker, P., Wohlfahrt, H., Macherauch, E. Subsurface crack initiation during fatigue as a result of residual stresses. *Fatigue of Engineering Materials and Structures, Vol. 1, 1979*, pp. 319-327.
23. Saunders, G., G., Claxton, R., A. *VSR – a current state-of-the-art appraisal. Residual stress in welded construction and their effects*. London: The welding institute; 1978. p. 173–83.
24. Yang Xu, Mao Cai Sun, Qing Ben Li. Effectiveness criterion for the in situ evaluation of vibratory stress relieving process. *Transaction of China welding institution (Chinese) 2002; 23(2): 63–7*.
25. James, M., Paterson, A., Sutcliffe, N. Constant and variable amplitude loading of 6261 aluminum alloy I-beams with welded cover plates – influence of weld quality and stress relief. *International Journal of Fatigue 1997; 19(2): 125–33*.
26. Rao, D., Zhu, Z., Chen, L., Ni, C. Reduce the residual stresses of welded structures by post-weld vibration. *Material Science Forum, 2005; 490–491: 102–106*.
27. Kuuluvainen, O. Email sent to Cronvall, O. Teollisuuden Voima Oy (TVO), 24.1.2008. 1 p.
28. Mitman, J. (Project Manager). *Revised Risk Informed In-Service Inspection Evaluation Procedure*. Electric Power Research Research Institute, Interim Report EPRI TR-112657. California, April 1999.
29. Viswanathan, R. *Damage Mechanisms and Life Assessment of High-Temperature Components*. ASM International, U.S., Third Printing, September 1995. 497 p.
30. *Welding of Stainless Steels and Other Joining Methods, A Designers' Handbook Series No. 9002*. Distributed by Nickel Development Institute (NiDI), Produced by American Iron and Steel Institute, U.S. 47 p.
31. *ASM Specialty Handbook: Stainless Steels*. Edited by Davis, J., R. ASM International, U.S., January 1994. 576 p.
32. Morrow J, Sinclair G., M. Cycle-dependent stress relaxation. In: *Symposium on Basic Mechanisms of Fatigue, ASTM STP 237*. American Society for Testing and Materials, 1958.

33. Jhansale, H., R., Topper, T., H. Engineering analysis of the inelastic stress response of a structural metal under variable cyclic strains. In: *Cyclic Stress-Strain Behavior - Analysis, Experimentation, and Failure Prediction*. American Society for Testing and Materials, 1973:246–70.
34. Landgraf, R., W., Chernenkoff, R., A. Residual Stress Effects on Fatigue of Surface Processed Steels, Analytical and Experimental Methods for Residual Stress Effects in Fatigue, ASTM STP 1004, Champoux, Underwood, and Kapp, Editors, American Society for Testing and Materials, 1988. pp. 1-12.
35. Kodama S. The behavior of residual stress during fatigue stress cycles. In: *Proceedings of the International Conference on Mechanical Behavior of Metals II*. Kyoto: Society of Material Science, 1972; 2 :111–118.
36. Zhuang, W., Z., Halford, G., R. Investigation of Residual Stress Relaxation Under Cyclic Load. *International Journal of Fatigue*, Vol. 23, 2001, pp. S31-S37.
37. Rao, D., Wang, D., Chen, L., Ni, C. The effectiveness evaluation of 314L stainless steel vibratory stress relief by dynamic stress. *International Journal of Fatigue* 29 (2007) 192–196.
38. Han, S. H., Kang, S. B. and Shin, B.C., 2001. Relaxation of welding residual stresses under fatigue loads. Korean society of mechanical engineers, Proceedings of annual spring conference, Part A. Pp. 424-429.
39. Han, S. H, Lee, T. K and Shin, B. C., 2002. Residual stress relaxation of welded steel components under cyclic loads, *Materials Technology (Steel Research)*, Vol. 73, No. 9, pp. 414-420.
40. Li, L., Wan, Z., Wang, Z., Ji, C. Residual stress relaxation in typical weld joints and its effect on fatigue and crack growth. *Acta Metall. Sin. (Engl. Lett.)* Vol.22, No.3, pp. 202-210, June 2009.
41. Kwofie, S. Plasticity model for simulation, description and evaluation of vibratory stress relief. *Materials Science and Engineering A* 516 (2009) 154–161.
42. Smith, D., J., Farrahi, G., H., Zhu, W., X., McMahon, C., A. Experimental measurement and finite element simulation of the interaction between residual stresses and mechanical loading. *International Journal of Fatigue*, Vol. 23 (2001) 293–302.
43. Vöhringer, O. Relaxation of Residual Stresses. *Proc. European Conference on Residual Stresses*, Karlsruhe, E. Macherauch and V. Hauk, Editors, DGM Informationsgesellschaft, 1983. pp. 47-80.
44. Sandström, R., Malén, K., Otterberg, R. Prediction of Stress Relaxation under Multiaxial Stresses and Application to the Reactor Pressure Vessel Steel A533B. *Res. Mechanica*, 6(1983)215-232.
45. Goo, B., C, Yang, S., Y., Seo, J., W. Fatigue Life Evaluation Model for Welded Joints with Residual Stresses. *Key Engineering Materials*, Vol. 297-300 (2005), pp. 762-767.
46. Takanashi, M., Kamata, K., Iida, K. Relaxation Behavior of Welding Residual Stresses by Fatigue Loading in Smooth Longitudinal Butt Welded Joints. *Welding in the World*, Vol. 44, No. 4 (2000), pp. 28-34.
47. Löhe, D., Vöhringer, O. Stability of Residual Stresses. In: Totten, G., Howes, M., Inoue, T (Ed.). *ASM International Handbook of Residual Stress and Deformation of Steel*, 2002.

48. Impellizzeri, L., F. Cumulative Damage Analysis in Structural Fatigue. Effects of Environment and Complex Load History on Fatigue Life, ASTM STP 462, American Society for Testing and Materials, 1970. pp. 40-68.
49. Hoffmeister, J., Schulze, V., Wanner, A., Hessert, R. Thermal Relaxation Of Residual Stresses Induced By Shot Peening In IN718. Conference Proceedings of ICSP-10 Tokyo, Japan, 2008.
50. Viereck, D., Löhé, D., Vöhringer, O., Macherauch, E. Relaxation of residual stresses in a nickel-base superalloy due to dislocation creep. In: Brandon, D., G., Chaim, R., Rosen, A. (editors), Proceedings of International Conference of Strength of Metals and Alloys 9. Freund Publishing, London, 1991. pp. 14-19.
51. Morrow, J, Ross, A., S., Sinclair, G., M. Relaxation of residual stresses due to fatigue loading. SAE Transactions 68, 1960. pp. 40-48.
52. Rotvel, F. On Residual Stresses During Random Load Fatigue. Advisory Group for Aerospace Research and Development. Symposium on Random Load Fatigue, AGARD CP 118, Lyngby, Denmark, 1972.
53. Webster, G., A., Ainsworth, R., A., 1994. High Temperature Component Life Assessment. Chapman and Hall, London.
54. Arcari, A., De Vita, R., Dowling, N., E. Mean stress relaxation during cyclic straining of high strength aluminum alloys. International Journal of Fatigue 31 (2009) 1742–1750.
55. Rovinskiy, B., M., Lutsau, V., G. Relaxation of microstresses. Zh Tech Fiz 1957;27(2):345-50 (in Russian).
56. Borzdyka, A., M., Getsov, L., B. Relaxation of stresses in metals and alloys. Moscow: Metallurgia, 1972 (in Russian).
57. Kwangsoo, H. A unified constitutive law for cyclic viscoplasticity. International Journal of Solids and Structures 46 (2009) 1007–1018.
58. Potter, J., M. The Effect of Load Interaction and Sequence on the Fatigue Behavior of Notched Coupons. Cyclic Stress-Strain Behavior – Analysis, Experimentation, and Failure Prediction. ASTM STP 519, American Society for Testing and Materials, 1973. pp. 109-132.
59. Holzapel, H., Schulze, V., Vöhringer, O., Macherauch, E. Residual stress relaxation in an AISI 4140 steel due to quasistatic and cyclic loading at higher temperatures. Material Science Engineering, A 248 (1998) 9.
60. Altenberger, I., Noster, U., Scholtes, B., Ritchie, R., O. High temperature fatigue of mechanically surface treated materials. In: Wagner, L. (Editor), Shot Peening. Wiley-VCH, Weinheim, 2003. 483 p.
61. Nikitin, I., Altenberger, I., Scholtes, B. Residual stress state and cyclic deformation behaviour of deep-rolled and laser-shock peened AISI 304 at elevated temperatures. Material Science Forum, 490 (2005) 376.
62. Teng, H., Bate, S., K., Beardsmore, D., W. STATISTICAL ANALYSIS OF RESIDUAL STRESS PROFILES USING A HEURISTIC METHOD. Article PVP2008-61378, Proceedings of PVP2008, 2008 ASME Pressure Vessels and Piping Division Conference, July 27- 31 2008, Chicago, Illinois, USA. 5 p.
63. Brahim, N., Bouchard, P., J., Truman, C., E., Smith, D., J. A STATISTICAL FRAMEWORK FOR ANALYSING WELD RESIDUAL STRESSES FOR STRUCTURAL INTEGRITY ASSESSMENT. Article PVP2008-61339, Proceedings of

- PVP2008, 2008 ASME Pressure Vessels and Piping Division Conference, July 27- 31 2008, Chicago, Illinois, USA. 8 p.
64. Kariya, T., Kurata, H. Generalized Least Squares. John Wiley & Sons, Chichester, U.K. 2004.
 65. Goudar, D., M., S. Hossain, S., Truman, C., E., Smith, D., J. UNCERTAINTY IN RESIDUAL STRESS MEASUREMENTS. Article PVP2008-61343, Proceedings of PVP2008, 2008 ASME Pressure Vessels and Piping Division Conference, July 27- 31 2008, Chicago, Illinois, USA. 8 p.
 66. Brahim, N., Smith, M., C., Truman, C., E., Smith, D., J., Bouchard, P., J. A STATISTICAL ANALYSIS OF PIPE GIRTH WELD EXPERIMENTAL RESIDUAL STRESS DATA. Article PVP2009-77571, Proceedings of PVP2009, 2009 ASME Pressure Vessels and Piping Division Conference, July 26-30, 2009, Prague, Czech Republic. 10 p.
 67. Sivia, D., S., Skilling, J. Data Analysis: A Bayesian Tutorial. Second Edition 2006: Oxford University Press Inc., New York.
 68. Sivia, D., S. Dealing with Duff Data. In: Maximum Entropy and Bayesian Methods. 1996. Kruger, South Africa.
 69. Abdel-Tawab, K., Noor, A., K. Uncertainty analysis of welding residual stress fields. Comput. Methods Appl. Mech. Engrg. 179 (1999) 327-344.
 70. Elishakoff, I. Essay on uncertainties in elastic and viscoelastic structures: From: criticisms by Freudentahl, A., M., to modern convex modeling, Computers and Structures 56 (1993) 871-895.
 71. Radaj, D. Heat Effects of Welding, Springer, New York, 1992.
 72. Draper, N., Smith, H. Applied regression analysis. Second edition. 1980: John Wiley & Sons, Inc.
 73. Harris, D., O. et al. Fracture Mechanics Models Developed for Piping Reliability Assessment in Light Water Reactors. Report NUREG/CR-2301, U.S. Nuclear Regulatory Commission (USNRC), Washington D. C., 1981.
 74. Harris, D., O. et al. Theoretical and user's manual for PC-PRAISE. A probabilistic fracture mechanics computer code for piping reliability analysis. Report NUREG/CR-5864. U.S. Nuclear Regulatory Commission (USNRC), Washington D. C., 1992.
 75. Shack, W., J. et al. Environmentally Assisted Cracking in Light Water Reactors: Annual Report, October 1981 – September 1982. NUREG/CR-3292, Washington D.C., U.S. Nuclear Regulatory Commission, June 1983.
 76. Harris, D., O., Dedhia, D., D., Eason, E., D., Patterson, S., D. Probability of Failure in BWR Reactor Coolant Piping, Volume 3: Probabilistic Treatment of Stress Corrosion Cracking in 304 and 316NG BWR Piping Weldments, Report NUREG/CR-4792. Prepared for U.S. Nuclear Regulatory Commission (USNRC), 1989.
 77. Khaleel, M., A., Simonen, F., A. Evaluations of Structural Failure Probabilities and Candidate Inservice Inspection Programs. Report NUREG/CR-6986 (PNNL-13810). Prepared by Pacific Northwest National Laboratory for U.S. Nuclear Regulatory Commission (USNRC). March 2009.
 78. Rudland, D., L, Xu, H., Wilkowski, G., Scott, P., Ghadiali, N., Brust, F. Development of a New Generation Computer Code (PRO-LOCA) for the Prediction of Break Probabilities for Commercial Nuclear Power Plants Loss-of-Coolant Accidents. In: Proceedings of the

- ASME Pressure Vessels and Piping Conference, July 23-27, 2006, Vancouver, British Columbia, Canada. American Society of Mechanical Engineers, New York.
79. Rudland, D., Scott, P., Kurth, R., Cox, A. CONTINUING DEVELOPMENT OF PRO-LOCA FOR THE PREDICTION OF BREAK PROBABILITIES FOR LOSS-OF-COOLANT ACCIDENTS. Article PVP2009-77053, Proceedings of PVP2009, 2009 ASME Pressure Vessels and Piping Division Conference, July 26-30, 2009, Prague, Czech Republic. 10 p.
 80. Itoh, H., Katsuyama, J., Onizawa, K. A PROBABILISTIC EVALUATION MODEL FOR WELDING RESIDUAL STRESS DISTRIBUTION AT PIPING JOINT IN PROBABILISTIC FRACTURE MECHANICS ANALYSIS. Article PVP2008-61421, Proceedings of PVP2008, 2008 ASME Pressure Vessels and Piping Division Conference, July 27- 31 2008, Chicago, Illinois, USA. 6 p.
 81. Chapman, O., J., V., Simonen, F., A. PR-PRODICAL - Model for Estimating the Probabilities of Defects in Reactor Pressure Vessel Welds, Report NUREG/CR-5505, U.S. Nuclear Regulatory Commission (USNRC), Washington, D.C., 1998.
 82. Reliability Consulting Programs (RCP). STRUREL, a Structural Reliability Analysis Program-System, COMREL & SYSREL: Users Manual. Munich: RCP Consult, 2004.
 83. STRUREL. A Structural Reliability Analysis Program: Theoretical Manual. RCP GmbH, München, Germany, 1991.
 84. Shinokawa, H., Shibata, K., Isozaki, T. Program of Calculation Coolant Leakage Amount from Through Crack. JAERI-M 90-050, Japan Atomic Energy Research Institute, 1990 (in Japanese).
 85. Dillström, P., Zang, W. ProLBB - A Probabilistic Approach to Leak Before Break Demonstration. SKI Report 2007:43. Inspecta Technology AB for the Swedish Nuclear Power Inspectorate (SKI). Sweden, Stockholm, November 2007. 177 p.
 86. Bradford, R. Through-thickness distributions of welding residual stresses in austenitic steel cylindrical butt welds. Proceedings of sixth international conference on residual stresses (ICRS-6). London: IOM Communications Ltd: 2000, p. 1373–381.
 87. Bouchard, P., Bradford, R. Validated axial residual stress profiles for fracture assessment of austenitic stainless steel pipe girth welds, pressure vessel and piping. Proceedings of ASME conference, New York : ASME;2001;PVP-423: 93–99.
 88. Dong, P., Brust, F. Welding residual stresses and effects on fracture in pressure vessel and piping components: a millennium review and beyond, ASME Trans. J. of Press. Vessel Technol. 2000; 122(3): 328–38.
 89. Dong, P., Rahman, S., Wilkowski, G., Brickstad, B., Bergman, M., Bouchard, P., Chivers, T. Effect of weld residual stresses on crack opening area analysis of pipes for LBB applications. Proceedings of ASME pressure vessel and piping conference. New York: ASME; 1996; PVP-324. pp. 47–64.
 90. Cronvall, O. Practical inclusion and behaviour of welding residual stresses in structural integrity analyses of NPP primary circuit components. VTT Research report VTT-R-00962-09, Technical Research Centre of Finland (VTT), Espoo, Finland, 2009. 53 p.
 91. Cronvall, O. Simulated behaviour of welding residual stresses in NPP primary circuit components subject to cyclic loading. VTT Research report VTT-R-02199-10, Technical Research Centre of Finland (VTT), Espoo, Finland, 2010. 51 p.
 92. ASME Boiler and Pressure Vessel Code, Section II. 2005 Update of 2004 Edition.

93. Abaqus/Standard User's manual, Version 6.8. Dassault Systèmes Simulia Corp., 2008. Providence, Rhode Island, U.S.A.
94. Abaqus Theory manual, Version 6.8. Dassault Systèmes Simulia Corp., 2008. Providence, Rhode Island, U.S.A.
95. Nuclear standard NE F9-5T, Guidelines and Procedures for Design of Class 1 Elevated Temperature Nuclear System Components. U.S. Department of Energy, Nuclear Energy Programs, September 1986, U.S.A.
96. Ziegler, H. A Modification of Prager's Hardening Rule. *Quart. Appl. Math.* 17 (1955) 55–65.
97. Crisfield, M. *Non-Linear Finite Element Analysis of Solids and Structures, Volume 1: Essentials*. John Wiley & Sons. Chichester, U.K., 1991. 345 p.
98. Brickstad, B. The Use of Risk Based Methods for Establishing ISI-Priorities for Piping Components at Oskarshamn 1 Nuclear Power Station. SAQ/FoU-Report 99/05, SAQ Kontroll AB, 1999. 83 p.
99. R5 and R6 Panels. R5/R6 Newsletter. Number 38, January 2009. 11 p.

Appendix 1: Summary of input data parameters necessary for RS relaxation assessment procedures

Concerning the covered residual stress (RS) relaxation assessment procedures, here is presented procedure specifically a summary of the necessary input data parameters, see Table A1 in the next page. This is the same table as Table 4.2-4 in Section 4.2, only now it is fitted to one page. Equation numbers are used in the table, for actual equations, see Tables 4.2-1, 4.2-2 and 4.2-3 in Section 4.2.

